National Library
of Canada

Acquisitions and
Bibliographic Services Branch

395 Wellington Street
Ottawa, Ontario
K1A 0N4

Bibliothèque nationale
du Canada

Direction des acquisitions et
des services bibliographiques

395, rue Wellington
Ottawa (Ontario)
K1A 0N4

Your file Votre référence

Our file Notre référence

NOTICE

The quality of this microform is heavily dependent upon the quality of the original thesis submitted for microfilming. Every effort has been made to ensure the highest quality of reproduction possible.

If pages are missing, contact the university which granted the degree.

Some pages may have indistinct print especially if the original pages were typed with a poor typewriter ribbon or if the university sent us an inferior photocopy.

Reproduction in full or in part of this microform is governed by the Canadian Copyright Act, R.S.C. 1970, c. C-30, and subsequent amendments.

AVIS

La qualité de cette microforme dépend grandement de la qualité de la thèse soumise au microfilmage. Nous avons tout fait pour assurer une qualité supérieure de reproduction.

S'il manque des pages, veuillez communiquer avec l'université qui a conféré le grade.

La qualité d'impression de certaines pages peut laisser à désirer, surtout si les pages originales ont été dactylographiées à l'aide d'un ruban usé ou si l'université nous a fait parvenir une photocopie de qualité inférieure.

La reproduction, même partielle, de cette microforme est soumise à la Loi canadienne sur le droit d'auteur, SRC 1970, c. C-30, et ses amendements subséquents.

Canada

Conversion of Bioacids/Bioacetone to Isobutylene and Other Hydrocarbons over ZSM-5 Zeolite Catalysts

Li Huang

A Thesis

in

The Department

of

Chemistry and Biochemistry

Presented in Partial Fulfillment of the Requirements
for the Degree of Master of Science at
Concordia University
Montreal, Quebec, Canada

August 1992

ISBN 0-315-80924-8

Canada

ABSTRACT

Conversion of Bioacids/Bioacetone to Isobutylene and Other Hydrocarbons over ZSM-5 Zeolite Catalysts

Li Huang

The direct catalytic conversion of very dilute aqueous solutions (10 wt%) of acetic acid, usually obtained from fermentation products, to hydrocarbons (mainly isobutylene) was carried out via the formation of acetone as the primary step, using a two-bed reactor.

The formation of acetone was base catalyzed using the CaO catalyst, and the reaction conditions were as follows: space velocity (WHSV) of 0.2 h^{-1}, and temperature ranging from 425 to 450^{0}C.

The formation of isobutylene from aqueous solution (5 wt%) of acetone was acid catalyzed using the ZSM-5 type zeolite catalysts having a Si/Al ratio of 18. High yields of isobutylene were obtained at a reaction temperature as low as 210^{0}C and a space velocity of 0.1 h^{-1}.

Two successful catalyst modifications were found to be beneficial.

(i) The activity and isobutylene selectivity were significantly improved by loading with 2 wt% TFA superacid, and performing the reaction at 220^{0}C.

(ii) The isobutylene selectivity showed a significant increase after the parent HZSM-5 was treated with a strong base solution of KOH containing $Al_2(SO_4)_3$ at a KOH

concentration of 1.2-1.5N.

The reaction sequence for aqueous acetone conversion followed the pathway in which diacetone alcohol acts as the intermediate and this was followed by an acid catalyzed cracking. The presence of water in the feed promoted the catalytic selectivity toward isobutylene.

The apparent activation energy and the pre-exponential factor were found to be 61.1 kJ/mole and 5.7E+5 h^{-1}, respectively.

Acknowledgements

I would like to express my sincere appreciation to Professor R. Le Van Mao for his advice, support and encouragement throughout all the facets of this work.

I would also like to thank:

Drs. O. S. Tee and R. H. Pallen as my committee members for their time and valuable suggestions;

Drs. J. Yao and L. Dufresne for many enjoyable discussions;

Dr. A. Lavigne and Miss A. Ramsaran for proofreading this thesis;

Mr. B. Sjiariel for his assistance with the equipment used in the research of this thesis;

Mr. C. Kowalewski for special glassware making;

office staff, in particular, Ms. C. J. Coutts for the assistance and help when needed;

and all my colleagues, past and present, for their cooperations.

Finally, I wish to express my deepest gratitude to my parents for their love, moral support and understanding. Without them, this work would have never been accomplished.

Dedicated

To my husband, Yining,

For his love and understanding

TABLE OF CONTENT

LIST OF FIGURES

LIST OF TABLES

LIST OF APPENDICES

CHAPTER 1 - INTRODUCTION

1.1 The B.A.T.H. (Bioacids/Bioacetone - to - Hydrocarbons) Process

The B.A.T.H. process is a process which converts acetic acid or acetone in fermentation effluents to hydrocarbons. The general idea to convert acetic acid or acetone into hydrocarbons in this project is based on the fact that acetic acid and acetone are currently produced by several industrial processes ranging from direct manufacturing to fermentation of biomass materials.

Three main methods are available for manufacturing concentrated acetic acid (mp = 16.6^0C, bp = 118.5^0C):[1]

(a) Liquid phase oxidation of acetaldehyde.

The catalytic oxidation of acetaldehyde in the liquid phase to acetic acid by air or oxygen is still widely used, and accounts for about 40 per cent of installed worldwide production capacity.

(b) Direct or indirect oxidation of hydrocarbons in the liquid phase.

This method can be applied to the oxidation of any paraffinic or olefinic hydrocarbons. Most industrial plants mainly process paraffins such as propane, *n*-butane and light gasoline and the first commercial plant built by Celanese, dates from 1952. The oxidation of light gasoline has also been industrialized worldwide.

(c) Methanol carbonylation.

Acetic acid has been produced by the carbonylation of methanol for a very long time, with the earliest industrial development dating back to 1925 (*British Celanese, BASF: Badische Anilin and Soda Fabrik*). An important technological breakthrough in this area was achieved by Monsanto workers to overcome the severe reaction conditions previously required for this process.

Acetic acid can also be obtained by glucose fermentation or pyrolysis of wood, hemicelluloses or lignin.[2]

Acetone is commonly used as a solvent. About one-third of the acetone (mp = -94.6^{0}C, bp = 56.1^{0}C) produced worldwide is derived from the dehydrogenation of isopropanol,[1] however, it can also be obtained by various other methods, mainly the following:[1]

(a) Oxidation of cumene and splitting of the hydroperoxide formed into phenol and acetone

(b) Direct oxidation of propylene by air.

(c) Acetone-butanol fermentation.

The most valuable hydrocarbon fraction in this work is isobutylene since it is a precursor of new and very effective octane enhancers.

1.2 Isobutylene and Octane Enhancement

Isobutylene (IB) has an enormous industrial potential since it is widely used in the field of elastomers for the manufacture of butyl rubber by co-polymerization with small amounts of isoprene.[3] In petrochemistry, isobutylene is obtained by:[3]

(a) extraction of C_4 components from steam cracking or catalytic cracking.

(b) dehydrogenation of isobutane.

Since it is a precursor for the synthesis of methyl tert-butyl ether (MTBE) and ethyl tert-butyl ether (ETBE), isobutylene plays an important role in the production of octane boosters. Gasolines produced over zeolite catalysts by the cracking of heavy oil have lower octane numbers (research octane number, RON, and motor octane number,

MON).[4] The octane rating of a gasoline measures its knocking characteristics as determined in a standard laboratory engine test. The higher the octane number, the lower the tendency for a gasoline to produce knocking phenomena in an automobile engine. The consequent decrease of octane number in gasoline can be partially regained by adding octane-boosters such as tetraethyl or tetramethyl lead to the gasoline (1.1 gram/gal). However, the average gasoline lead level has been necessarily lowered significantly (0.1 gram/gal), since lead is an air pollutant. This forced the refiners to look for alternatives to meet octane blending requirements and then, methyl tert-butyl ether (MTBE), ethyl tert-butyl ether (ETBE) and tert-amyl methyl ether (TAME) have proven to be effective as gasoline octane boosters and are now used in several countries as substitutes for tetraethyl lead.[4]

Isobutylene (IB) can be used to produce MTBE or ETBE by reaction with methanol or ethanol according to the following reactions:

$$\underset{\text{(IB)}}{(CH_3)_2CHCH_2} + CH_3OH \longrightarrow \underset{\text{(MTBE)}}{(CH_3)_3COCH_3} \qquad (1)$$

$$\underset{\text{(IB)}}{(CH_3)_2CHCH_2} + CH_3CH_2OH \longrightarrow \underset{\text{(ETBE)}}{(CH_3)_3COCH_2CH_3} \qquad (2)$$

1.3 Interest in Biomass

Presently, most of our organic chemicals and subsequent synthetic organic polymeric materials are obtained from petroleum (mainly paraffins, cycloparaffins and aromatic compounds in varying proportions), and natural gas (methane). Problems associated with this reliance on petroleum include fluctuating petroleum costs, uncertainty of supply and ultimately concerns relating to the depletion of these non-renewable fossil fuels. Coal as a raw material can also be used to supply energy and

chemicals, but coal, like petroleum, is a non-renewable resource, and so a gradual transition to the use of biomass feedstocks is expected to provide solutions to the long-term problems associated with petroleum and coal depletion.

Considerable interest in the use of biomass has therefore emerged.[2,5] The basic biomass resource consists of energy farms, energy yielding crops such as corn and sugar cane, and waste materials from sources such as municipal wastes, animal manure, and crop and forestry residues. The conversion of the biomass to synthetic fuels can be accomplished by a variety of thermal and biochemical processes.[6] Fermentation has been performed for many centuries for wine-making since 10 000 BC and recently, developments in hybrid technology and genetic engineering have extended the scope and potential of industrial fermentation technology.[7]

Dilute aqueous solutions of acetone or various acids, such as acetic acid, are produced by fermentation of biomass and/or organic wastes. However, their low concentration in the fermentation broth makes their recovery uneconomical. Furthermore, waste treatment processes must be used to reduce the concentration of organic matter in waste water, so that the effluent may be safely discharged into the environment. Therefore, it would be of great interest to convert these oxygenates such as acids and alcohols into hydrocarbons so as to approach the solution to both energy and environmental problems.

Fortunately, the preliminary work done by R. Le Van Mao[8] and co-workers has shown that an aqueous solution of acetone (with concentration ranging from 5 to 10 wt%) can be selectively converted, with very high yields, into isobutylene over ZSM-5 and Y zeolites treated with trifluoromethane sulfonic acid. Therefore, before describing the experimental part, it is worth mentioning zeolites, an important material widely used in heterogeneous catalysis.

1.3 Zeolites

Zeolites are finding applications in many areas of catalysis, generating interest in these materials both in industrial and academic laboratories due to their unique intercrystalline pore-channel systems and the excellent maintenance of catalyst activity.[9] Subsequently, a great number of techniques have been developed for identifying and characterizing zeolite materials.[10,11] The number of zeolite-related U.S. patents published through 1981 exceeds 5,000 and the zeolite scientific and technical literature contains over 25,000 articles.[9]

The major part of zeolite catalysis work has been related to reactions where the zeolite is used as a "solid acid", e.g., isomerization, cracking, hydrocracking etc. The catalysts chosen for catalytic cracking, which is the greatest use of zeolites, are zeolites X and/or Y. Large savings in petroleum resources have been made through the use of catalysts over the last 15 years in the U.S.A..[12] The second greatest use, hydrocracking, is based on zeolite catalysts Y, mordenite, erionite or ultrastable faujasites to produce kerosine, toluene, xylenes and jet-fuels. Further applications have been achieved since the syntheses of ZSM-5 and ZSM-11 which are widely used as catalysts for methanol conversion, xylene isomerization, dewaxing and a number of other processes.[13]

1.3.1 What are zeolites?

Structurally, zeolites are crystalline aluminosilicates with a framework based on an extensive three-dimensional network of oxygen ions. The fundamental unit is the individual tetrahedral TO_4 unit, where T is either Si or Al (Figure 1.1).[9] These tetrahedra are arranged in such a way that each of the four oxygen anions is shared in turn with another silica or alumina tetrahedron. The number of AlO_2^- tetrahedra in the structure determines the framework charge which is balanced by cations located in the cages or channels of the framework. Since such cations in most cases are not "locked in", they are free to move and are exchangeable with other cations and this is known as an ion-

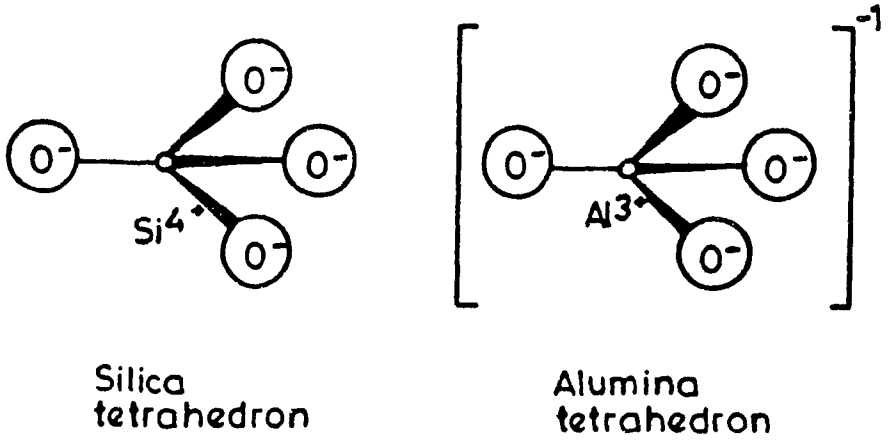

Figure 1.1 Primary building blocks of zeolites

exch .ngeable property of zeolites. A representative empirical formula for a zeolite is written as follows:

$$M_{2/n}.ZAl_2O_3.XSiO_2.YH_2O,$$

where n is the charge on the cation M, coefficient X is greater than Z, and Y is the hydration number. Each zeolite has a unique crystal lattice structure even though their chemical composition may be the same.

The secondary building unit (SBU) consists of selected geometric groupings of those primary units and there are nine of such building units which can be used to describe all of the known zeolite structures. These secondary building units consist of 4, 6 or 8-membered single rings and some branched rings (Figure 1.2).[9] Also reported in such a figure are the symbols used to describe them. These secondary building units form the building blocks of the framework zeolite crystal structure. In Figure 1.3, faujasite sodalite cages and the ZSM-5 building units along with the structures they form are shown. These structures spread out into a three-dimensional network which has the properties of a crystal.

There are several ways to classify zeolites. The simplest one is based on the pore size of the zeolite pore openings which will determine the size of molecules being admitted in the zeolite pores and this is determined by the number of tetrahedral units, or alternatively, oxygen atoms required to form the pore as well as the nature of the cations that are present in the pore. There are only three pore openings that are of practical interest for catalytic applications; they are referred to as the 8, 10, and 12 ring openings. The sizes corresponding to these ring openings for three representative zeolites are shown in Figure 1.3.

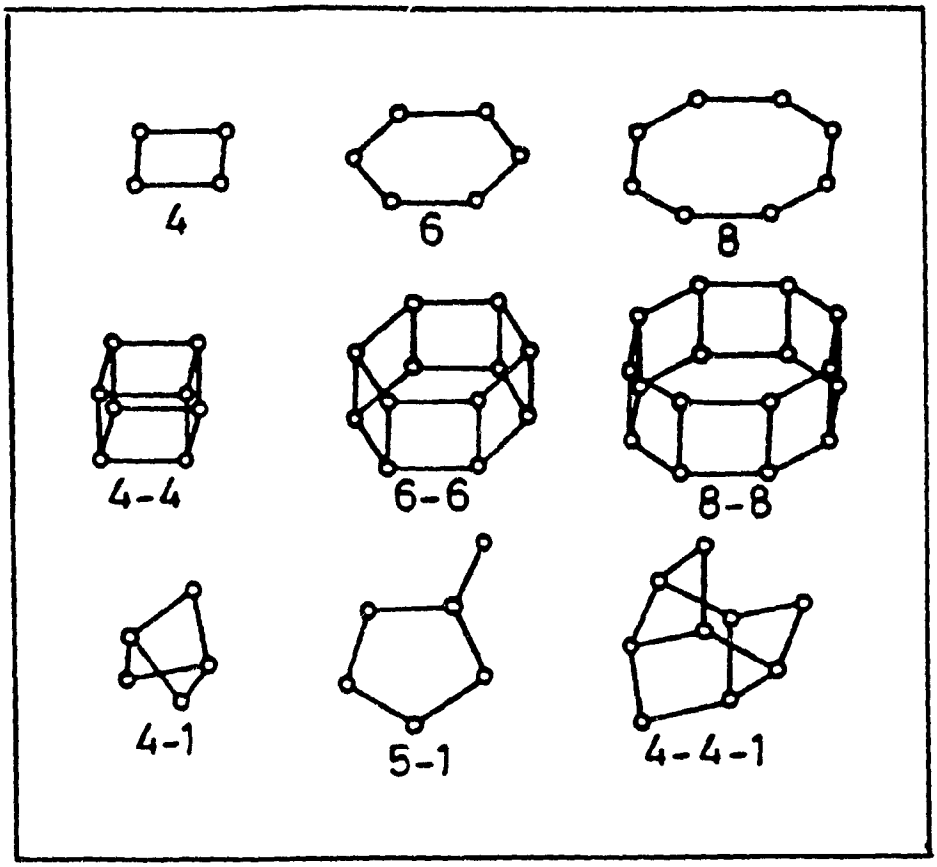

Figure 1.2 Secondary building units

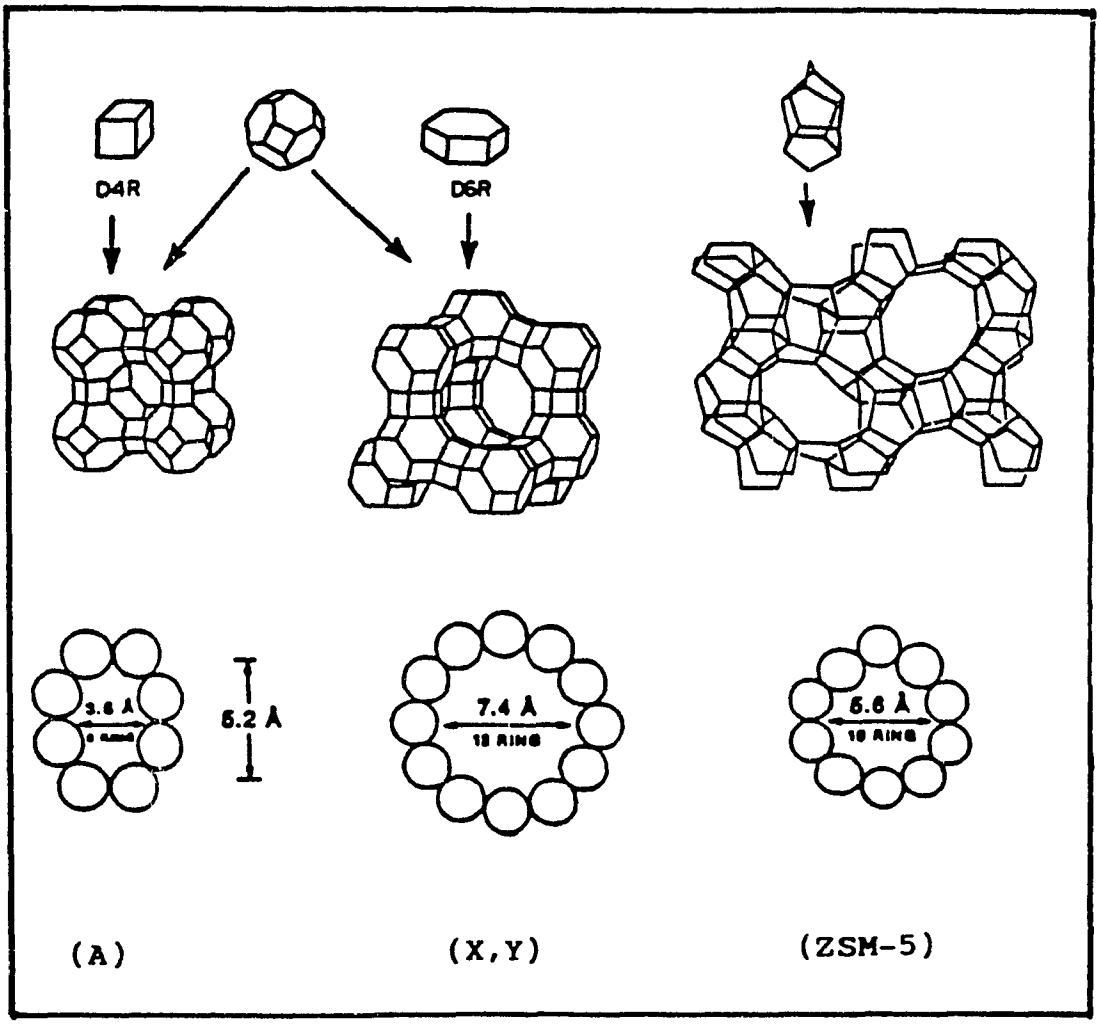

Figure 1.3 Different building units, the zeolite frameworks resulting from their linking and the pore size of their opening

1.3.2 Shape-Selectivity

Shape-selectivity is a consequence of specific geometric constraints imposed by the zeolite crystal structure on foreign molecules in the system. Since the interior of a zeolite is practically a unique catalytic environment for chemical transformations, shape selectivity plays a very important role in zeolite catalysis and operates by either reactant shape selectivity, product shape selectivity, or transition-state shape selectivity (Figure 1.4).[4]

Reactant shape selectivity (also known as sieving effect) is observed when only certain reactant molecules can pass through the catalyst pores, the remaining molecules being too large to diffuse into the pores.

Product shape selectivity occurs when, among all the product species formed within the pores, only those with the proper dimensions can diffuse out and be recovered. Bulky products, if formed, are either converted to less bulky molecules (e.g., by equilibration) or eventually deactivate the catalyst by blocking the pores.

Restricted transition-state shape selectivity occurs when certain reactions are prevented because the corresponding transition state would require more space than available in the cavities. Neither reactant nor potential product molecules is prevented from diffusing through the pores, and reactions requiring smaller transition states proceed unhindered since no blocking of pores should occur.

Molecular traffic shape selectivity occurs in zeolites with two types of channel systems (e.g. in ZSM-5), having different pore openings and geometry. In this case, the reactant molecules enter the zeolite pore system preferentially through one type of channels and the products, due to size or shape limitations, leave the zeolite particle through the other type of channels, thus minimizing the eventual detrimental effects of the product counter-diffusion with respect to the reactant-diffusion.

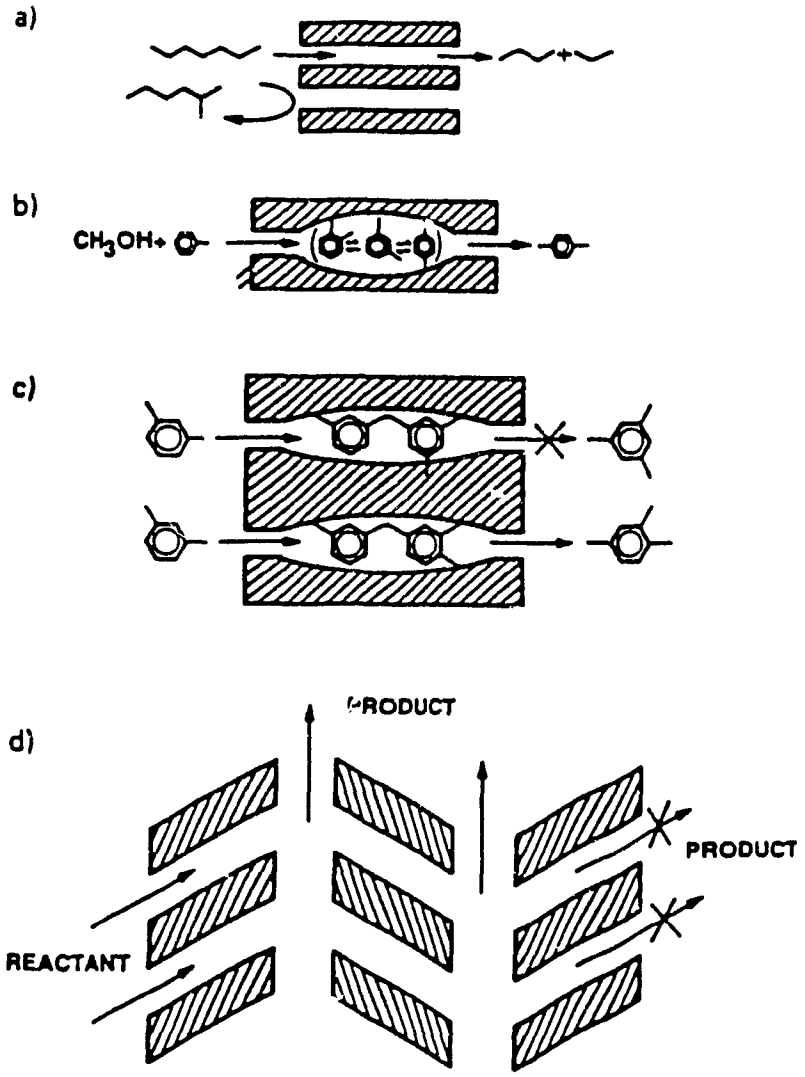

Figure 1.4 Schematic representation of molecular shape selectivity effects: (a) reactant selectivity, (b) product selectivity, (c) restricted transition state selectivity, and (d) molecular traffic selectivity (in ZSM-5)

1.3.3 Surface Acidity

Another important feature of zeolites is the surface acidity present on the zeolite surface when the cations in the exchangeable sites are replaced by protons. Studies carried out on cracking catalysts revealed that their activity is connected with their acidic properties, first noted in 1933 by Gayer.[14] However, the exact nature of the surface sites generating acidity has not been definitely clarified. Figure 1.5 depicts a zeolite surface, showing possible types of surface structures due to various treatments of a silica rich zeolite.[11] Part (a) shows the as-synthesized material, where M^+ represents a metal cation (typically sodium). Ammonium exchange of the alkali cations results in the surface structure as represented in (b) and subsequent deammoniation by calcination produces the active proton-exchanged sites (c). The proton adjacent to an alumina site is the classical Bronsted-acid site. It is generally associated with the bridged Si-O-H (silanol) as is a classical Bronsted-acid site which is proposed to exist in equilibrium with that depicted in (d). The proton acidity is a result of the interaction between the unshared pair of electrons on the oxygen atom and the unoccupied orbital of the aluminum atom, which weakens the bond between the oxygen atom and the proton coordinated to it in such a way that the proton has donor acidity. Therefore, any efforts which can affect these interactions will influence the surface acidity accordingly. Upon dehydroxylation (by calcination at high temperature, for instance), a trigonally coordinated aluminum is formed: this constitutes a Lewis acid (electron acceptor) site (e).

The number and strength of the acid sites are complex functions of the nature and concentration of AlO_2^- tetrahedral groups, as well as the location and concentration of exchangeable cations that are present on the zeolite surface. As the Si/Al ratio increases, the thermal, hydrothermal, and acid stability increases,[9] However, it is now well known that, the lower the Si/Al ratio of the zeolite framework, the higher the acid site density.[15-17] A good way to control the acidity of zeolite catalysts and their stability is to modify the Si/Al ratio of their framework and such a modification can be achieved by the

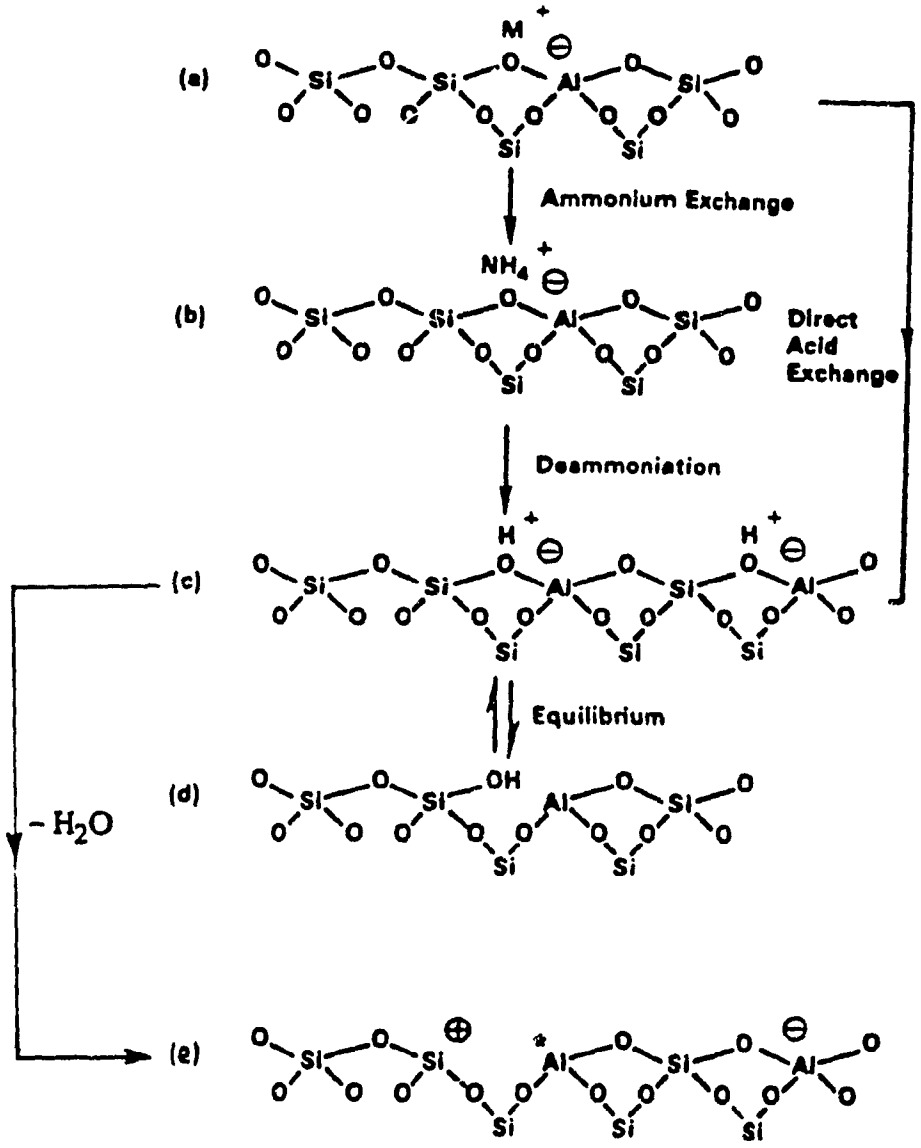

Figure 1.5 Diagram of the "surface of a zeolite framework

following two ways: (i) by dealumination which results in a framework Al content reduction,[18,19] and (ii) by alumination which leads to a framework Al content increase.[20-23]

Another way to enhance zeolite acidity is by loading superacids such as FSO_3H and FSO_3H:SbF_5 (Magic Acid) onto the zeolite surface.[24] The thermal stability of active superacid complexes on the zeolite surface is one of the major factors limiting the use of this method.

1.3.4 Zeolite ZSM-5

Zeolite ZSM-5, belonging to the pentasil family, has a unique channel structure which differs from those of the large pore faujasite and small pore zeolites such as Linde A and erionite and it possesses unusual catalytic properties and has a high thermal stability. ZSM-5 is used commercially in synthetic fuels (conversion of methanol to gasoline), petroleum refining (dewaxing of distillates) and petrochemicals (xylene isomerization, toluene disproportionation, ethylbenzene manufacture).

In Figure 1.6,[4] the structure of ZSM-5 zeolite according to Kokotailo and co-workers is shown.[25] The framework contains (Si, Al)O_4 tetrahedrons which, in turn, are joined together forming two types of intersecting channels with 10-membered ring openings. The size of these openings is between that of the large pore, 12-membered ring opening of faujasite and the small-pore, 8-membered ring opening of zeolite A. One channel system runs parallel to the *a* axis of the orthorhombic unit cell; and has near-circular (5.4 to 5.6 Å) openings and the other channels are straight, parallel to the *b* axis, and have elliptical openings (5.1 to 5.7 Å). The channel intersections have a diameter of about 9 Å.

ZSM-5 zeolites have been synthesized with SiO_2/Al_2O_3 molar ratios from 20 to greater than 8000 and many properties of ZSM-5, such as ion exchange capacity and catalytic activity, vary with the SiO_2/Al_2O_3 ratio. Other properties, such as degree of

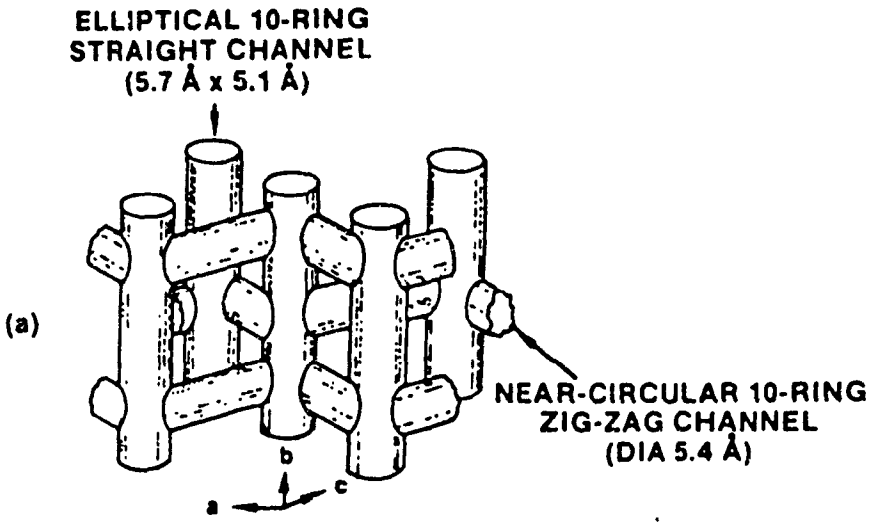

Figure 1.6 Structure of ZSM-5: channel system

crystallinity, pore size and volume, depend primarily on the framework structure and are independent of the SiO_2/Al_2O_3 ratio.

In the hydrogen form, ZSM-5 zeolites have Bronsted and Lewis acid sites and the latter is specifically present in samples which have been activated at high temperatures. The infrared spectra show a strongly acidic band at 3600 cm^{-1} , most likely due to OH groups and a weakly acidic band at 3720-3740 cm^{-1} which is probably due to terminal silanol groups on the surface of the zeolite.[4] The concentration of acid sites (acid density) is proportional to the concentration of framework aluminum.

The particular shape-selective properties of ZSM-5 are due to the presence of two intersecting channel networks resulting from the conjunction of four different features.[9]

1. Pore openings with medium size;
2. Free space of dimensions larger than that of the pores at channel intersections;
3. The absence of cages along the channels;
4. The occurrence of slightly differentiated channel networks.

1.4 Conversion of Acetic Acid into Acetone

The synthesis of isobutylene both from glacial acetic acid and acetone had not been studied until 1974 when a shape-selective catalyst, HZSM-5, was synthesized and successfully used for the methanol to gasoline conversion,[26] even though the catalytic properties of zeolites had been extensively used for hydrocarbon transformation such as reforming, isomerization and catalytic cracking. ZSM-5 zeolite has made possible the one-step conversion of oxygenated natural compounds such as alcohols, carboxylic acids and ketones directly into hydrocarbons.[27]

Under the experimental conditions, such as T = 371 ^0C, WHSV = 1 h^{-1}, the major products from acetic acid over HZSM-5 catalysts included isobutylene and small

amounts of acetone, as found by C. D. Chang et al. in 1977.[27] The hydrocarbon selectivity to isobutylene in this case was interesting (66.5%) but the total conversion was relatively low (only 29.9%) with considerable production of carbon dioxide. However, the production of acetone increased dramatically when a base catalyst of alkaline metal-ion exchanged zeolite was used in L. M. Parker's work which suggested that acetic acid conversion into acetone could be achieved by a base catalytic process.[28]

Most recently, S. Sugiyama and co-workers used silica-supported alkaline earth oxides and obtained excellent activity to convert acetic acid selectively into acetone in a vapor-phase fixed-bed flow system.[29] They concluded that the alkaline earth silicate should retain the nature of the basic oxide for the synthesis of ketones from carboxylic acid. Thus, for supported magnesium oxide, the following reaction scheme was given, which showed how the major products, acetone and carbon dioxide were produced:

$$MgO + 2CH_3COOH \longrightarrow Mg(OCOCH_3)_2 + H_2O$$

$$Mg(OCOCH_3)_2 \longrightarrow MgCO_3 + (CH_3)_2CO$$

$$MgCO_3 + 2CH_3COOH \longrightarrow Mg(OCOCH_3)_2 + CO_2 + H_2O$$

1.5 Aldolization of Acetone and Further Cracking

Acetone (CH_3COCH_3) conversion has been studied by several researchers and ZSM-5 zeolite catalysts were mostly used due to their strong acidity and shape-selectivity.[24,26,30-37] The major products were found to be hydrocarbons (mainly isobutylene), and it has been postulated that the formation of isobutylene is basically via a classic aldol condensation and further cracking of these condensation products (diacetone alcohol and mesityl oxide). However, the detailed mechanism has not been well established since the role of the condensation intermediates is not yet understood.

The role of aldol condensation products in acetone conversion over zeolite catalysts originated from the well known acid-catalyzed condensation reaction of acetone to mesitylene.[38] In this synthesis, R. Adams and co-workers used H_2SO_4 as a catalyst to obtain a 20% yield of mesitylene. But again, the reaction mechanism was incompletely understood. According to Whitemore,[39] mesityl oxide is produced primarily by condensation and quick dehydration as shown in scheme I. Therefore mesityl oxide was suggested to be the precursor of the mesitylene with isophorone as an intermediate. According to such a scheme, the production of some other aromatics and mono-olefins (C_2 and isobutylene) over heterogeneous zeolite catalysts of faujasites in 1972 has to be via a cracking reaction of mesityl oxide (MO).[40]

In 1981, Clarence D. Chang and co-workers of Mobil RD Corporation reacted acetone over ZSM-5 zeolite at 260-399^{0}C,[41] and significant amounts of acetic acid and isobutylene were produced in addition to the expected condensation products of acetone. Based on this evidence they believed that the cracking reactions had occurred, both acetic acid and isobutylene might be formed as a consequence of the cracking of diacetone alcohol (the primary condensation product without dehydration). In this mechanism (scheme II), C. D. Chang tried to explain the formation of mesitylene by isobutylene condensation-dehydrocyclization rather than via cyclization of isophorone as proposed by Whitemore.[36] However, neither experimental evidence nor further explanation about this isobutylene condensation-dehydrocyclization process were offered in their paper. We are of the opinion that this process, being so difficult, does not favor significant production of mesitylene over HZSM-5 under such conditions.

In C. D. Chang's work,[27] acetone conversion was 3.9% at 250^{0}C and 95.3% at 399^{0}C with a weight hourly space velocity (WHSV) of 8.0 h^{-1}. A significant amount of isobutylene was formed but the selectivity was low (19.1% and 3.6% at 250^{0}C and 399^{0}C respectively). The principal requirement of industrial catalysts is the preferential activation of those reactions that yield the wanted products, and the selectivity of a

Scheme I:

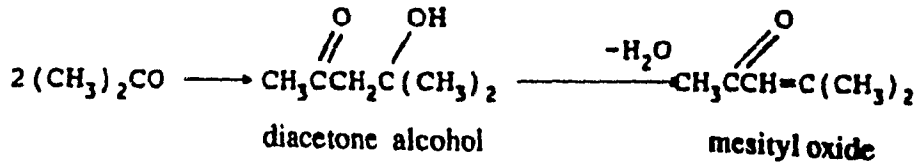

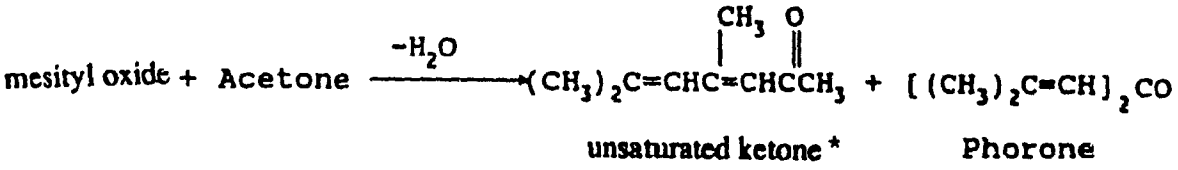

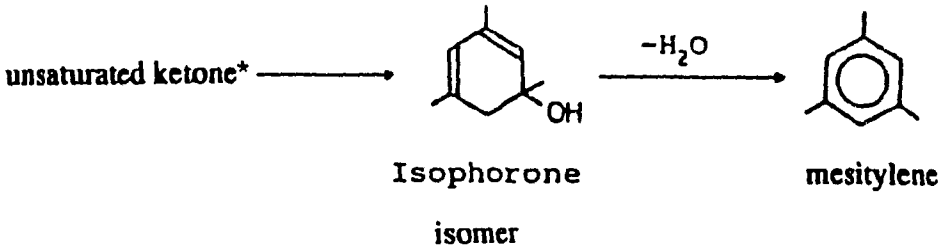

Scheme II:

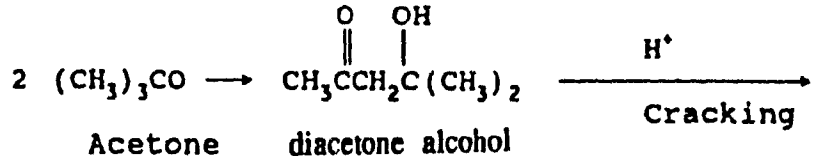

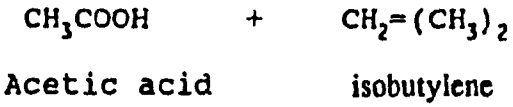

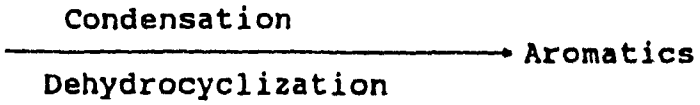

* 4,6 dimethyl hepta-3,5 diene-2 one.

Scheme III:

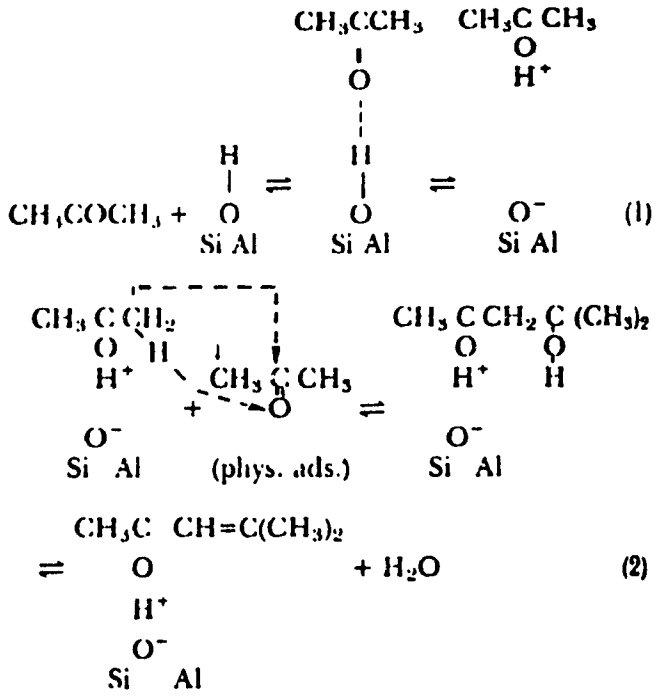
CH3CCH3
CH3C CH3
O
H+
H
O
Si Al
CH3COCH3 +
O⁻
(1)
CH3 C CH2
CH3 C CH2 C (CH3)2
O H
O O
H+
H+ H
CH3 C CH3
O⁻
O⁻
Si Al
(phys. ads.)
Si Al
CH3C CH=C(CH3)2
O
+ H2O
(2)
H+
O⁻
Si Al

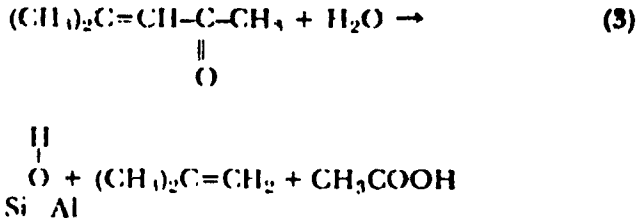
(CH3)2C=CH–C–CH3 + H2O →
O
(3)
H
O + (CH3)2C=CH2 + CH3COOH
Si Al

catalyst is often its most important property because it minimizes as much as possible the formation of by-products. Yet, no modification on these catalysts has been seen so far. Some results were obtained over Y zeolite (larger pore size than ZSM-5 zeolite) with a high production of isobutane.[8] But this reaction was accompanied by extensive coke formation and fairly rapid deactivation.[31,41]

More recently, Kubelkova and co-workers investigated the mechanism of formation of isobutylene over ZSM-5 at low temperature.[30,31,33-35,42] Based on the experimental evidence obtained with solid state NMR, FTIR and other surface techniques, they concluded that mesityl oxide was one of the intermediates in the acetone transformation. They demonstrated that acetone was converted at low temperature by zeolitic-bridging hydroxyls () to mesityl oxide, which then underwent further condensation and cracking between 150^{0}C and 250^{0}C, releasing mainly gaseous isobutylene (scheme III). However, according to McAllister mesityl oxide was not appreciably cracked in the absence of water.[43]

1.6 Effects of Water in the Feed

The effect of water has to be considered because feeds obtained from fermentation contain a large amount of water. One of the advantages of having water in the fermentation conversions is to prevent catalyst deactivation.[44] This beneficial effect of water takes place inside the zeolite pores and on the outer surface of HZSM-5, where coke formation is said to occur.[45] There is an equilibrium present between Bronsted-acid sites and Lewis-acid sites as in:

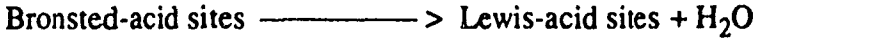

The presence of water in the feed decreases the rate of coke formation by shifting the dehydroxylation equilibrium to the left and decreasing the number of Lewis-acid sites

because the rate of coke formation is faster for Lewis-acid sites than on Bronsted-acid sites.[46] On the other hand, the possible interference of water with selective adsorption on active sites results in a partial inhibition of coke formation.[46] Furthermore, it is expected that the presence of water could affect the product distribution because production of hydrocarbons from oxygenates involves the dehydration process. But no investigation into this has been reported.

1.7 Objective of the Thesis

The objective of my research project was to attempt a direct conversion of bioacids to hydrocarbons (B.A.T.H. process), mainly isobutylene, using a reaction system of two catalytic reactors placed in series. Two catalysts, modified on the basis of the parent ZSM-5 zeolite catalysts, were prepared for the acetone conversion to isobutylene. Variations in reaction parameters, such as temperature, contact time and reactant concentration, were studied. A detailed examination of aqueous acetone conversion was made in order to elucidate the reaction mechanisms. The activation energy of the aqueous acetone conversion was determined.

1.8 Organization of the Thesis

The thesis is divided into four chapters.

In Chapter 1, the research work related to the subject of this thesis has been reviewed briefly. The appropriate background regarding the properties of the zeolites is also included in this Chapter.

The experimental details are given in Chapter 2.

The results of the thesis research are presented in Chapter 3.

Finally, the conclusion of this work is presented in Chapter 4.

CHAPTER 2 - EXPERIMENTAL

2.1 Chemicals

The chemicals used in the synthesis, preparation and characterization in this work were obtained from the suppliers as listed below,

CHEMICALS	GRADES	SUPPLIERS
Acetic Acid	reagent	Allied Chemical Ltd.
Acetone	reagent	Baker Analyzed Co.
Alumina Sulfate	reagent	The McArthur Chemical Co. Ltd.
Ammonium Chloride (99%)	reagent	Fischer Scientific Co.
Bentonite, U.S.P.	technique	Fischer Scientific Co.
Potassium Hydroxide	reagent	Fischer Scientific Co.
Silica gel (60-200 mesh)	technique	J. T. Baker Chemical
Sodium Aluminate	reagent	Anachemia
Sodium Hydroxide	reagent	Aldrich Chemicals
Tetrapropyl ammonium reagent		
Bromide (98%) (TPA)	reagent	Aldrich Chemicals
Trifluoromethane sulfonic acid	analytical	Fluka

2.2 Synthesis of Zeolite ZSM-5

The molecular shape-selective zeolites used as catalysts were synthesized by the following procedure:[47a] 110 grams of silica gel (pre-oven dried at 120^0C overnight), 110 grams of TPA (Br) and 7 grams of sodium hydroxide were dissolved in 250 ml of distilled water pre-heated to 80^0C. After 1 hour of stirring, a solution of 13 grams of sodium aluminate in 50 ml H_2O was added and mixed for another 15 minutes. The resulting gel-like mixture was introduced into the autoclave and heated under self-

induced pressure to 170^{0}C for 10 days, after which the liquid was filtered and the crystalline product was rinsed with 4 l of H_2O and dried at 120^{0}C overnight. The sample was then calcined at 550^{0}C overnight in order to decompose the organic ammonium ions. This procedure is designed to produce the sodium form of the ZSM-5 zeolite with a Si/Al ratio of 18 and XRD analysis of this sodium form showed that the product was crystalline and in good agreement with those found in the literature for the ZSM-5 zeolite structure.[47] To get the protonic form, the NaZSM-5 was ion-exchanged with a 10 wt% aqueous NH_4Cl solution at 80^{0}C for 3 hours. After repeating this exchange procedure five times, the formation of NH_4ZSM-5 was considered complete and the sample was then calcined at 550 ^{0}C overnight, which produced the a form of the zeolite, HZSM-5.

2.3 Other Treatments on ZSM-5

2.3.1 TFA Super Acid Loading

0.2 gram of trifluoromethane sulfonic acid (TFA) was dissolved in 15 ml of pure acetone and the resulting solution was slowly added to 10 grams of HZSM-5 zeolite while stirring. The sample was dried in air for 1 hour and then in an oven at 120^{0}C overnight to completely evaporate the solvent. This zeolite, with a 2 wt% super acid loading, was then ready for use.

2.3.2 Realumination

In order to insert alumina into the zeolite framework, "realumination" was performed: 80 ml of aqueous KOH solution containing 24 grams of aluminum sulfate $Al_2(SO_4)_3$ was allowed to contact with 10 grams of HZSM-5 zeolite at 80^{0}C for 3 hours. The mixture was filtered and the solid washed with double deionized water until the pH value of the washing solution was nearly neutral. The sample was then washed with 80

ml of 0.2N HCl and ion-exchanged with 10 wt% aqueous NH_4Cl solution as explained earlier in section 2.2. The dried sample was finally calcined at 550^0C overnight.

2.4 Preparation of Extrudates

Zeolite ZSM-5 in extrudate form was used as a catalyst in order to prevent any serious pressure drop in the reactor, which would occur if the powder form were used. The extrudates were made of 20% bentonite and 80% zeolite powder. Bentonite is a mineral clay and is believed to be just a binder which does not affect the catalyst activity.[47b] About 0.6 ml distilled water per gram of this powder mix was used to make the paste which was extruded into small catalyst extrudates (2 mm in diameter) from a 3 ml plastic syringe. After drying at 120^0C overnight, the extrudates were cut into short pieces (4 mm) manually.

2.5 Physical and Chemical Characterization

2.5.1 Atomic Absorption Spectroscopy

Atomic absorption spectroscopy was used to determine the zeolite's elemental composition.

0.1 gram of zeolite contained in a platinum crucible was placed in the oven at 750^0C for 1 hour. After cooling to room temperature, 0.9 gram of the fusion mixture (potassium carbonate and lithium tetraborate in ratio 2:1) was added into the sample and mixed gently. The sample was replaced in the oven at 750^0C for another 45 minutes. 10 ml of 10 wt% sulfuric acid and 4 ml of concentrated HCl were used to dissolved the zeolite, and 4 ml of hydrogen peroxide (30%) was added to remove oxygen. The resulting solution was diluted to 100 ml. The intensity measurements were taken from a Perkin Elmer Model 503 Atomic Absorption Spectrophotometer and concentration

calculations were obtained using external standards (NaCl and $AlCl_3$ were used for Na^+ and Al^{3+} respectively).

Two chemical characteristics were obtained from the atomic absorption results:

(1) the Si/Al ratio was calculated from SiO_2 and Al_2O_3 contents by the equation:

$$\frac{Si}{Al} = \frac{Moles(SiO_2) \times MW(Si)}{2 \times Moles(Al_2O_3) \times MW(Al)}$$

(2) the sodium content was taken directlyfrom the sodium oxide measurement.

2.5.2 Powder X-ray Diffraction

X-ray powder diffraction was used for the characterization of the solid isolated from the synthesis. The most significant information obtained from such a technique includes:[11]

1. Confirmation of the formation of a crystalline material;
2. Presence of a single phase or mixture of phases;
3. The identification of the structure type, if sufficient peaks are obtained;
4. The level of crystallinity obtained from that synthesis batch compared to a standard sample (degree of crystallinity, DC).

Powder X-ray diffraction patterns of the zeolites were recorded on a Philips X-ray powder diffractometer automated by a Sietronics (Sie 112) with a Micro Powder diffraction search by the March System (JCPDS file) obtained from Fein Marquat. The goniometer scan parameters are shown in Table 2.1.

Table 2.1 X-ray scan parameters

Start 2-THETA Angle	22 Degrees
End 2-THETA Angle	33 Degrees
Step size	0.02 Degrees
Tube type, Lambda	Cu, 1.5418
Scan Speed	0.5 Degrees/minute

Table 2.2 Chemical composition and degree of crystallinity of the parent zeolites

Catalysts	Al_2O_3 (%)	Na_2O (%)	SiO_2 (%)	Others[a] (%)	Si/Al (%)	DC (%)
HP-(18)	4.67	0.10	95.23	0	18.0	100
HP-(45)	1.93	0.17	97.90	0	44.7	98
HA-(15)	5.24	0.16	89.06	5.64	15.0	92
HP-(21)	4.00	0.30	95.70	0	21.1	108
HP-(19)	4.33	0.20	95.47	0	19.4	106
HP-(24)	3.54	0.38	96.08	0	23.9	95
HP-(20)	4.26	0.42	95.32	0	19.7	100

[a] MgO plus Fe_2O_3

The samples were prepared for the X-ray diffractometer by the following methods. 200 mg. of zeolite sample and 40 mg. NaCl (internal standard) were intimately mixed and spread on a glass microscope slide (which acted as sample holder). A typical diffraction pattern thus recorded is shown in Figure 2.1. For the determination of the DC, a selected crystalline reference sample (the most crystalline sample available) was assigned a degree of crystallization of 100%. We determined the largest relative intensity to that of NaCl, I_0 (ca $2\theta = 23.25^0$). The same procedure was then applied to the sample being studied, with I being the largest relative intensity to that of NaCl. The DC is then obtained as a percentage using the following expression:

$$DC\% = \frac{I}{I_0} \times 100\%$$

This technique has the advantage of being totally independent of the homogeneity of the sample coat on the sample holder.

The chemical compositions and the DC of synthesized zeolites are listed in Table 2.2.

2.5.3 Magic Angle Spinning NMR

^{29}Si, ^{27}Al and ^{1}H NMR results have been used in order to provide useful information about the structural features of the ZSM-5 zeolite. These characteristics were then related to the catalytic activity of the material.

All solid state NMR spectra of ^{29}Si, ^{27}Al and ^{1}H were recorded at 59.592, 78.159 and 299.95 MHz respectively on a VARIAN VXR 300 FT-NMR spectrometer (Universite de Montreal), equipped with KEL-F Doty solid-state probes. The ^{27}Al, ^{29}Si and ^{1}H chemical shifts are in ppm and relative to the external $Al(H_2O)_6^{3+}$ and TMS respectively. The spinning rate for ^{29}Si was 4680 Hz.

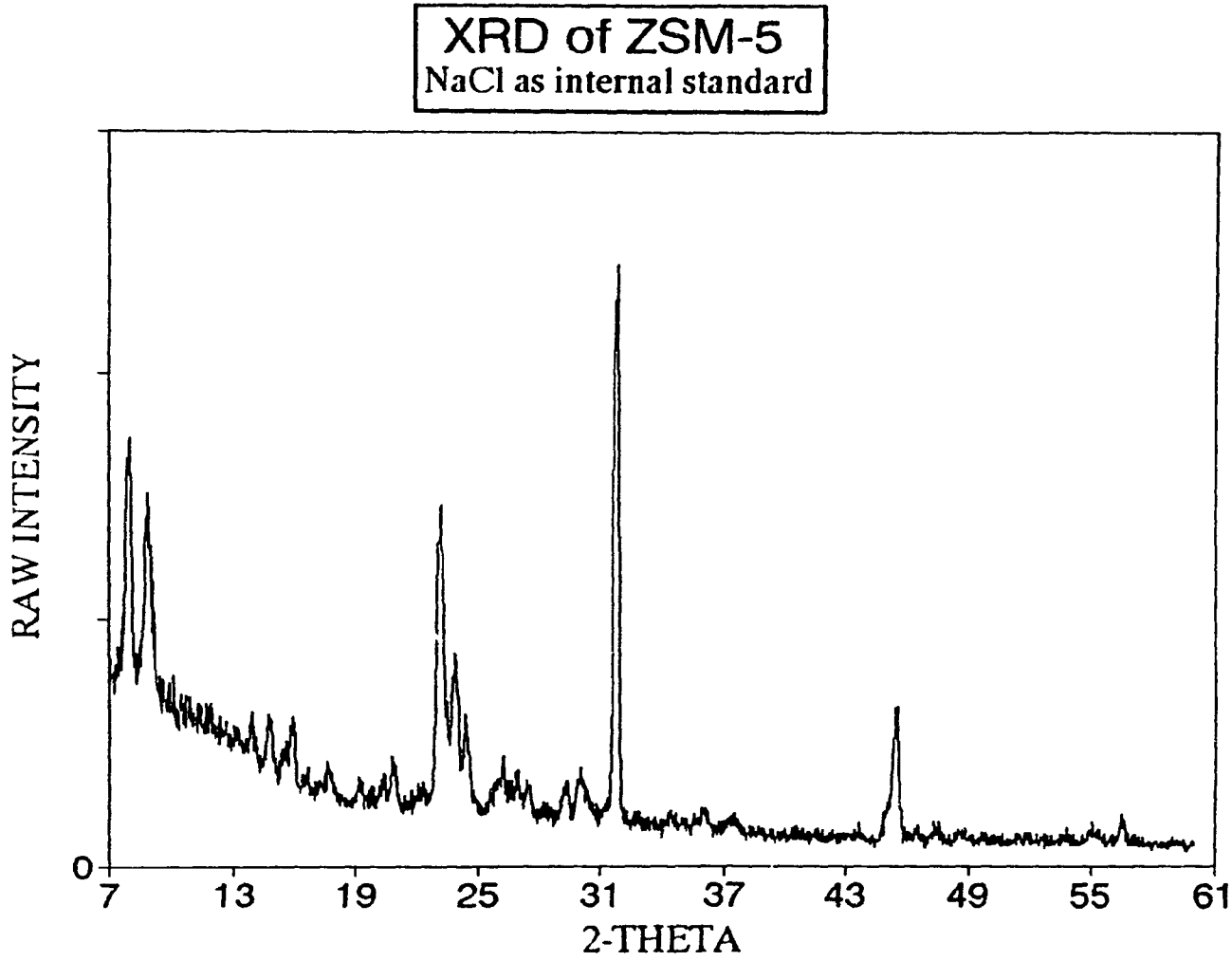

Figure 2.1a Typical X-ray diffraction pattern of ZSM-5 with internal standard of NaCl: before the baseline subtraction

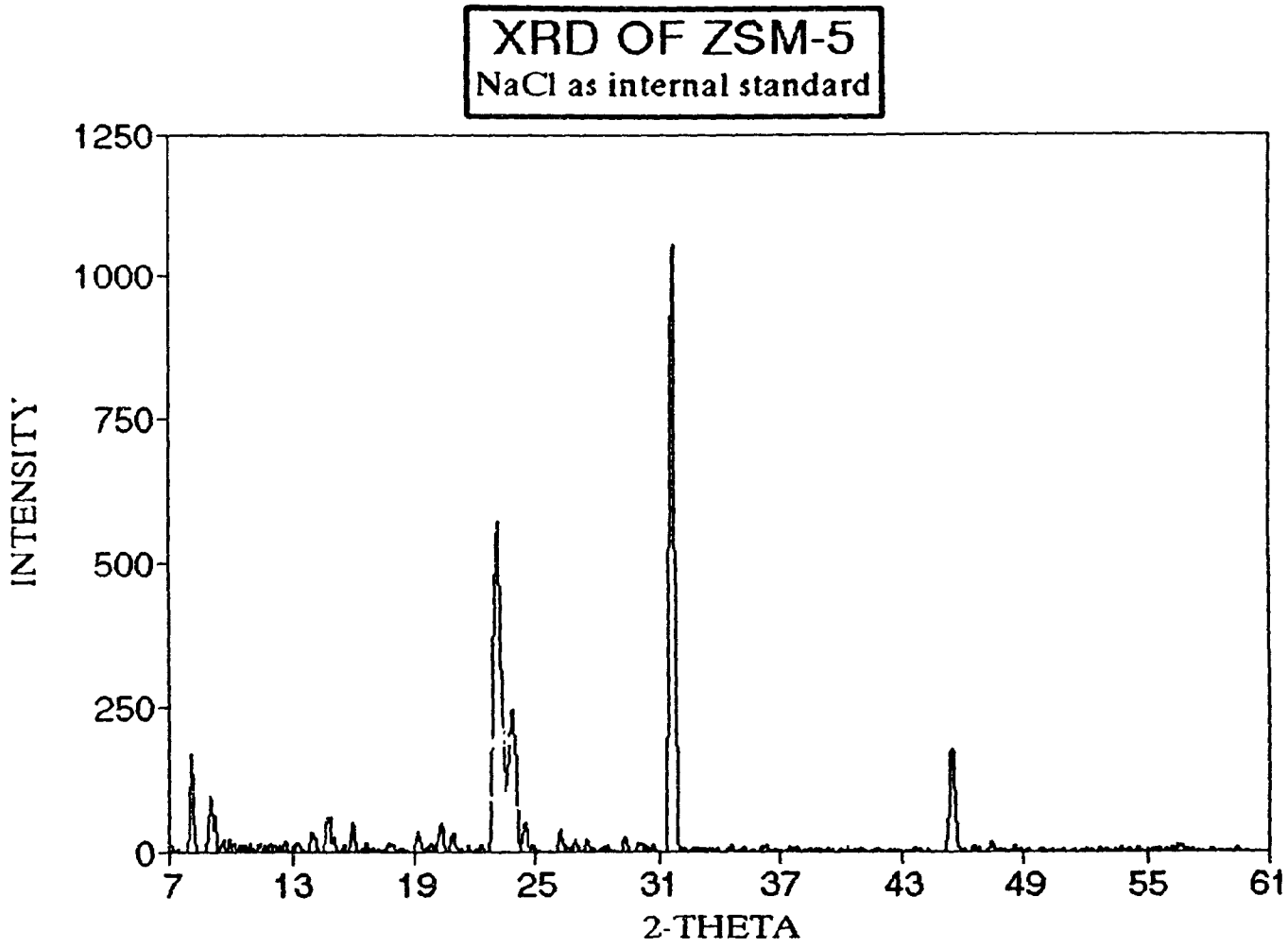

Figure 2.1b Typical X-ray diffraction pattern of ZSM-5 with internal standard of NaCl: after the baseline subtraction

2.5.4 Surface Area Measurement (BET)

Zeolites are porous materials with the pore structure and the total surface area being related to each other. Both the total surface area and the pore size distribution can be determined from physical sorption measurements.

The surface area of a powder zeolite was measured by a Micromeritics ASAP 2000 surface area & porosimetry Instrument. About 0.5 grams of powder sample was used for each test. Sample degassing, calibration of the dead volume and nitrogen adsorption isotherms were performed automatically. Both the surface area and porosity distribution were obtained in a single operation.

2.5.5 Infrared Measurements (FT-IR)

The IR spectra were recorded on a Bomem Michelson-102, FT-IR Spectrometer at room temperature and atmospheric pressure using the reflectance technique. To minimize the interference of water, the sample was calcined at 550^0C and dehydrated under vacuum at 350^0C immediately before taking the measurement. These procedures were carried out at 150^0C for samples loaded with TFA in order to prevent any acid loss.

2.5.6 Thermogravimetric and differential Thermal Analyses (TGA - DTA)

In order to determine the thermal stability of the incorporated TFA surface species, TGA-DTA scans were recorded on a Setaram B70 TGA/DTA apparatus both in the presence of air and argon. The scan temperature ranged from room temperature to 575^0C.

2.5.7 Temperature Programmed Desorption of Ammonia (TPD - NH_3)

The temperature programmed desorption of ammonia was used to study the total acidity (acid density) and the acid strength distribution of both parent zeolite and realuminated ZSM-5 samples. The TPD-NH_3 experiments were performed according to

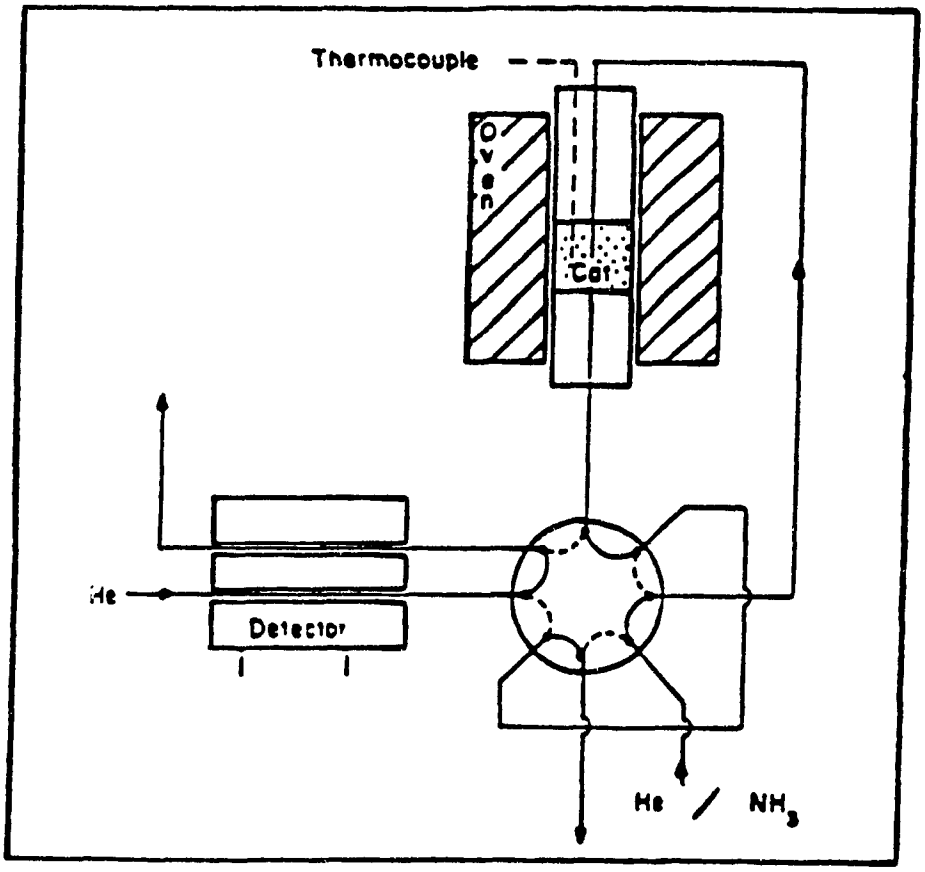

Figure 2.2 TPD-NH_3 apparatus

the technique described by Le Van Mao and co-workers,[48] using the apparatus shown schematically in Figure 2.2. Ammonia TPD spectra were recorded with a conventional TPD experimental set-up. The temperature of the furnace was monitored with a multi-program controller. Desorbed ammonia molecules were quantitatively detected with a gas-chromatograph equipped with a thermal conductivity detector (TCD, Perkin Elmer F11 Model) and a Hewlett-Packard 3392 A integrator. In a typical run, 1.0 g of pellet sample was placed in a small quartz tube and heated to 540^0C over helium (flow rate of 20 ml/min) for 10 hours. The temperature was lowered to 100^0C and the catalyst sample was exposed to ammonia (previously dried over calcium chloride) with a flow-rate of 20 ml/min for 40 minutes. The sample was then flushed for another 40 minutes with helium (20 ml/min) to remove ammonia molecules that might be physically adsorbed onto the zeolite surface. Under this condition, the desorption was done with the programmed temperature increasing from the initial temperature of 100^0C to a final temperature of 600^0C. The amount of the ammonia desorbed, based on TCD signals, was obtained from calculations against an external standard obtained by the injection of a specific amount of ammonia into the gas chromatograph.

2.6 Testing of Catalyst Activity

There are four factors which are important in considering a useful catalyst. (1) activity, (2) selectivity, (3) life and (4) cost. The objective of catalyst testing in the laboratory is to define the first three factors.

All the runs for catalyst testing were carried out on a fixed bed, continuous plug-flow reactor, made of quartz, which has the following dimensions: diameter = 30 mm and, length = 300 mm. The length of the catalyst bed is 40 mm (weight of catalyst = 4 grams).

Figure 2.3 is the schematic diagram of the experimental set-up. The reactor was placed in an electric furnace and the reactants were introduced into a vaporizer-gas mixer

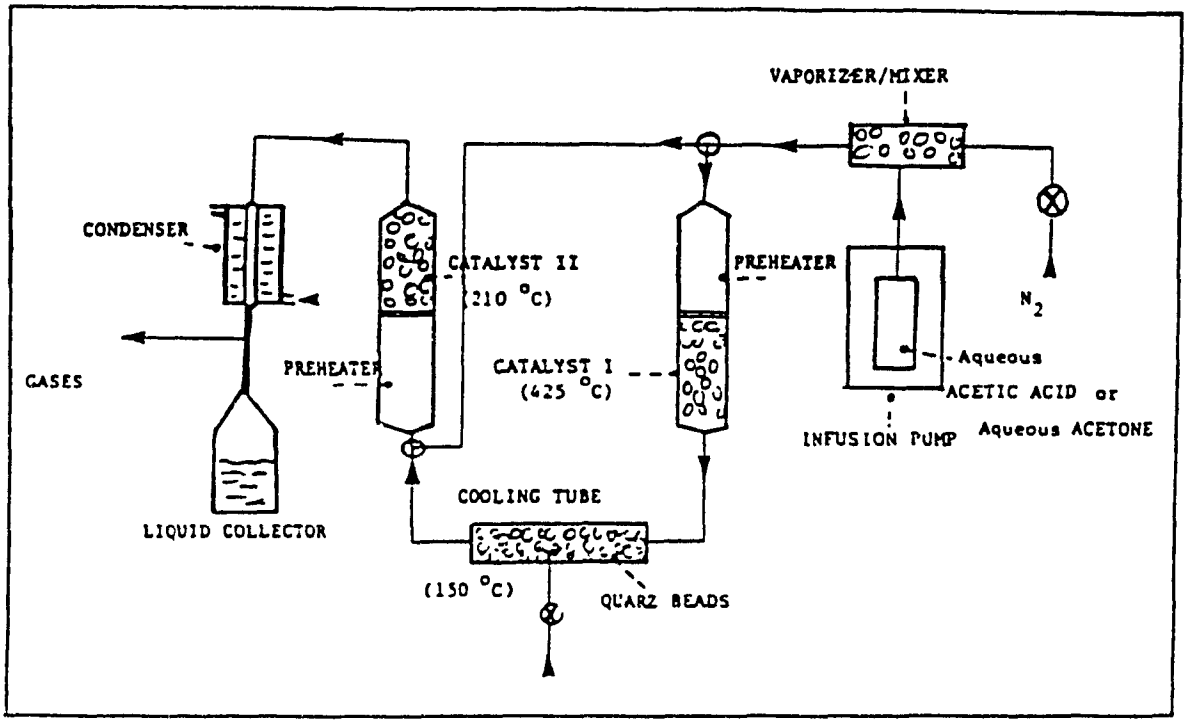

Figure 2.3 Schematic diagram of experimental set-up for acetic acid or acetone conversion

through a syringe-type pump. Nitrogen gas (carrier gas) was led to the vaporizer-gas mixer at a fixed flow rate (20 ml/min). The temperature of the catalyst bed was read from a digital thermometer unit (built by the Concordia workshop) equipped with a thermocouple placed on the catalyst bed. The liquid products were collected in an ice bath trap and gaseous products were analyzed quantitatively by gas chromatography, using a 1/8" diameter x 3 m long stainless steel column packed with chromosorb-P coated with 20 wt% of squalane. A PONA column (from Hewlett-Packard) was utilized for analyzing the liquid phase after each run. Both columns were used in a Hewlett-Packard model HP-5890A gas chromatograph equipped with a flame-ionization-detector. The temperature of the columns was program-controlled. The data were processed in an integrator-recorder (Hewlett Packard 3392A). The calculations are done according to the following procedures.

(i) Acetic acid to acetone

The total conversion of the reaction was calculated by the following expression:

$$\text{Total (\%)} = \frac{(\text{Acetic acid})_{in} - (\text{Acetic acid})_{out}}{(\text{Acetic acid})_{in}} \times 100$$

where $(\text{Acetic acid})_{in}$ and $(\text{Acetic acid})_{out}$ are the number of carbon atoms (C-atoms) of acetic acid in the feed and acetic acid recovered in the outstream, respectively.

The number of carbon atoms of a organic compound was determined by the expression:

$$\text{C-atom} = \frac{(\text{Weight Injected})}{(\text{Molecular weight})} \times (\text{N-carbon})$$

where N-carbon is the number of carbons in the structure.

The conversion to acetone was calculated by:

$$\text{Acetone \%} = \frac{(\text{Acetone})_{out}}{(\text{Acetic acid})_{in}} \times 100$$

where $(\text{Acetone})_{out}$ is the C-atoms of acetone recovered in the product.

The conversion to hydrocarbons, HC, was calculated by:

$$\text{HC \%} = \frac{(\text{Acetic acid})_{in} - (\text{Acetic acid})_{out} - (\text{O-compounds})_{out}}{(\text{Acetic acid})_{in}} \times 100$$

or

$$\text{HC \%} = \frac{\text{HC}}{(\text{Acetic acid})_{in}} \times 100$$

where $(\text{O-compounds})_{out}$ is the C-atoms of the product oxygenated compounds such as acetone and alcohols and HC is the hydrocarbon yield. The hydrocarbon selectivity to the reaction product "i" was defined as follows:

$$\text{Selectivity } (\%)_i = (Y_i/\text{HC}) \times 100$$

where Y_i is the yield of the product "i".

(ii) Acetone to Isobutylene and Other Hydrocarbons

The total conversion of the reaction is expressed as follows:

$$\text{Total (\%)} = \frac{(\text{Acetone})_{in} - (\text{Acetone})_{out}}{(\text{Acetone})_{in}} \times 100$$

where $(\text{Acetone})_{in}$ and $(\text{Acetone})_{out}$ are the number of carbon atoms (C-atoms) of acetone in the feed and acetone recovered in the outstream, respectively.

The conversion to hydrocarbons, HC, was calculated by:

$$\text{HC \%} = \frac{(\text{Acetone})_{in} - (\text{Acetone})_{out} - (\text{O-compounds})_{out}}{(\text{Acetone})_{in}} \times 100$$

or

$$\text{HC \%} = \frac{\text{HC}}{(\text{Acetone})_{in}} \times 100$$

where $(\text{O-compounds})_{out}$ is the C-atoms of product oxygenated compounds such as acetic acid and mesityl oxide and HC is the hydrocarbon yield.

The definitions of the number of carbon atoms of an organic compound and the product selectivity of the reaction product "i" are the same as those in (i).

The reaction conditions used in this experiment were as follows:

Temperature	160 - 450^{0}C
Weight of catalyst	1 - 4 g
System pressure	1 atm.
Flow rate of inner gas	20 ml/min
Weight hourly space velocity	0.008 - 0.50 h^{-1}
Duration of run	200 mins.

The effect of the reaction temperature was thoroughly investigated. Kinetic studies involve the determination of the reaction rate constant k, which depends on several operating variables such as the temperature , as well as, the state of the catalyst. The effect of temperature on the rate constant is described by the Arrhenius exponential law:

$$k = A \exp\left(-\frac{E}{RT_{rea}}\right)$$

where

A is the frequency factor,

E is the activation energy expressed in cal/mol, which is always positive,

T_{rea} is the absolute temperature of the reactor.

Thus, the reaction rate constant is influenced by the temperature of the reactor which affects the conversion of the feed into other products.

The weight hourly space velocity (WHSV) is directly connected with the contact time which is measured by the ratio of the weight of catalyst to the weight flow rate of the feed. This ratio is in fact a fairly approximate measure of the time of contact between the reactant and the catalyst bed. The contact time is directly proportional to the amount (weight) of the catalyst and inversely proportional to the feed flow rate. In industrial practice, the WHSV is commonly used. This key operating variable is therefore expressed as grams of feed processed per hour per gram of catalyst used:

$$WHSV = \frac{\text{Flow rate (gram/hour)}}{W_{cat}\text{ (gram)}}$$

The data for reproducibility are given in Appendix I.

CHAPTER 3 - RESULTS AND DISCUSSION

3.1 Aqueous Acetic Acid Conversion

As mentioned earlier, it has been demonstrated that acetic acid conversion over a base catalyst, such as an alkaline metal ion-exchanged zeolite and supported alkaline earth oxide produces significant amounts of acetone,[28,29] while over an acid catalysts it produces isobutylene.[27] However, nothing was mentioned about the conversion of very dilute aqueous acetic acid solutions. For this reason, three types of catalysts including CaO, HZSM-5 and CaY embedded within a clay (bentonite) matrix have been used to examine the feasibility of conversions using a very dilute aqueous acetic acid solution. The results are reported as total conversion and product selectivity of which the latter represents the selectivity of each product expressed in carbon atom percent. The hydrocarbon distribution is reported as the selectivities to various hydrocarbon fractions expressed in carbon atom percent and the total conversion is also expressed in carbon atom percent.

3.1.1 Activity of CaO

CaO, like other metal oxides, has been used as a strong base catalyst for the conversion of acetic acid into acetone. Results with 10 wt% aqueous acetic acid solution are listed in Table 3.1. Experiments were carried out at 400^{0}C, 425^{0}C and 450^{0}C, respectively. At each temperature, three different weight hourly space velocities (WHSV) were used.

The products were mainly acetone and carbon dioxide with small amounts of hydrocarbons. The carbon selectivity to acetone was much higher than that to hydrocarbons (Which is less than 1% in all cases). Therefore, we consider acetone as the major product in the conversion of very dilute aqueous acetic acid solutions. In order to

Table 3.1 Conversion of aqueous acetic acid (10 wt%) over CaO catalyst at various temperatures and WHSVs

Temp. (^{0}C)	WHSV (h^{-1})	Total Conversion (C-Atom %)	Product Selectivity (C-atom %)				
			Acetone	Hydrocarbons	Other	O-compounds[a]	CO_2+CO
450	0.06	100	40.8	0.4		3.2	55.6
	0.14	97.6	68.6	0.2		4.9	26.3
	0.20	95.8	71.7	0.1		4.1	24.1
425	0.05	100	63.8	0.3		0	35.9
	0.12	97.0	69.6	0.1		0	30.3
	0.24	92.4	63.0	0.1		0	36.9
400	0.05	100	62.4	0.9		0	36.7
	0.13	92.5	58.6	0.3		0	41.1
	0.22	81.1	61.8	0.1		0	38.1

[a] Acetate-like species

obtain optimum reaction conditions, the effects of temperature and contact time on the conversion were studied and the results are presented below.

In Figure 3.1 a - c, the effect of the reaction temperature on the conversion of 10 wt% aqueous acetic acid solution over a CaO catalyst is shown. Total conversion, and carbon selectivity to acetone and carbon dioxide, are plotted in Figures 3.1a 3.1b and 3.1c for WHSV of 0.22, 0.13 and 0.05 h^{-1} respectively. The total conversion of acetic acid was consistently high and increased with increasing temperature. For longer contact times, the conversion attained practically the 100% level. Carbon selectivities to acetone, carbon dioxide and monoxide showed different variation patterns with temperature. They also exhibited some dependence on the contact time. The major hydrocarbon product was methane which appeared in small amounts in all cases, implying that some thermal cracking of acetic acid had occurred.[28] The acetate species in O-compounds were found in small amounts (Table 3.1) and probably the intermediates in the formation of acetone, according to the alternative mechanism proposed by Parker and co-workers.[26] Part of the carbon dioxide evolution was also due to the thermal cracking and decomposition of acetic acid:

$$\underset{\text{(acetic acid)}}{CH_3COOH} \longrightarrow \underset{\text{(carbon dioxide)}}{CO_2} + \underset{\text{(methane)}}{CH_4}$$

In fact, at constant temperatures, the total conversion of acetic acid increased with increasing contact time (Figure 3.2). The carbon selectivity to acetone varied differently with contact time depending on the reaction temperature. At 400^0C and 425^0C, it was found to be almost constant. At 450^0C, more carbon dioxide was produced at the expense of acetone mostly at longer contact times, indicating that some acetone had been converted to carbon dioxide through a secondary reaction.

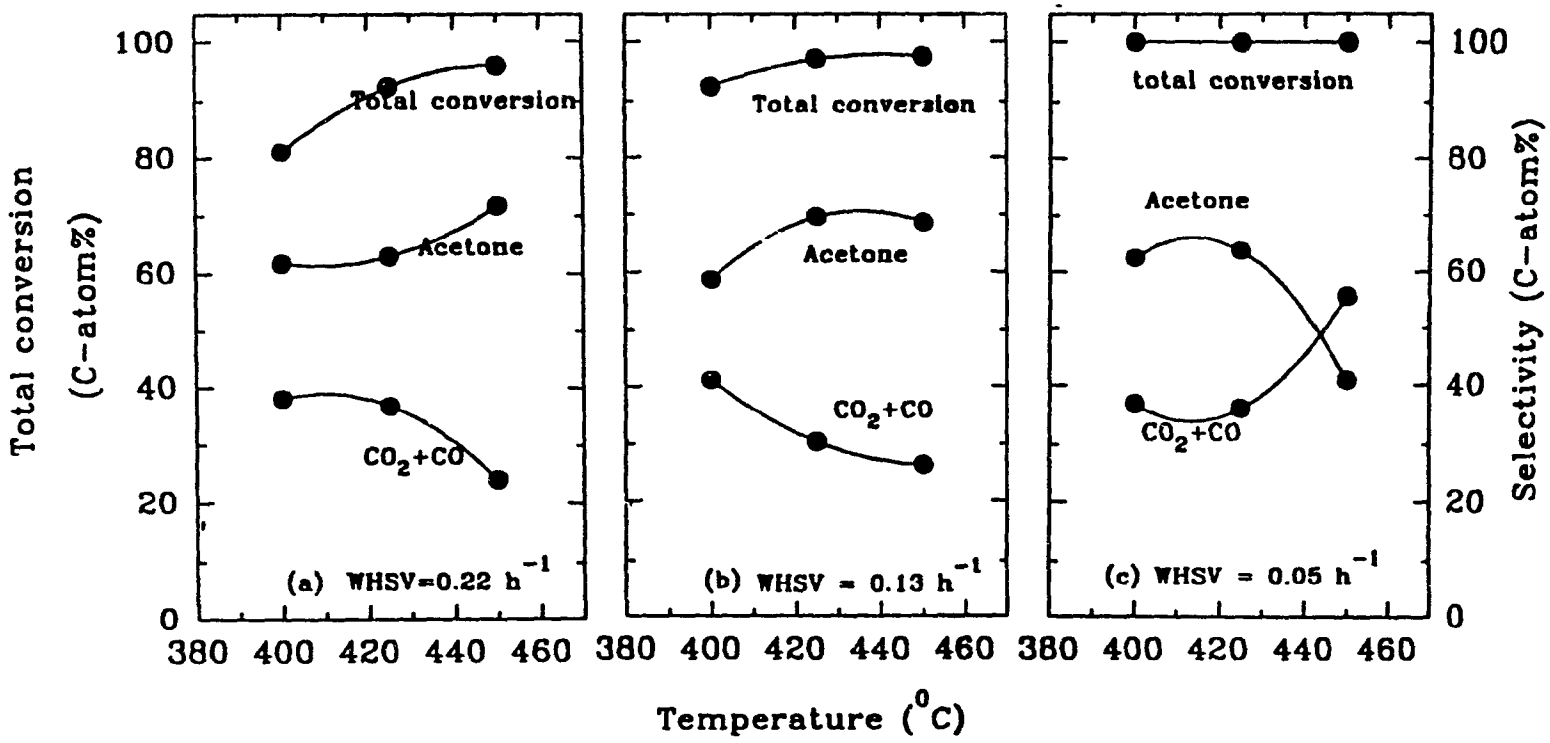

Figure 3.1 Effect of temperature on aqueous acetic acid (10 wt%) conversion over CaO catalyst at: (a) 0.22 h^{-1}, (b) 0.1 h^{-1}, and (c) 0.05 h^{-1}

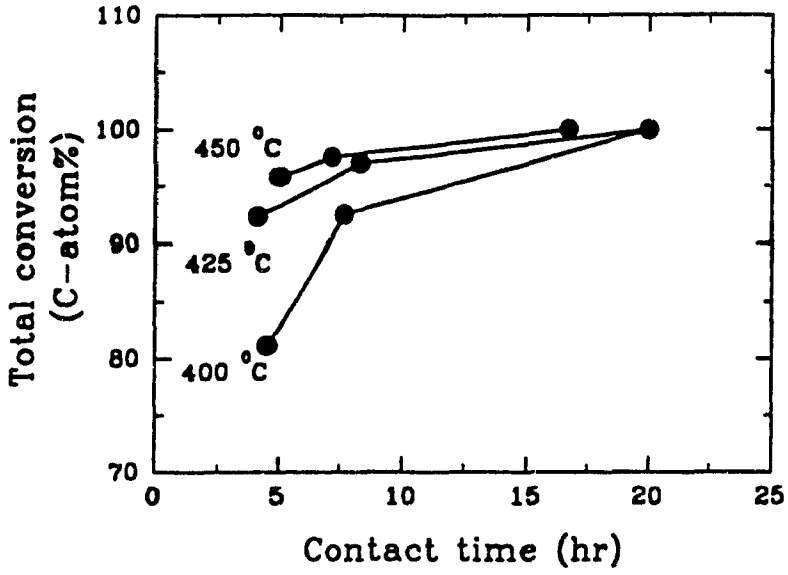

Figure 3.2 Effect of contact time on total conversion of aqueous acetic acid (10 wt%) over CaO catalyst

However, a crossing effect of temperature and contact time shows that at higher temperature and shorter contact time (or larger WHSV), the production of acetone was favoured over that of carbon dioxide and monoxide. Therefore, the optimum conditions for acetone production from the 10 wt% aqueous acetic acid solution were as follows:

temperature = 450^0C, and

WHSV = 0.2 h^{-1}.

3.1.2 Activity of Ca-Y Zeolite

The results of aqueous acetic acid (10 wt%) conversion over Ca-Y catalyst are listed in Table 3.2. The reactions were carried out at 400^0C, 425^0C and 450^0C using a constant WHSV of about 0.5 h^{-1}.

Comparing these results obtained over CaO catalyst (Table 3.1), the total conversion and the conversion to acetone were both lower. Carbon dioxide was produced in fairly large amounts due to the thermal cracking and decomposition of acetic acid.[34] This also led to significant production of hydrocarbons mostly at higher temperature.

Y zeolite belongs to the faujasite family of low-silica zeolites having 12-membered rings as basic units. Therefore, HY zeolite has a weaker surface acidity and larger pore size than that of the HZSM-5. Ca-Y, an alkaline metal-exchanged zeolite, normally exhibits basic surface property.[28] But, some Bronsted-acid sites may be generated on the zeolite surface by hydrolysis of the Ca^{2+} in the same manner as La^{3+}:[49]

$$Ca^{2+} + H_2O \longrightarrow Ca(OH)^+ + H^+$$

Table 3.2 Conversion of aqueous acetic acid (10 wt%) over Ca-Y catalyst at various temperatures

Reaction Conditions			
Temp (^{0}C)	400	425	450
WHSV (h^{-1})	0.06	0.06	0.04
Conversion (C-Atom%)	71.5	72.6	93.1
Carbon Selectivity (C-Atom%)			
Acetone	7.6	7.7	5.6
Other O-compounds	3.6	1.9	1.7
Hydrocarbons	16.3	11.7	29.4
CO_2+CO	72.5	78.7	63.3
Hydrocarbon Distribution (C-Atom%)			
Isobutylene	9.2	7.6	4.2
Other C_2 -C_4 Olefins	25.7	26.3	18.4
C_1 -C_4 Paraffins	59.1	55.2	49.3
C_5^+ Aliphatics	2.5	0	0
Aromatics	3.5	10.9	28.1

Table 3.3 Conversion of aqueous acetic acid (10 wt%) over HZSM-5 catalyst at various temperatures

Reaction Conditions			
Temp (^{0}C)	275	333	406
WHSV (h^{-1})	0.18	0.19	0.20
Conversion (C-Atom%)	2.9	17.7	70.7
Carbon Selectivity (C-Atom%)			
Acetone	0	11.8	5.6
Hydrocarbons	48.7	18.8	41.9
CO_2+CO	51.3	69.4	52.5
Hydrocarbon Distribution (C-Atom%)			
Isobutylene	0	27.8	19.5
Other C_2 -C_4 Olefins	0	49.6	60.9
C_1 -C_4 Paraffins	78.4	1.7	3.3
C_5^+ Aliphatics	0	1.1	6.3
Aromatics	21.6	19.8	10.0

3.1.3 Catalytic Activity of the ZSM-5 Zeolite

According to the results obtained by C. D. Chang, acetic acid over acidic ZSM-5 catalysts could produce isobutylene and a small amount of acetone.[27] With very dilute acetic acid aqueous solution (10 wt%), the results obtained with the HZSM-5 zeolite catalyst having a Si/Al ratio of 18 are reported in Table 3.3. The reaction was carried out at 275^{0}C, 333^{0}C and 406^{0}C respectively, using a WHSV of about 0.19 h^{-1}. The total conversion was 2.9%, 17.8% and 70.7% at 275, 333 and 406^{0}C respectively, showing that the conversion increased with increasing temperatures.

On the other hand, the isobutylene selectivity was found to be 0%, 27.8% and 19.5% at 275, 333 and 406^{0}C respectively with the highest value at 333 ^{0}C. The carbon selectivity to acetone was found to be 0%, 11.8% and 5.6% with the highest value obtained at 333^{0}C. But the total conversion at this temperature was low (17.7%).

Large amounts of carbon dioxide were produced, and this was partially due to the thermal cracking of acetic acid. Such an explanation is supported by the fact that methane was found in the C_1-C_4 paraffins. Furthermore, the decomposition of acetic acid itself normally produces CO_2.

As mentioned in the introduction, activity and selectivity are two important properties of industrial catalysts. At low temperatures, the activity of the catalyst was low, resulting in the low conversions. At 406^{0}C the conversion increased to 70.7%, however, the selectivities for both isobutylene and acetone were rather low.

Compared to the results obtained by C. D. Chang,[27] the carbon distribution in our tests was similar, implying similar pathways for both reactions. This leads to the assumption that acetone is formed by the zeolite catalyzed ketonization of acetic acid[50], whereas isobutylene is formed by the aldolization of acetone and cracking reactions. This will be further discussed in section 3.2.

3.1.4 Reaction Mechanism

Through the results obtained with CaO, Ca-Y and HZSM-5 catalysts, it is found that a high yield of acetone from very dilute aqueous acetic acid conversion can be obtained over CaO catalyst, indicating that the conversion of acetic acid to acetone is base catalyzed. According to the mechanism proposed by S. Sugiyama,[29] the formation of acetone and carbon dioxide arises from the decomposition of alkaline earth acetate intermediates. The first stage of decomposition produces acetone and carbonate which is subsequently converted into the acetate by displacement desorption of carbon dioxide in the presence of acetic acid. Based on the above hypothesis, we assume that in our case also, acetone is produced from acetic acid with calcium carbonate as intermediates. This is expressed in the following scheme.

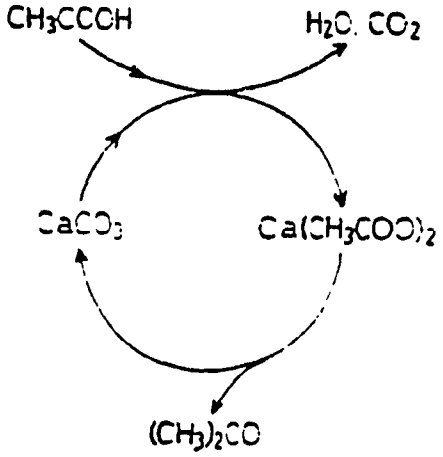

The reactions involved are:

$$CaO + 2CH_3COOH \longrightarrow Ca(OCOCH_3)_2 + H_2O$$

$$Ca(OCOCH_3)_2 \longrightarrow CaCO_3 + (CH_3)_2CO$$

$$CaCO_3 + 2CH_3COOH \longrightarrow Ca(OCOCH_3)_2 + CO_2 + H_2O$$

3.2 Conversion of Aqueous Acetone to Isobutylene

The conversion of aqueous acetone to isobutylene is the final step in the production of isobutylene from aqueous acetic acid. Much work has been done with pure acetone over ZSM-5 zeolite catalysts, and it was recognized that the products included acetic acid, other o-compounds, carbon dioxide and monoxide, and hydrocarbons (mainly isobutylene).[27,30,31,33-35,42] Untill now the study of these reactions has not been done with very dilute solutions.

In our work, the activities of the parent and chemically treated ZSM-5 zeolite catalysts were studied using very dilute aqueous solutions of acetone. These results are reported in the following sections, and expressed as product selectivity which is the selectivity of each product in carbon atom percent. The total conversion is also given in carbon atom percent.

3.2.1 Catalytic Activity of the ZSM-5 Type Zeolites

Previous results on acetic acid conversion with HZSM-5 did not indicate advantages for acetone production, since HZSM-5 is a strong acid catalyst and the process is base catalyzed. However, it is well known that acid catalysts can promote aldol condensation of acetone and further cracking.[14] Therefore, our work on aqueous acetone began with ZSM-5 zeolites. The study covered many aspects of catalysis including the intrinsic properties of the catalyst and the reaction conditions such as temperature and contact time.

3.2.1.A Effects of Chemical Composition

Many properties of zeolites, such as surface acidity, are affected by their chemical composition. The effects of chemical composition were examined in this work since the acidity is very important to the reaction being studied.

(1) Si/Al Ratio of Zeolite ZSM-5

As mentioned earlier, framework Al content influences the acidity of zeolites. The conversion of aqueous acetone (5 wt%) was studied over HZSM-5 with Si/Al ratios of 18 and 45 at both 270^0C and 300^0C using a WHSV of 0.1 h^{-1}.

The results are reported in Table 3.4. At the temperature of 270^0C, the total conversion and the selectivities to hydrocarbons and isobutylene are higher over HZSM-5(18) than those over HZSM-5(45), indicating that the formation of isobutylene in particular was favoured by the greater amount of acidic sites on the catalyst surface provided by a lower Si/Al ratio.

At the higher temperature of 330^0C, however, selectivity to isobutylene over HZSM-5(18) was lower than that over HZSM-5(45), which produced more light paraffins and C_5^+. This was probably due to the higher activity of the catalyst with the lower Si/Al ratio in terms of oligomerization and cracking.

(2) Effects of La^{3+} Ion Exchange

Cations which balance the charge in zeolites are ion-exchangeable and their presence can affect both the acidity and pore size. La^{3+}, a rare earth metal ion, can generate Bronsted-acid sites on the zeolite surface. Such an acidity arises from the hydrolysis of La^{3+} as in:[11]

$$La^{3+} + H_2O \longrightarrow La(OH)^{2+} + H^+$$

The $La(OH)^{2+}$ can react with another water molecule to yield $La(OH)_2^+$ and another H^+. These lanthanum-hydroxy ions occupy sites in the zeolite framework which contribute to increasing its thermal stability.[49]

The conversion of 5 wt% aqueous acetone solution was carried out over 1 wt% La^{3+} ion exchanged ZSM-5(18) (hereafter called LaZSM-5(18)) at 250^0C, 300^0C and

Table 3.4 Effect of Si/Al ratio on conversion of aqueous acetone (5 wt%) over HZSM-5 catalysts at 0.1 h^{-1}

Reaction Conditions				
Si/Al	45	18	45	18
Temperature (^{0}C)	269	272	329	330
Conversion (C-Atom%)	72.4	76.7	88.5	96.7
Carbon Selectivity (C-Atom%)				
Acetic Acid	13.0	16.6	3.8	3.8
Hydrocarbons	41.3	52.7	41.7	46.5
CO_2+CO	45.7	30.7	54.5	49.7
Hydrocarbon Distribution (C-Atom%)				
Isobutylene	20.7	28.8	27.0	9.0
Other C_2 -C_4 Olefins	52.4	36.3	36.5	30.4
C_1 -C_4 Paraffins	7.5	7.3	4.2	19.7
C_5^+	19.4	27.6	32.3	40.9

Table 3.5 Conversion of aqueous acetone (5 wt%) over LaZSM-5(18) catalyst at various temperatures and 0.1 h^{-1}

Reaction Conditions			
Temperature (^{0}C)	250	300	352
Conversion (C-Atom%)	66.6	76.7	83.7
Carbon Selectivity (C-Atom%)			
Acetic Acid	17.3	7.7	6.2
Hydrocarbons	19.7	43.3	68.4
CO_2+CO	63.0	49.0	25.4
Hydrocarbon Distribution (C-Atom%)			
Isobutylene	24.7	17.2	16.7
Other C_2 -C_4 Olefins	19.4	29.9	39.5
C_1 -C_4 Paraffins	7.3	11.9	15.5
C_5^+	48.6	41.0	28.3

352^{0}C, respectively. The results reported in Table 3.5 shows that the total conversion and the carbon selectivity to hydrocarbons increases, with increasing the temperature.

The catalytic activities of the LaZSM-5(18) and the HZSM-5(18) are shown in Figure 3.3 (data are in Table 3.5). At the lower temperature of 250^{0}C, LaZSM-5 showed poorer activity and isobutylene selectivity than the parent zeolite. However, at 352^{0}C, the LaZSM-5 was more selective to isobutylene than the parent zeolite.

Based on the function of La^{3+} described above, the increase in acidity should at least promote the activity and selectivity. However, according to R. Carvajal,[51] La^{3+} incorporation does not automatically result in a stronger acidity in zeolites, which requires a complex interaction of some aluminum atoms with the polyvalent cations located in special positions within the framework. No further work was attempted at this point.

(3) Chryso-zeolite ZSM-5

The chryso-zeolite ZSM-5 was prepared in our labs according to a technique described by R. Le Van Mao et al.,[52,53] Such materials were obtained by acid leaching of the chrysotile asbestos fibers and the resulting solids were used as the silica source in the synthesis of ZSM-5. The total acid density of chryso-zeolite ZSM-5 is lower than that of regular zeolite ZSM-5 of similar Si/Al ratio due to the presence of the leftover Mg. Such Mg component generates basic sites which may neutralize some of the adjacent Bronsted-acid sites. The possible interaction between adjacent acidic and basic sites is illustrated in Figure 3.4 (the chemical composition of chryso-zeolite, HA, was previously given in the experimental part).[54]

The catalytic tests were carried out at 273^{0}C and 329^{0}C using a WHSV of 0.1 h^{-1} and the results are reported in Table 3.6. At both temperatures, selectivities to hydrocarbons and isobutylene are relatively high when compared with those obtained with the regular HZSM-5 (Table 3.7), although the total conversion is relatively low.

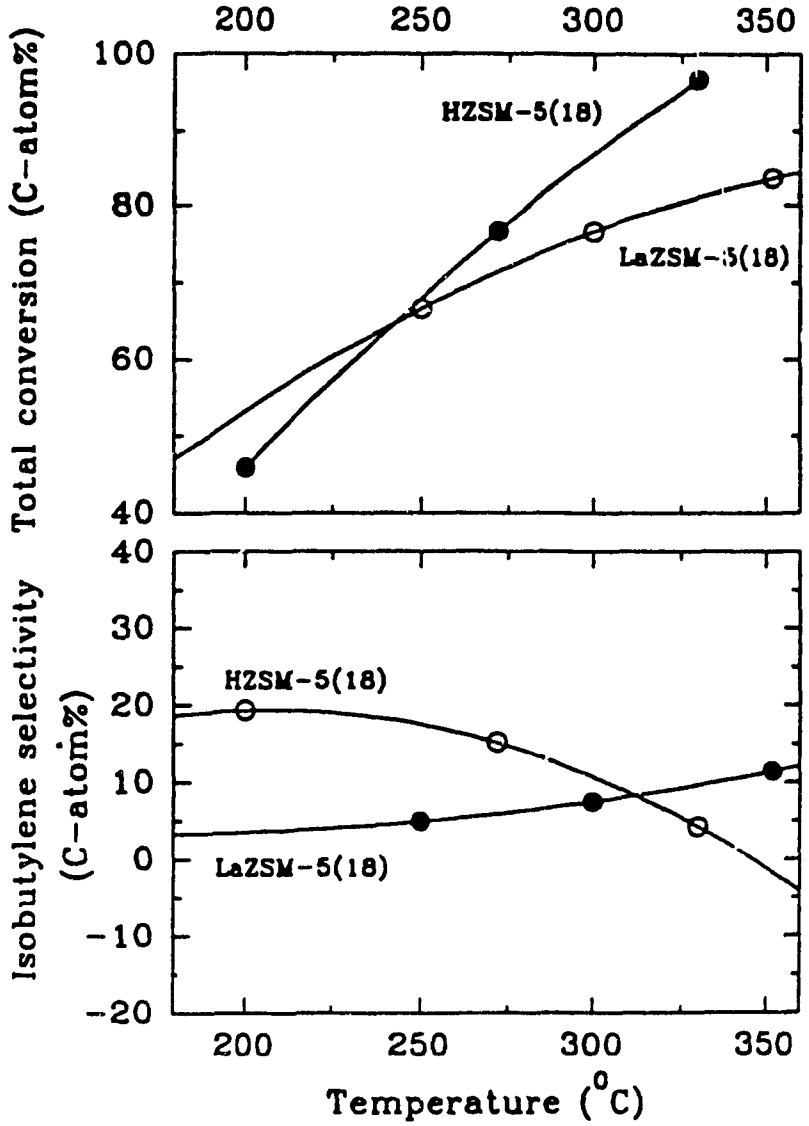

Figure 3.3 Effect of temperature on aqueous acetone (5 wt%) conversion over HZSM-5(18) and LaZSM-5(15) catalysts at 0.1 h^{-1}

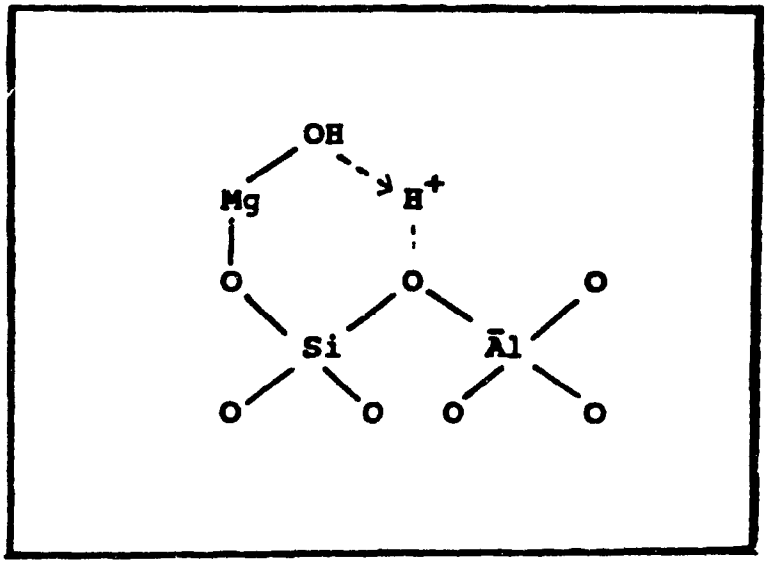

Figure 3.4 Possible interaction between adjacent acidic and basic sites in chryso-zeolite ZSM-5

Table 3.6 Conversion of aqueous acetone (5 wt%) over chryso-ZSM-5(15) catalyst at various temperatures and 0.1 h^{-1}

Reaction Conditions		
Temperature (^{0}C)	273	329
Conversion (C-Atom%)	24.1	45.9
Carbon Selectivity (C-Atom%)		
Acetic Acid	11.0	17.1
Hydrocarbons	56.5	64.5
CO_2+CO	32.5	18.4
Hydrocarbon Distribution (C-Atom%)		
Isobutylene	71.8	46.6
Other C_2 -C_4 Olefins	3.0	30.1
C_1 -C_4 Paraffins	0	0.8
C_5^+	25.2	22.5

Table 3.7 Effect of temperature on conversion of aqueous acetone (5 wt%) over HZSM-5(18) catalyst at 0.1h^{-1}

Reaction Conditions			
Temperature (^{0}C)	200	272	330
Conversion (C-Atom%)	45.8	76.7	96.7
Carbon Selectivity (C-Atom%)			
Acetic Acid	16.3	16.6	3.8
Hydrocarbons	35.9	52.7	46.5
CO_2+CO	47.8	30.7	49.7
Hydrocarbon Distribution (C-Atom%)			
Isobutylene	53.9	28.8	9.0
Other C_2 -C_4 Olefins	13.4	36.3	30.4
C_1 -C_4 Paraffins	1.3	7.3	19.7
C_5^+	31.4	27.6	40.9

This indicates that there might be some beneficial effects from the influence of basic sites during the formation of isobutylene over HZSM-5, since aldol condensation of acetone can also be base catalyzed.[36,38]

3.2.1.B Effects of Temperature

Table 3.7 shows the effect of the reaction temperature over the HZSM-5 zeolite catalyst. The total conversion increased with increasing temperature, as expected. The carbon selectivity to hydrocarbons increased dramatically with the temperature, reached a maximum at 270^0C, and then decreased slightly. At 330^0C, there were more paraffins and C_5^+ formed at the expense of the olefins. The isobutylene selectivity was higher at lower temperature.

It is worth noting that as clearly shown in Figure 3.5 (data are in Table 3.7 and the conversion to each product is equal to the product of the selectivity and the totol conversion). the conversion to acetic acid, isobutylene and light olefins varies in the same manner, indicating that the formations of isobutylene and light olefins might be related to that of the acetic acid.

3.2.1.C Effects of the Concentration of Acetone

In order to study the role of water during the formation of isobutylene, acetone containing different amount of water was injected into the reaction system using a constant WHSV of about 0.1 h^{-1}. The experimental results are listed in Table 3.8. The following results are obtained:

(i) acetic acid and isobutylene were produced in significant amounts;

(ii) mesityl oxide and C_9 aromatics including mesitylene were produced in significant amounts only at higher acetone concentration. This is most evident when

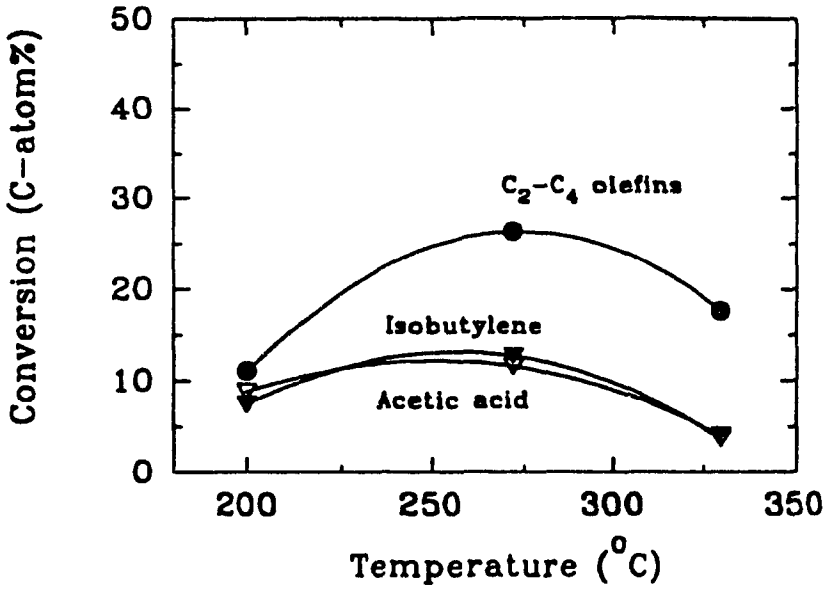

Figure 3.5 Variations of the selectivity towards isobutylene, light olefins and acetic acid with the reaction temperature at 0.1 h^{-1}

Table 3.8 Effect of aqueous acetone concentration on acetone conversion over HZSM-5(22) catalyst at 210^{0}C

Reaction Conditions					
Concentration (wt%)	5.00	16.47	35.01	59.54	100
WHSV (h^{-1})	0.10	0.10	0.10	0.09	0.10
Conversion (C-Atom%)	57.9	67.1	71.9	75.4	47.1
Carbon Selectivity (C-Atom%)					
Acetic Acid	11.8	19.3	26.0	48.0	46.6
Mesityl Oxide	0	0	0.2	0.2	0.8
Other O-compounds[a]	0.6	0.9	1.4	2.1	3.2
Hydrocarbons	19.4	13.4	18.6	17.6	24.1
CO_2+CO	68.2	66.4	53.8	32.1	25.3
Hydrocarbon Distribution (C-Atom%)					
Isobutylene	64.3	55.3	48.3	42.1	67.4
Other C_2-C_4 Olefins	11.6	10.9	14.1	13.8	12.8
C_1-C_4 Paraffins	0.9	3.1	3.3	4.0	0.9
C_5^+ Aliphatics	19.8	19.8	22.4	22.7	6.2
C_9 Aromatics	0	0	0	0	8.3
Other Aromatics	3.4	10.9	11.9	17.4	4.4

[a] Mainly C_4 alcohols

pure acetone was used as the feed, resulting in a mesityl oxide selectivity of 0.8% and a selectivity of C_9 aromatics of 8.3%. However, the amounts of these products were still very low;

(iii) Isobutylene selectivity went through a minimum for an acetone concentration around 60%.

These findings were in agreement with the results of C. D. Chang who proposed that the reaction pathway includes acid catalyzed cracking of the diacetone alcohol intermediate.[41] According to such a proposal, the dehydration reaction leading to mesityl oxide and subsequently to mesitylene is strongly inhibited by a large amount of water present in the feed. Oligomers (C_5^+) and some other aromatics obtained with acetone in the presence of a large amount of water could result from the dimerization of isobutylene, and subsequent dehydrocyclization of the intermediates so produced.

Some of our results are plotted in Figure 3.6. where it can be seen that the total conversion first slightly increased with increasing acetone concentration and then decreased as the acetone concentration reached around 50%. The lowest conversion was obtained at a acetone concentration of 100%. The carbon selectivity to hydrocarbons remains practically constant, while O-compounds, mainly acetic acid, increased dramatically with increasing acetone concentration to reach a plateau at around 60% concentration. Carbon dioxide and monoxide selectivity decreased from the start.

3.2.1.b Effects of Contact Time

The reaction was carried out at 210^{0}C over HZSM-5(22) zeolite catalyst. The contact time ranged from 2 to 114 hours.

The results for total conversion, conversion to hydrocarbons, to light olefins, isobutylene and acetic acid at different contact times are shown in Figure 3.7. The data are reported in Table 3.9. It can be seen that the production of isobutylene goes through an early maximum at around 20 hours (contact time), indicating that isobutylene was

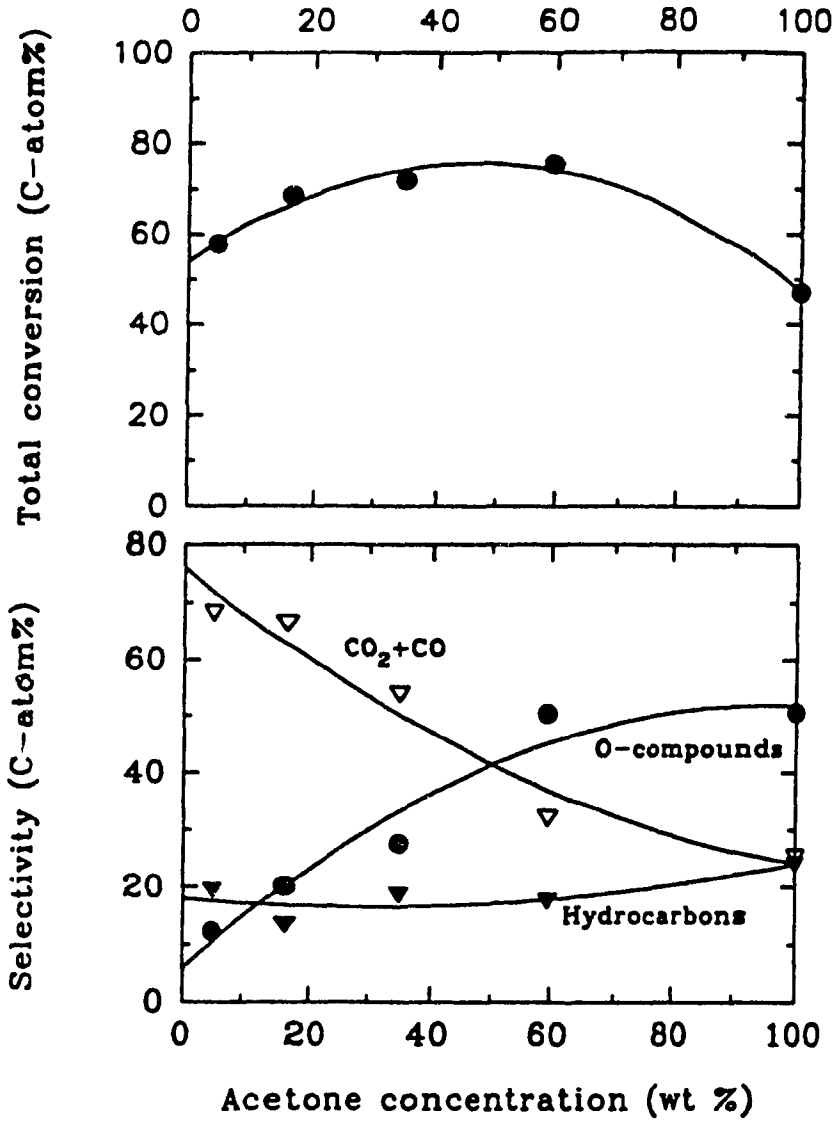

Figure 3.6 Effect of acetone concentration on aqueous acetone conversion over HZSM-5(22) catalyst at 210^{0}C and 0.1 h^{-1}

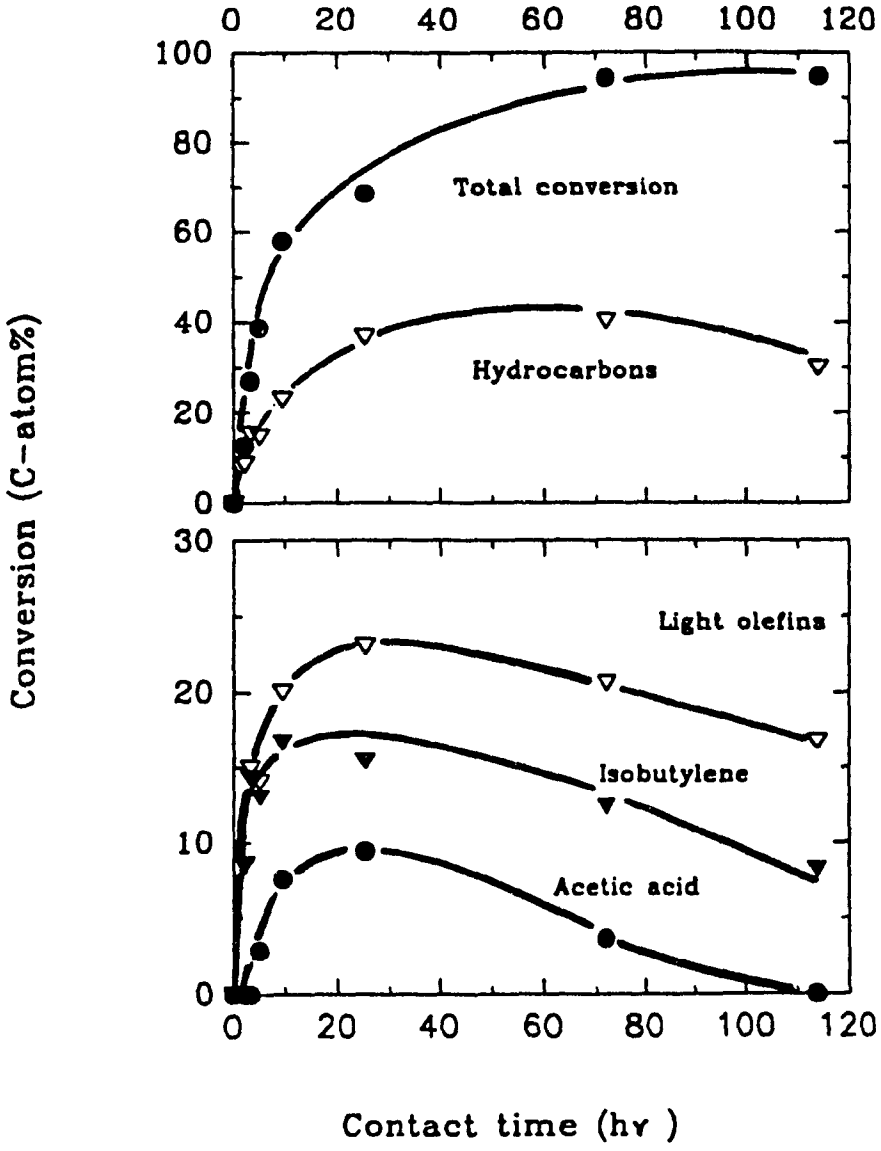

Figure 3.7 Effect of contact time on aqueous acetone (5 wt%) conversion over HZSM-5(22) catalyst at 210^{0}C

Table 3.9 Effect of contact time on aqueous acetone (5 wt%) conversion over HZSM-5(22) catalyst at 210 °C

Reaction Conditions							
Contact time (hr)	2.0	3.1	5.0	9.5	25.1	74.	114.
Conversion (C-Atom%)	12.7	27.0	38.8	57.9	68.5	94.4	94.8
Carbon Selectivity (C-Atom%)							
Acetic Acid	0	0	7.4	13.1	13.7	3.9	0
Other O-compounds	0	0	0	0.9	0	0	0
Hydrocarbons	68.1	56.7	38.2	39.5	53.6	42.6	31.5
CO_2+CO	31.9	43.3	54.4	46.5	32.7	53.5	68.5
Hydrocarbon Distribution (C-Atom%)							
Isobutylene	98.8	93.7	88.1	73.0	42.1	30.8	27.4
Other C_2-C_4 Olefins	1.2	4.4	6.9	14.4	20.7	27.9	28.6
C_1- C_4 Paraffins	0	1.9	0.2	0.7	1.6	4.8	14.3
C_5^+ Aliphatics	0	0	4.8	11.9	32.6	27.8	25.6
Aromatics	0	0	0	0	3.0	8.7	4.1

probably the primary reaction product. On the other hand, acetic acid was formed in significant amounts and its yield varies in the same manner as isobutylene (similar results was reported previously with HZSM-5 in changing temperature), indicating that acetic acid was also a primary reaction product in addition to isobutylene. Light olefins as the cracking products of isobutylene showed the same trend as acetic acid.

It can also be seen that the production of hydrocarbons went through an early maximum, attaining a constant value later on. However, the total conversion increased abruptly within a contact time of 25 hours and kept increasing gradually up to a contact time of 70 hours. After 25 hours as contact time, heavy hydrocarbons (C_5^+ aliphatics and aromatics) appeared in the products and increased with contact time at the expense of other light olefins and acetic acid, due probably to an increase in the activity of thermal cracking and polymerization. More carbon dioxide was produced at longer contact time and this was also due to the thermal cracking.

3.2.2 Activity of the TFA Loaded ZSM-5 Zeolite

Considerable success of the liquid superacids FSO_3H, CF_3SO_3H (trifluoromethane sulfonic acid, shortly called TFA below) and FSO_3H:SbF_5 (Magic Acid) at acidity has led to efforts to transfer this chemistry to solid systems for heterogeneous catalytic processes. It is well recognized that these acids are of incomparable acid strength.[24]

Several kinds of liquid superacids including magic acid, boron trifluoride-methanol complex ($BF_3.CH_3OH$), and triflic acid, were used in attempt to enhance the acidity of zeolite materials. Among these, it was found that HZSM-5 catalyst with TFA loading showed significant improvement with respect to the results obtained with the parent HZSM-5. For this reason, our discussion in this section will be limited to TFA loading and its effects on conversion.

Table 3.10 Effect of TFA concentration on conversion of aqueous acetone (5 wt%) over HZSM-5(18)/TFA catalysts

Reaction Conditions				
Temperature (^{0}C)	200	200	211	212
TFA (wt%)	1	2	2	3
WHSV (h^{-1})	0.09	0.09	0.10	0.10
Conversion (C-Atom%)	50.5	45.9	61.0	53.4
Carbon Selectivity (C-Atom%)				
Acetic Acid[a]	18.7	22.2	26.6	24.9
Hydrocarbons	22.0	54.0	65.4	55.5
CO_2+CO	59.3	23.8	8.0	19.6
Hydrocarbon Distribution (C-Atom%)				
Isobutylene	47.6	46.4	39.5	41.6
Other C_2 -C_4 Olefins	13.8	13.3	19.1	17.3
C_1 -C_4 Paraffins	1.4	2.1	4.0	3.4
C_5^+	37.2	38.2	37.4	37.7

[a] Plus small amount of other o-compounds.

3.2.2.A Effects of TFA Concentration

Table 3.10 lists the conversion of aqueous acetone (5 wt%) over TFA loaded HZSM-5(18) with TFA concentration ranging from 1 wt% to 3 wt%.

At 200^0C, the tests were performed with HZSM-5 (18) containing 1 wt% and 2 wt% TFA and at 210^0C, 2 wt% and 3 wt% TFA. The data show that at each temperature, the catalyst with a 2 wt% TFA loading offers improved results in terms of total conversion and carbon selectivity to hydrocarbons since the hydrocarbon selectivity to isobutylene remained essentially unchanged. The reason why the activity of such a catalyst showed a maximum at a 2 wt% TFA loading is not clear. According to R. Le Van Mao,[8] TFA loading can significantly enhance the product shape selectivity of that catalyst by reducing its pore size. The best loading for adsorption of ethanol is 4 wt%, which is the same for the adsorption of n-hexane (having the same molecular size) on TFA loaded zeolite. Since the critical dimension of isobutylene is larger than that of ethanol or ethylene, a larger pore size would be needed for transformation of acetone into isobutylene. Such a pore size requirement is better fulfilled at the 2 wt% TFA loading.

3.2.2.B Effects of Temperature

The effect of temperature was studied in order to examine its effect in the stability of TFA in the zeolite. The results obtained over HZSM-5(18)/2%TFA at temperature ranging from 180^0C to 220^0C (contact time = 0.1 h^{-1}) are plotted in Figure 3.8 (The data are given in Appendix II). The total conversion and carbon selectivity to hydrocarbons increased with increasing temperature. The isobutylene selectivity decreased very slightly, and such changes, observed with increasing temperature, are considered to be due to kinetic effects of the temperature on the reactions.

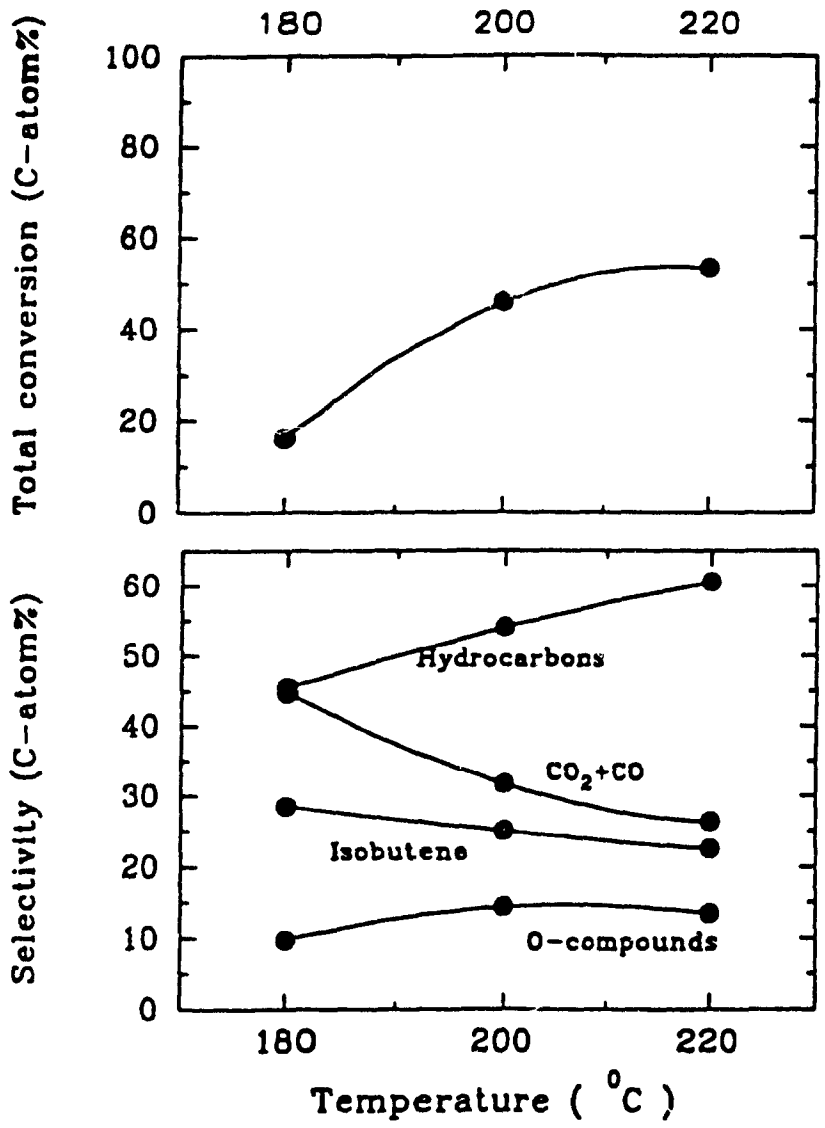

Figure 3.8 Effect of temperature on aqueous acetone (5 wt%) conversion over HZSM-5(18)/2%TFA catalyst at 0.1 h^{-1} (see also Appendix II)

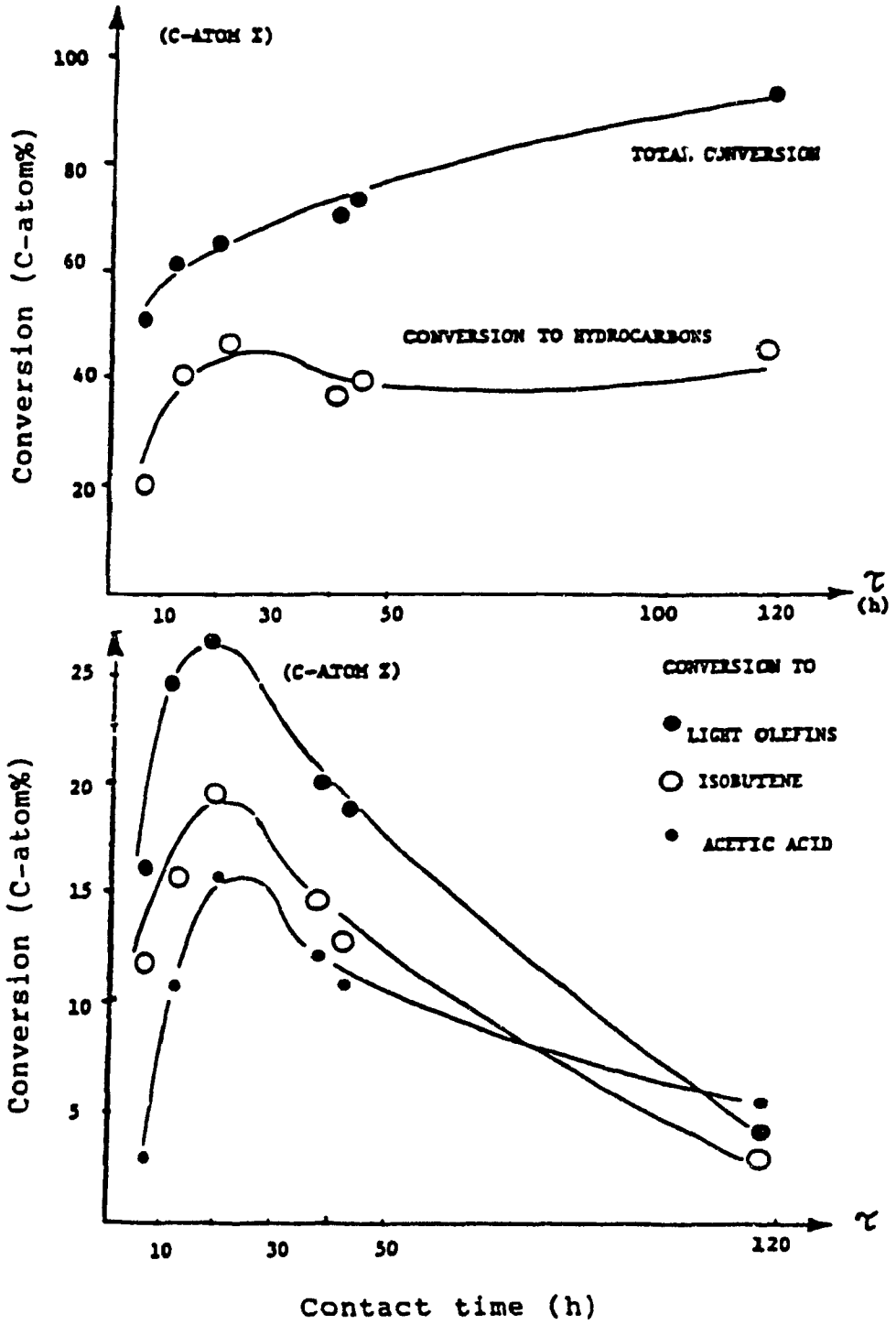

Figure 3.9 Effect of contact time on aqueous acetone (5 wt%) conversion over HZSM-5(18)/2%TFA catalyst at 210°C (see also Appendix II)

3.2.2.C Effects of Contact Time

The tests were carried out at 210^{0}C over HZSM-5(18)/2wt%TFA using contact time from 7 to 120 hours (concentration of acetone = 5 wt%). The results for total conversion, conversion to hydrocarbons, to light olefins, isobutylene and acetic acid at different contact times are plotted in Figure 3.9 (The data are given in Appendix II). It can be seen that the production of isobutylene and other light olefins went through an early maximum (around 20 h), indicating that isobutylene was probably the primary reaction product. On the other hand, acetic acid was formed in significant amounts and its yield varies in the same manner as isobutylene (this was also observed with HZSM-5 in the previous section), indicating that acetic acid was also the primary reaction product and that isobutylene and acetic acid were both produced from the cracking of the same intermediates. It can also be seen that the production of hydrocarbons went through an early maximum, attaining a constant value later on. However, after this duration of contact time, more carbon dioxide and heavy hydrocarbons were produced at the expense of other light olefins and acetic acid.

It has been noticed that the maximum yield for isobutylene was about 27%, while the previous results with parent HZSM-5 (Figure 3.7) showed a maximum of 17% for isobutylene. This has evidently shown the improvement of TFA loaded HZSM-5 catalyst in isobutylene production, due to enhanced acidity.

3.2.2.D Stability of the Supported TFA Species

Comparing the results of acetone conversion over HZSM-5(18) (Table 3.7) with those over HZSM-5(18)/2wt%TFA (Table 3.10) it can be seen that the hydrocarbon selectivity and isobutylene selectivity at 272^{0}C with HZSM-5 can be reached with HZSM-5(18)/2wt%TFA at 210^{0}C. In order to gain some understanding about the nature of TFA in the zeolite, some work has been done to characterize the surface of TFA loaded zeolites.

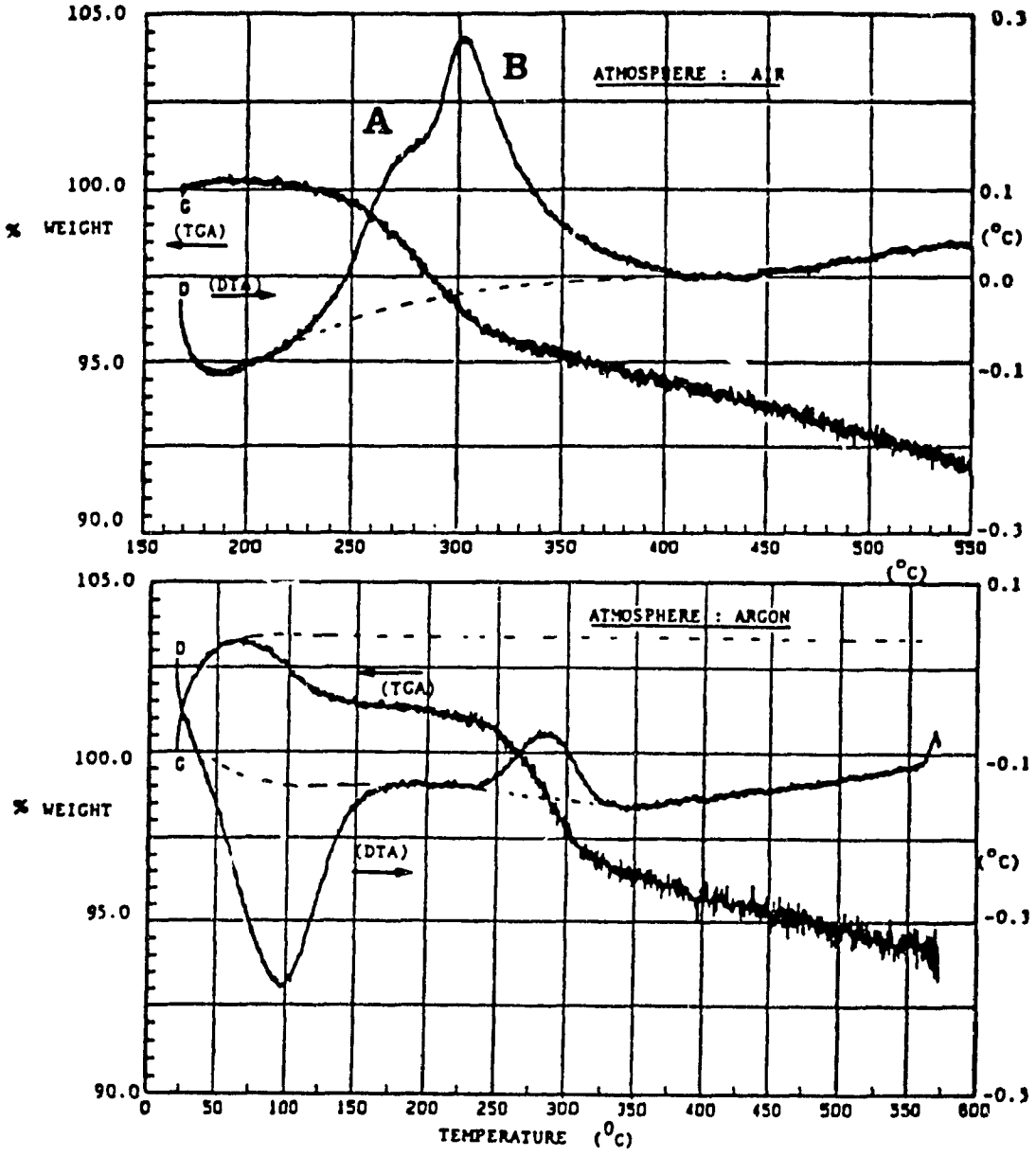

Figure 3.10 TGA-DTA curves with HZSM-5(18)/4%TFA in air and in argon

Figure 3.10 shows the TGA/DTA results obtained with TFA loaded ZSM-5(18) zeolite. From these results it can be seen that:

(i) in the presence of air, the triflic acid, which has a boiling point of 161^{0}C, is quantitatively removed only at the temperature well above 240^{0}C (TGA curve), indicating that the TFA is, upon chemisorption, strongly bound on the zeolite surface;

(ii) in the presence of air, two exothermic peaks with maxima located at 275^{0}C (peak A) and 310^{0}C (peak B) are seen on the DTA curve, implying that there might be two kinds of species associated with the chemisorbed TFA on the zeolite surface, and these two TFA species undergo an oxidation type reaction, instead of decomposition or desorption;

(iii) in the absence of air (atmosphere: argon), however, DTA spectrum shows one exothermic peak (B), indicating that the lesser bound TFA species can desorb without any oxidation reaction while the more firmly bound TFA species (B) can react with the surface silanol groups (or labile framework oxygens) when the sample is heated in argon to 275^{0}C. Therefore, the more firmly bound TFA might be located in the proximity of the Al sites, and the higher thermal stability of species B may be due to the stabilizing interactions of its fluorine atoms with the OH groups associated with the framework Al atoms.

^{1}H and ^{27}Al MAS solid state NMR spectra of parent HZSM-5 and HZSM-5 loaded with TFA (1 wt% and 3 wt%) are shown in Figure 3.11. From ^{1}H spectra, two different proton species are seen with the HZSM-5/1wt%TFA. One at 6.49 ppm is downfield with respect to bridging (acidic) OH groups at 5.870 ppm which as seen in the spectrum of parent HZSM-5, means that the species has a smaller electron density around the atom than that with the parent HZSM-5. The other at 3.420 ppm is upfield, indicating that the species has a greater electron density around. Two peaks are seen in all ^{27}Al

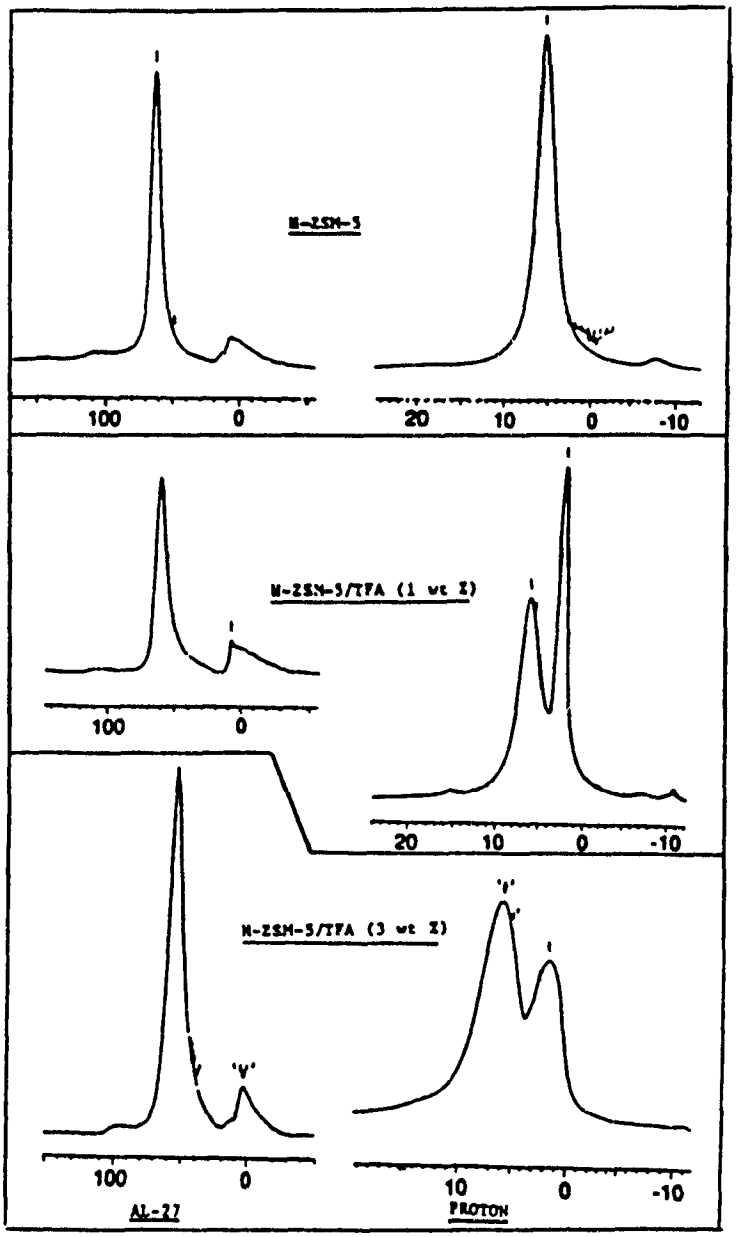

Figure 3.11 MAS solid state NMR spectra with HZSM-5(18)/TFA: (a) ^{1}H and (b) ^{27}Al

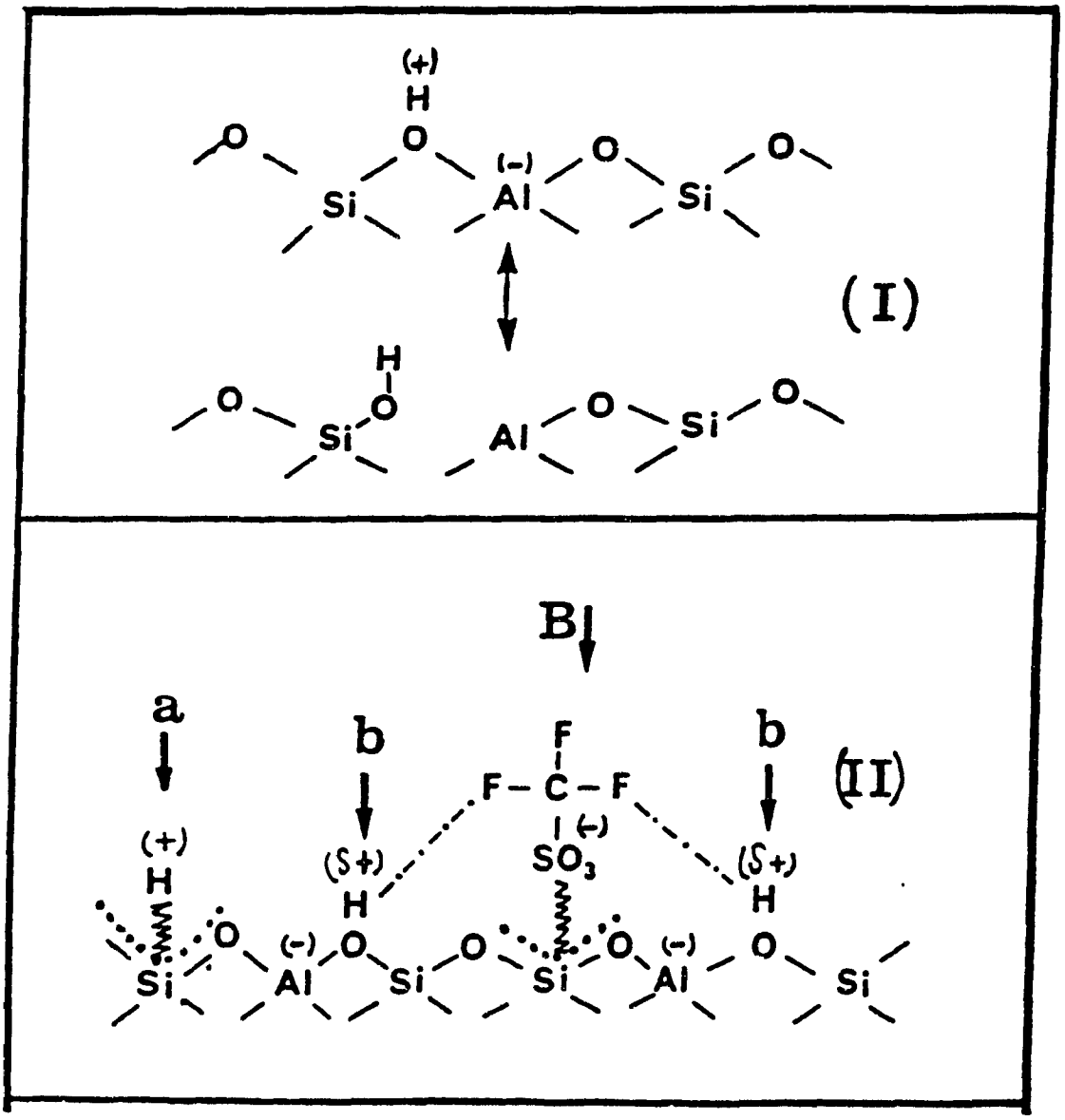

Figure 3.12 Hypothesis on the nature of TFA species on the zeolite surface: (I) acid sites on the parent zeolite surface and (II) dissociative adsorption of TFA and its stabilization by formation of hydrogen bonds

spectra and they are almost the same, indicating that TFA loading did not change the distribution of Al content. In ^{27}Al spectra, the peak at about 60 ppm is assigned to tetrahedral Al atoms and the peak at about 0 ppm is assigned to octahedral Al atoms.[55]

Based on the experimental evidence obtained above, the hypothesis on the nature of the TFA species on the zeolite surface is represented in Figure 3.12. The Bronsted-acid sites are given in diagram (I), and the hypothesis is shown in diagram (II). Species *a* is located further apart from framework oxygen atoms and as such is distanced from their lone-pair electrons, representing a smaller electron density around the proton *a* than that of the bridging OH group in (I). Species *b* is located at the same position as the bridging OH groups, but closer to one of the fluorine atoms in chemisorbed TFA. Such species *b* are probably stabilized by formation of hydrogen bonds and thus show greater electron density around the protons.

IR spectra of the parent zeolite showed two vibrations at 3740 and 3610 cm^{-1} which are assigned to a weakly acidic band and terminal silanol groups on the surface. Upon TFA loading, three additional bands were observed, two at 3780-3800 cm^{-1} and one at 3640 cm^{-1}. These are tentatively assigned to the two types of TFA related OH group (*b* and *a* in Figure 3.12).

3.2.3 Activity of Base Realuminated ZSM-5

Acidity and ion-exchange properties of zeolites are intimately related to the type of occupancy of the tetrahedral sites. Modification of the composition of the framework is intimately involved with thermal stability and with catalytic activity for a variety of reactions by altering the number and strength of acidic site.[23,51] It is therefore desirable to be able to alter the Si/Al ratio of the framework.

However, an attempt to introduce more Al into the ZSM-5 framework so as to attain a Si/Al ratio of less than 10 by simply adding more of the Al component to the gel mixture was unsuccessful as revealed by an extremely low degree of crystallinity of the

resulting products (the results are not shown). Many variables influence the structure of crystallized zeolites such as the composition of the gel mixture, temperature, and the duration of the formation. The production of a particular crystalline phase is very sensitive to the Si/Al ratio. For example, very high silica content in the gel produces α-quartz, whereas increasing the aluminum content of the gel first produces the ZSM-5 phase and then the mordenite phase.[11] In general, ZSM-5 zeolite crystallizes in the TPA (tetrapropylammonium cation) system at Si/Al between 18 and infinity and at ratios below 18 the mordenite phase begins to appear.[11]

Post-synthesis realumination and dealumination have been attempted by many workers in different ways. It is well known that severe steaming of hydrogen zeolites reduces the number of framework tetrahedral aluminum sites and the catalytic acid activity.[18,19] There are equally interesting new ways of enhancing acidity by inserting aluminum into high-silica zeolite frameworks, which have recently been reported in the literature. For example, aluminium can be isomorphously substituted for Si in the framework of the highly siliceous zeolite ZSM-5 with Si/Al ratios of 400-5000 by $AlCl_3$ vapor or alumina at elevated temperatures.[20,22] At least some of the added aluminum is shown to be incorporated into the zeolite as a tetrahedrally coordinated species by ^{27}Al MAS NMR, NH_3-TPD, and FTIR. The treated catalysts show increased acidic activity in methanol conversion and paraffin cracking reactions and give products similar to that of conventional HZSM-5 catalysts.[56]

J. Klinowski reported that aluminium atoms eliminated from the framework of zeolite Y by hydrothermal treatment can be subsequently reinserted into the framework by treatment with aqueous solutions of strong bases (preferably KOH).[17] The results showed that the insertion was successful and sufficient. However, insertion of aluminum into low silica zeolite frameworks of ZSM-5 as tetracoordinate species has not yet been reported.

Table 3.11 Effect of KOH concentration on conversion of aqueous acetone (5 wt%) over HZSM-5(22)/KOH catalysts at 210^{0}C

Reaction Condition					
KOH Concentration	0	0.5	0.8	1.2	1.5
WHSV (h^{-1})	0.10	0.10	0.09	0.10	0.10
Si/Al Ratio	21.75	20.08	19.33	13.46	2.43
Conversion (C-Atom%)	56.2	52.0	61.1	56.1	46.0
Carbon Selectivity (C-Atom%)					
Acetic Acid	11.6	8.9	15.9	11.6	12.7
Other O-compounds[a]	0.8	0.6	1.3	0.6	0.7
Hydrocarbon	27.7	22.0	38.3	31.1	32.5
CO_2+CO	59.9	68.5	44.5	56.7	54.1
Hydrocarbon Selectivity (C-Atom%)					
Isobutylene	48.7	43.7	48.2	53.2	72.9
Other C_2 -C_4 Olefins	6.3	8.5	14.0	8.9	7.9
C_1 -C_4 Paraffins	3.7	0.9	0.9	1.1	0.7
C_5^+ Aliphatics	29.8	32.3	30.3	23.7	16.6
Aromatics	11.5	14.6	6.6	13.1	1.9

[a] Mainly C_4 alcohols.

The following section reports the results of treating ZSM-5(22) zeolite with an aqueous solution of KOH containing $Al_2(SO_4)_3$ as the aluminum source.

3.2.3.A Effects of the Preparation Procedure (KOH Concentration)

The results obtained on aluminated HZSM-5 with different KOH concentrations are reported in Table 3.11. The experiments were carried out at 210^{0}C. The KOH concentration "0" corresponds to the result for parent zeolite. Carbon selectivities to hydrocarbons for KOH concentrations higher than 0.5 N were higher than that obtained with the parent zeolite.

The most interesting improvement was that isobutylene selectivity increased with increasing KOH concentration and was much higher than that obtained with the parent HZSM-5(22) when the KOH concentration was larger than 1.0N (Figure 3.13).

However, the total conversion started to decrease slightly at high KOH concentration, indicating that the zeolite structure might be partially destroyed at these levels. Therefore the most effective KOH concentration for a KOH/$Al_2(SO_4)_3$ solution is between 1.2 and 1.5N.

In order to gain some understanding of what occurred in the zeolite structure during treatments, x-ray powder diffraction, chemical analysis, MAS solid state NMR and BET surface area techniques were performed and the results are tabulated in Table 3.12.

(i) The degree of crystallinity (DC) started to decrease when the KOH concentration in the preparation solution increased to 0.8N, showing that there was some effect on the structure by treatment with very strong base. Since zeolites, being crystalline solids with a regular structure, have a characteristic diffraction pattern, this can be used to identify the particular zeolite, determine the degree of crystallinity of the material, and to possibly determine the presence of other crystalline impurities. A very

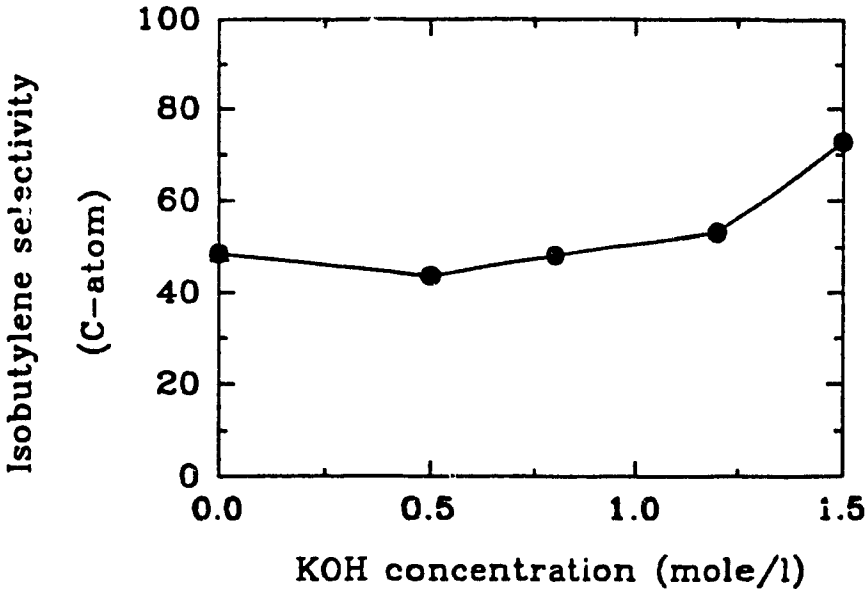

Figure 3.13 Effect of KOH concentration on isobutylene selectivity at 210^0C and 0.1 h^{-1}

Table 3.12 Physical and chemical properties of the realuminated ZSM-5

KOH Conc.(wt%)	0	0.5	0.8	1.2	1.5
DC (%)	100	100	95	81	76
Si/Al	21.8	20.1	10.3	13.5	2.4
A_{tetrd}/A_{oct}	5.77	--	--	4.61	3.66
Surface Area (m^2/gram)	362	--	--	326	217

Table 3.13 Total acidity and acid site distribution of the zeolite ZSM-5 before and after the alumination

Catalyst	Acid site distribution (%)			Total acidity
	S1	S2	S3	(mequiv/g)
HP-(18)	91.4	8.6	0	0.77
HP-(18)/0.8	67.5	32.5	0	0.85
HP-(18)/1.2	54.5	35.3	10.2	1.33

broad low base line was observed in the case of 1.5N KOH, indicating the presence of amorphous material in the structure.[9]

(ii) The Si/Al ratio obtained by chemical analysis showed a decrease with increasing KOH concentration, indicating that the Al content in the structure had been increased (assuming that there was no removal of Si from the structure). Unfortunately the results from atomic adsorption could not tell us about the possibility of insertion of the extra Al in the zeolite framework. However, at least part of this Al belonged to amorphous material which was observed in x-ray results reported above.

(iii) A_{tetra}/A_{oct} ratio was obtained from ^{27}Al MAS solid state NMR spectra (Figure 3.14). A_{tetra} and A_{oct} are the peak areas of tetrahedral and octahedral aluminium in the structure respectively. ^{27}Al MAS solid state NMR spectra of the tetrahedral lattice aluminium in a selected experimental system show only single resonances because every Al has the same environment (Al[4Si]). The main chemical distinction afforded by the ^{27}Al spectra is between (i) octahedral coordination which gives a peak at about 0 ppm (with reference to $Al(H_2O)_6^{3+}$·aq.) and (ii) tetrahedral (lattice) coordination, which results in signals in the range of 50-65 ppm.[55] Therefore, A_{tetra}/A_{oct} ratio can generally give the distribution of Al content (tetrahedral and octahedral) in the zeolite structure. Alumination caused a decrease in A_{tetra}/A_{oct}, indicating either a decrease in tetrahedral Al or (and) an increase in octahehral Al in the structure. However, if we take a close look at each change of Si/Al and A_{tetra}/A_{oct} corresponding to 1.2N and 1.5N KOH, it is found that the decrease in Si/Al (38% and 89% for 1.2N and 1.5N) was always quantitatively larger than that in the A_{tetra}/A_{oct} ratio (20% and 36% respectively). This observation implies that some Al atoms were inserted into tetrahedral sites, otherwise the decrease in Si/Al ratio would be fully caused by an increase in octahedral Al and the percentage change of A_{tetra}/A_{oct} values for HZSM-5/1.2NKOH and HZSM-5/1.5NKOH would have been almost the same as that of Si/Al ratio

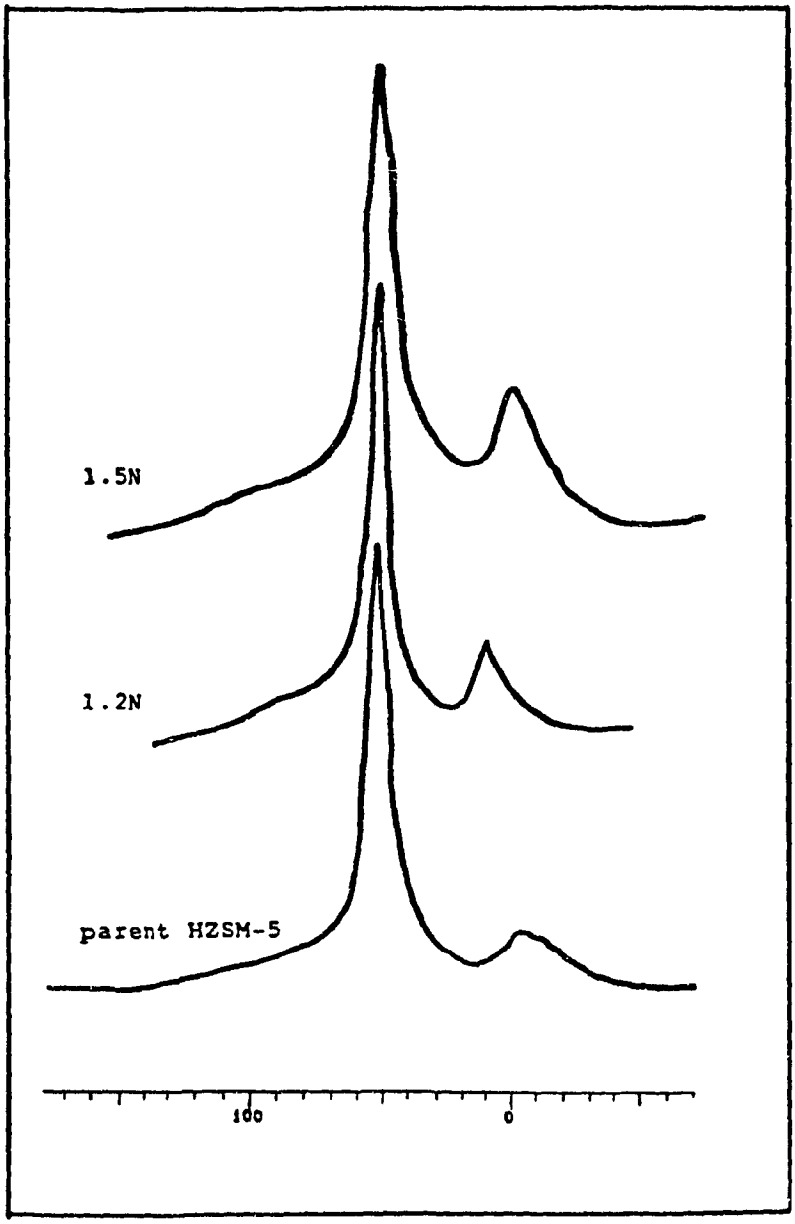

Figure 3.14 MAS solid state NMR spectra of ^{27}Al with HZSM-5(22) and HZSM-5(22)/KOH zeolites

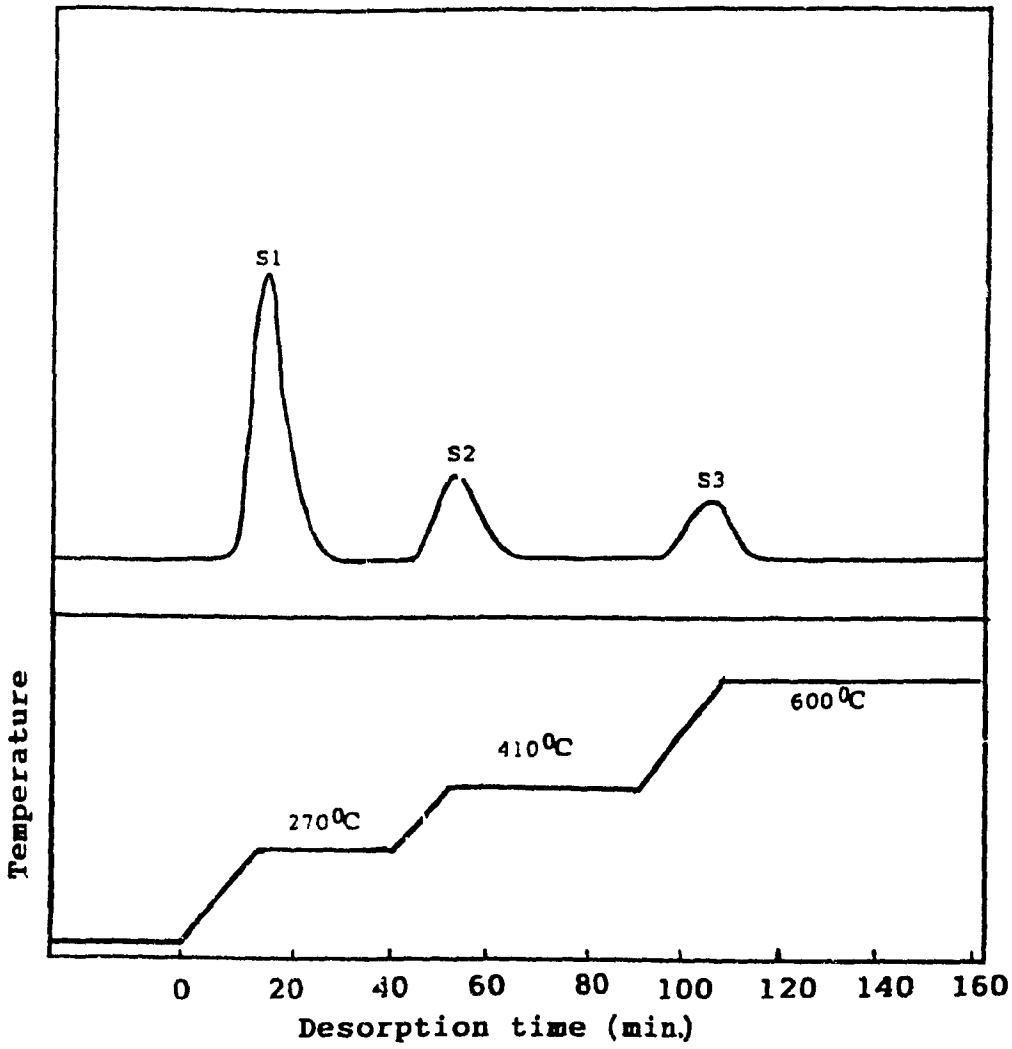

Figure 3.15 TPD profile of HZSM-5(18) zeolite catalyst

(iv) BET surface area reflects the total area of inner zeolite pores and also outside the particles. Usually if the pores are blocked by other materials such as the products from coke formation and amorphous substances, the BET surface area tends to decrease From our measurement, BET surface area decreased with increasing KOH concentration, indicating that there might be changes in pore volume and pore structure.[4] This is probably due to the blockage of pores by amorphous Al formed since this kind of Al can be trapped in the cavities as octahedral aluminium species.[17]

(v) Figure 3.15 illustrates the TPD-NH_3 profiles of the ZSM-5 zeolite. There are three desorption peaks corresponding to different strength of Bronsted-acid sites(S1, S2 and S3 respectively).

Table 3.13 is a summary of the acid density of such acid sites of zeolite ZSM-5 before and after alumination. It was observed that the acid density of S2 and S3 sites after alumination has significantly increased, and the higher the KOH concentration, the larger the increase. Total acid density also increased correspondingly after alumination. This observation indicates that the S2 and S3 should be responsible for the modification of the catalyst by alumination in the acetone conversion to isobutylene.

According to J. Klinowski,[17] extra-framework Al forms soluble (tetrahedral) aluminate anions upon contact with KOH and are reinserted into the framework. Part of the aluminate anions, therefore, could possibly be inserted into the framework of ZSM-5 zeolite and the rest of the aluminate anions formed AL_2O_3 (amorphous material) upon washing the zeolite with distilled water.

It remains unclear, however, whether these newly created acid sites have the same or different specific activity as the conventional protonic sites or the enhanced acid sites.

Based on E. Brunner's research results in which the enhanced activity for *n*-hexane cracking over dealuminated HZSM-5 was considered to be a result of the

Table 3.14 Effect of aqueous acetone concentration on acetone conversion over HZSM-5(22)/1.5NKOH catalyst at 210^{0}C

Reaction Conditions					
Concentration (wt%)	5.00	16.47	35.01	59.54	100
WHSV (h^{-1})	0.10	0.10	0.09	0.08	0.08
Conversion (C-Atom%)	31.0	40.5	53.7	65.7	35.6
Carbon Selectivity (C-Atom%)					
Acetic Acid	8.2	6.1	12.6	12.9	27.7
Mesityl Oxide	0	0	0	0	4.0
Other O-compounds[a]	0	0.3	0.3	0.2	2.6
Hydrocarbons	30.4	22.5	21.7	23.2	54.5
CO_2+CO	61.4	71.1	65.4	63.7	11.2
Hydrocarbon Distribution (C-Atom%)					
Isobutylene	96.5	84.7	79.5	75.1	39.3
Other C_2-C_4 Olefins	2.3	5.3	8.3	8.9	3.7
C_1-C_4 Paraffins	0.2	0.9	1.2	2.3	3.0
C_5^+ Aliphatics	1.0	5.1	4.6	5.8	4.6
C_9 Aromatics	0	0	0	0	47.4
Other Aromatics	0	4.0	6.4	7.9	2.0

[a] Mainly C_4 alcohols.

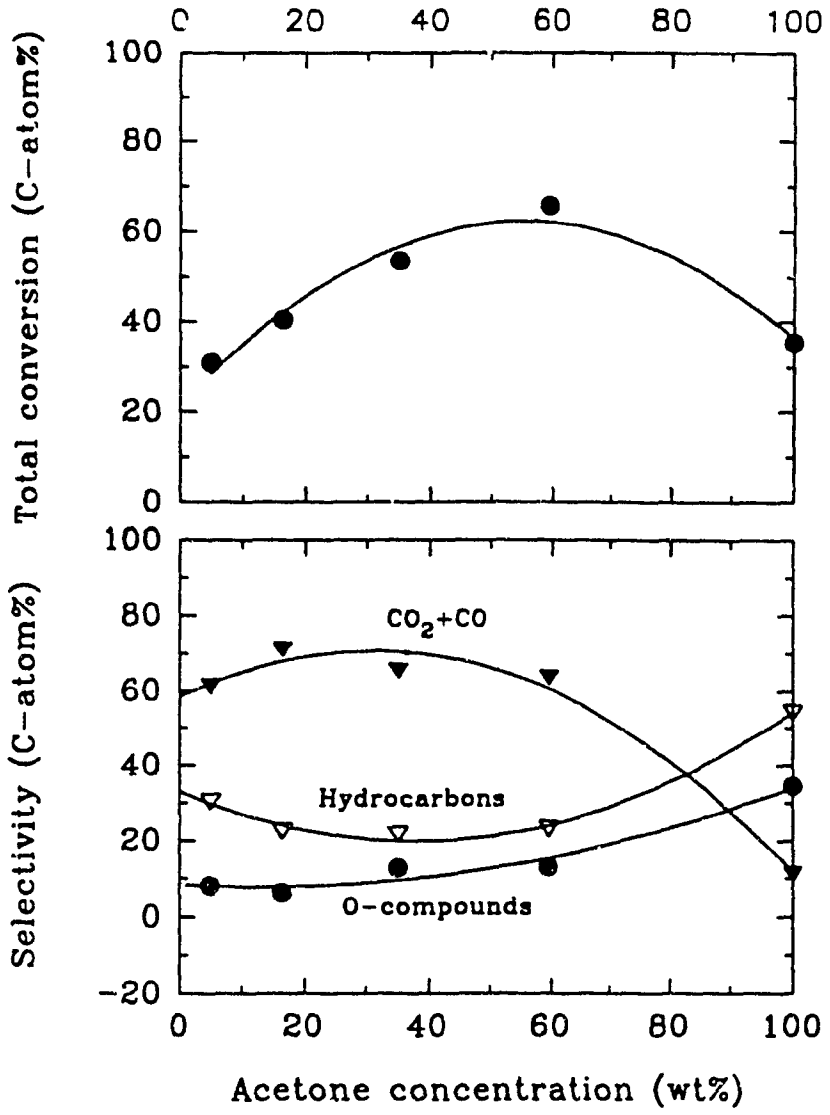

Figure 3.16a Effect of acetone concentration on aqueous acetone conversion over HZSM-5(22)/1.2NKOH catalyst at 210^{0}C and 0.1 h^{-1}

interaction of the n-hexane molecule with a bridging hydroxyl group and with extra-framework aluminum species,[16,18] enhancement in isobutylene selectivity over HZSM-5/KOH was possibly caused by the interaction of adsorbed molecules (acetone, diacetone, mesityl oxide) with both the bridging hydroxyl group and extra-framework aluminium species.

3.2.3.B Effects of the Concentration of Acetone

Results of such a series of tests are reported in Table 3.14 and in Figure 3.16a. Experimental conditions were the same for both the parent HZSM-5 and the treated ones. The figure shows that the total conversion went through a maximum at the acetone concentration of 50%. The carbon selectivity to hydrocarbons however, went through a minimum at the acetone concentration of 50%. The formation of o-compounds, mainly acetic acid, increased slightly with the acetone concentration while that of carbon dioxide and monoxide first increased and soon began to decrease dramatically.

Through the above observation, there is a similarity in the behavior between the aluminated and parent HZSM-5 catalysts, implying that the reaction mechanisms are similar to each other. However, carbon selectivity to hydrocarbons was much higher for treated HZSM-5, while that to o-compounds was lower.

Curves (a) and (b) in Figure 3.16b (data are in table 3.8, 3.14 and 3.16) show the isobutylene selectivity with changing acetone concentration over parent and aluminated HZSM-5 catalysts. At the acetone concentration lower than 60 wt%, the selectivity obtained over the aluminated HZSM-5 (b) was significantly higher than that over the parent HZSM-5 (a) and both catalysts showed decreases in isobutylene selectivity with increasing acetone concentration. After this concentration, the selectivity over the aluminated HZSM-5 (b) kept decreasing up to the acetone concentration of 100 wt%, while the selectivity over the parent HZSM-5 (a) started to increase till the end at which, in fact, the selectivity is higher than that over aluminated HZSM-5. The increase in

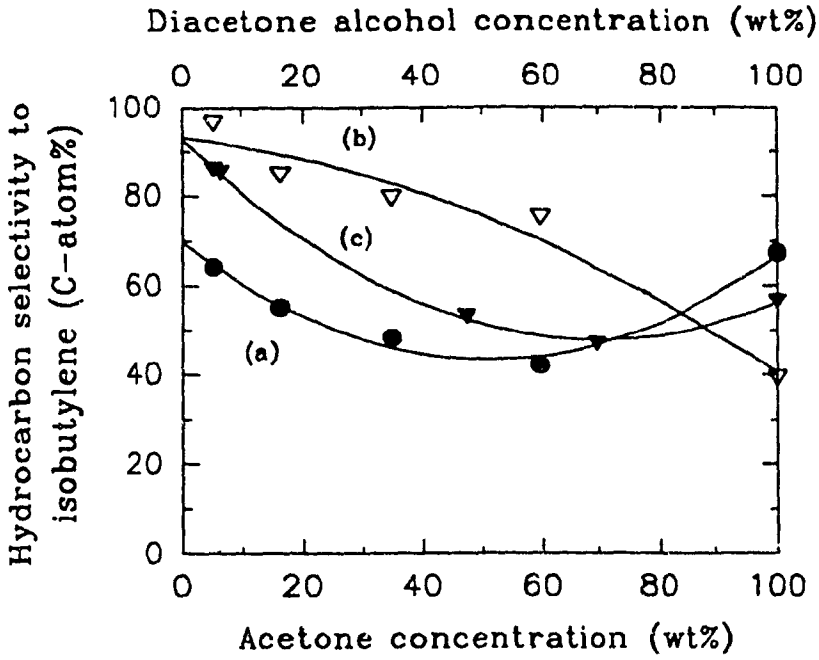

Figure 3.16b Variations of the selectivity to isobutylene at 210^{0}C and 0.1 h^{-1}: (a) with the acetone concentration on aqueous acetone conversion over HZSM-5(22) catalyst; (b) with the acetone concentration on aqueous acetone conversion over HZSM5(22)/1.2NKOH catalyst; and (c) with the diacetone alcohol concentration on aqueous diacetone alcohol conversion over HZSM-5(22) catalyst

isobutylene selectivity in the absence of water in the feed is probably caused by an increased amount of the Lewis-acid sites on the parent HZSM-5 zeolite surface.

3.2.4 Catalytic Activity of the Y Zeolite and Comparison with the HZSM-5 Zeolite

The interior of a zeolite (molecular sieve) is a unique catalytic environment for chemical transformation. Shape selectivity plays important roles in the process by imposing spatial limitations which, under certain conditions, may control the rate and the course of reactions.[41]

Of the natural and synthetic zeolite catalysts, the synthetic faujasites and the pentasils are the most successful in terms of commercial applications and thus have a large economic impact.[9] One of the contributing factors is their three-dimensional channel systems.[12] Y zeolite belongs to faujasitic zeolites and has a 12-member ring with a pore size of 7.4 Å which is larger than that of ZSM-5 zeolite (5.6 Å, 10-member ring). Y zeolite usually has a low Si/Al ratio within the range of 2-3 which generates a larger number of Bronsted-acid sites with relatively weak acidity.

In order to see the different effect between HZSM-5 and HY zeolites on aqueous acetone (5 wt%) conversion and gain some further understanding of this reaction, a set of tests were performed with various HY contents in the combined catalyst. The results are shown in Figures 3.17 (The data are given in Appendix II). Figure 3.17a shows the changes of acetone total conversion, carbon selectivities to hydrocarbons and carbon dioxide and monoxide, with increasing HY content in the combined catalyst. As can be seen, the total conversion decreased gradually from 71% to 52% with increasing HY content. The carbon selectivity to hydrocarbons decreased from 32% to 26%, while that to carbon dioxide (monoxide) selectivity increased with increasing HY content, indicating that adding HY generally reduced the activity and the carbon selectivity to hydrocarbons of the combined catalyst in the aqueous acetone conversion. Also, the

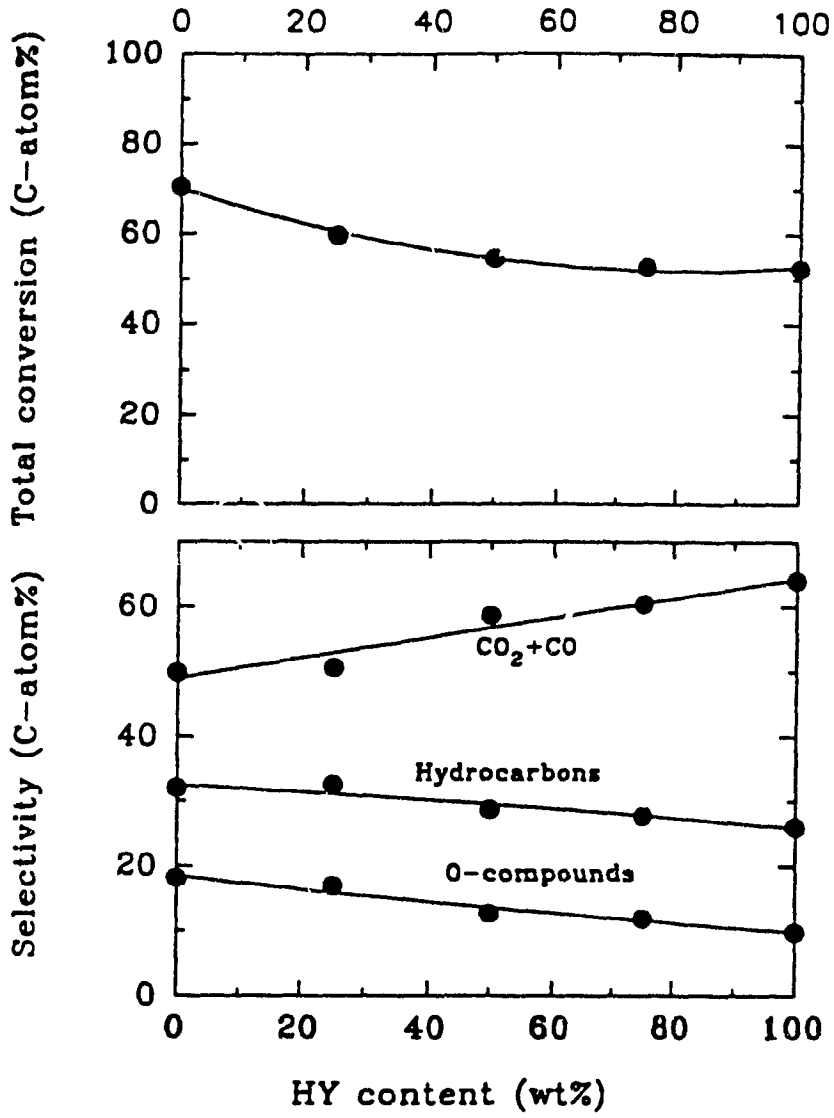

Figure 3.17a Effect of HY content in HZSM-5(22) catalyst on aqueous acetone (5 wt%) conversion at 210^{0}C and 0.1 h^{-1} (see also Appendix II)

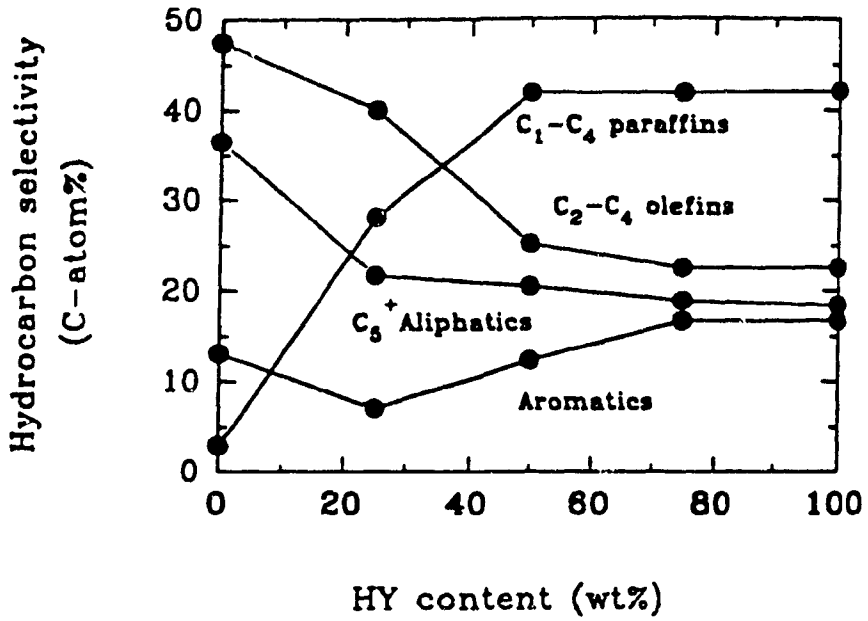

Figure 3.17b Effect of HY content in HZSM-5(22) catalyst on hydrocarbon selectivity at 210^{0}C and 0.1 h^{-1} (see also Appendix II)

carbon selectivity to o-compounds (mainly acetic acid and some C_4 alcohols) showed a slight decrease with increasing HY content in combined catalyst.

Concerning the hydrocarbon selectivity plotted in Figure 3.17b for hydrocarbon selectivity to light paraffins, light olefins, C_5^+ aliphatics and aromatics, with increasing HY content, aromatics showed a slight increase after the HY content was above 50%, indicating that the formation of aromatics was favoured with HY zeolite. On the other hand, light paraffins (mainly isobutane) were produced more and more at the expense of light olefins (mainly isobutylene) and heavier aliphatics, indicating that the formation of isobutane was easier over HY zeolite. This observation is in good agreement with those of R. Le Van Mao[8] and C. D. Chang[41]. The former believes that the change in product yield and selectivity with respect to the parent ZSM-5 and Y-type zeolites is due to the shape selectivity and the difference in acidity. The latter proposes that the formation of isobutane is likely via H-transfer associated with coking reactions in which fused aromatic rings are produced. This is in order to balance the overall hydrogen content in the cracking process, in which the hydrogen serving to saturate olefins must come from hydrocarbons which are converted into aromatics or coke.[9] Such an explanation is supported in this work by the fact that more aromatics were produced with increasing HY content in the HZSM-5 catalyst. As mentioned above, Y zeolite has a larger pore size than ZSM-5 zeolite, therefore, it is easier to form molecules with larger dimensions. However, less heavier aliphatics had been produced over HY zeolite catalyst probably because most of the light olefins had become paraffins before the dimerization and this occurs in a similar way as the formation of isobutane from isobutylene.

The conversion of pure acetone over HZSM-5 and HY was also examined. Table 3.15 shows the results of the reactions performed at 210 ^{0}C and 1 h^{-1}. Some mesityl oxide was obtained over both HY and HZSM-5 catalysts, indicating that the dehydration of diacetone alcohol had significantly occurred because of the absence of water favouring the following reaction:

Table 3.15 Conversion of acetone over HZSM-5 and HY catalysts at 210^0C and 1 h^{-1}

Reaction Condition		
Catalyst	HZSM-5	HY
Conversion (C-Atom%)	30.0	24.3
Carbon Selectivity (C-Atom%)		
Acetic Acid	4.0	7.0
Mesityl Oxide	4.7	2.4
Other O-compounds	2.4	3.8
Hydrocarbons	16.4	19.1
CO_2+CO	72.5	67.7
Hydrocarbon Distribution (C-Atom%)		
Isobutylene	27.1	26.8
Other C_2 -C_4 Olefins	2.2	3.1
C_1 -C_4 Paraffins[a]	0.1	2.8
C_5^+ Aliphatics	57.0	40.6
C_9 Aromatics	13.4	22.9
Other Aromatics	0.2	3.8

[a] Mainly isobutane.

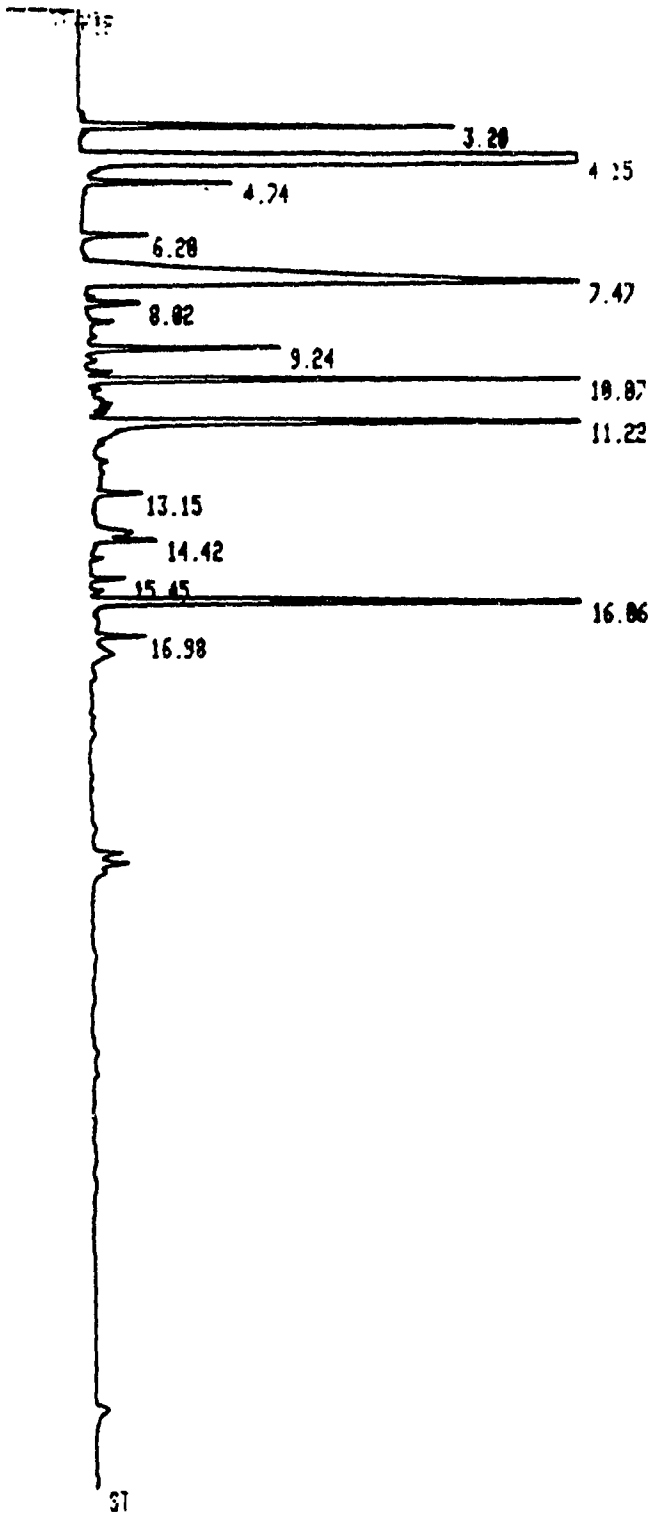

Figure 3.18a GC spectrum of liquid phase from acetone conversion over HZSM-5(22) catalyst at 210^{0}C and 0.1 h^{-1}

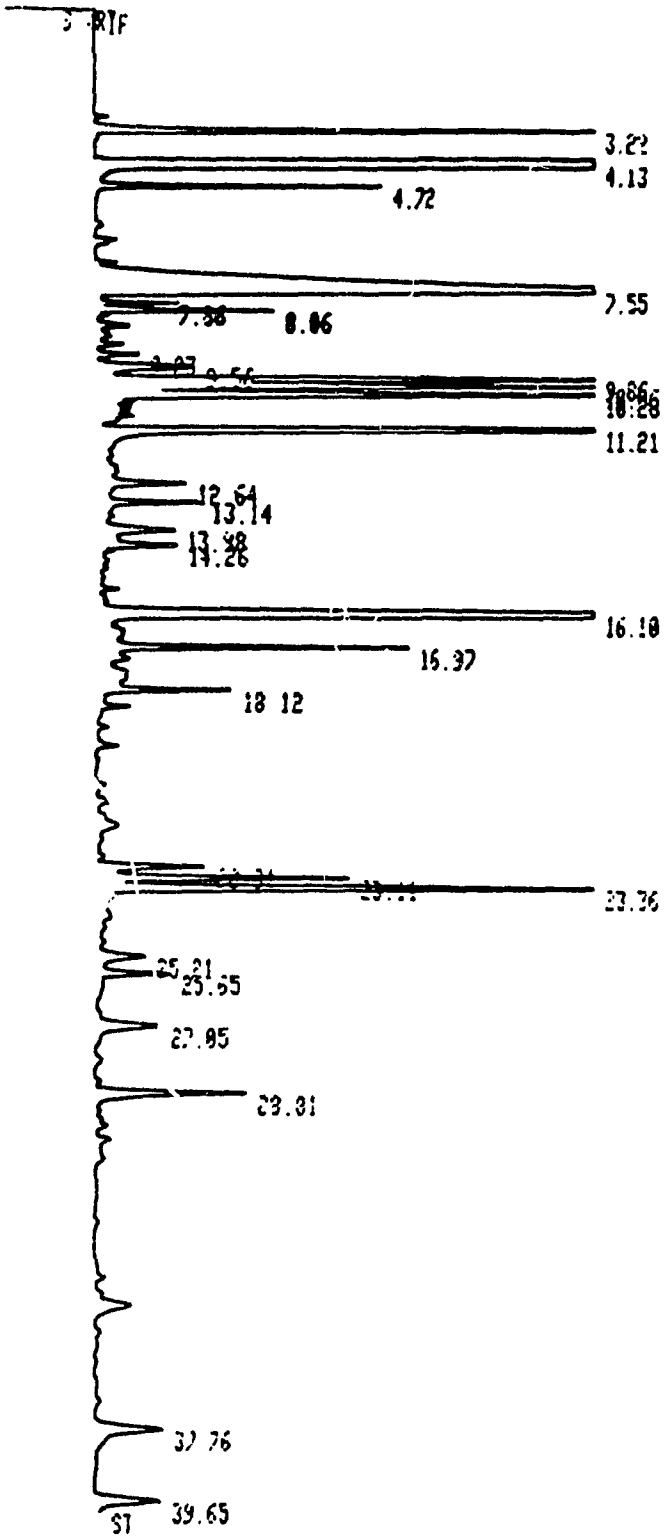

Figure 3.18b GC spectrum of liquid phase from acetone conversion over HY catalyst at 210^0C and 0.1 h^{-1}

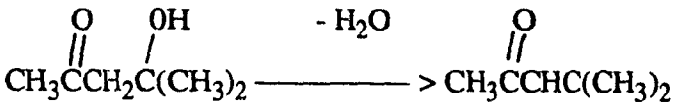

However C_9 (possibly mesitylene) was obtained both over HZSM-5 and HY zeolite catalysts, which is clearly shown in Figures 3.18, in which original graphs from the GC printout for the liquid phase of acetone conversion over HZSM-5 (Figure 3.18a) and HY (Figure 3.18b) are presented. The peaks having retention time values around 16.0 minutes were identified as C_9 aromatics of mainly mesitylene (1,2,3-trimethyl benzene) and isomers by GC and GC-MSD and those after 17.0 minutes were identified as larger molecules by GC-MSD. These observations are interesting because they reflect very important information about the mechanism. According to F. C. Whitmore,[39] mesityl oxide is the precursor of mesitylene. More mesitylene was produced over HY, indicating that the formation of large molecules such as mesitylene should be favoured over HY zeolite due to its relatively larger pore size. Conversely, less mesitylene was obtained since its formation, which occurred in HY, was suppressed in ZSM-5. This occurs firstly, because the critical dimensions of the product mesitylene are quite large and therefore its movement within the zeolite channels would be subject to spatial restrictions imposed by the ZSM-5 structure. Secondly, according to C. D. Chang,[41] the formation of mesitylene may proceed generally in two ways. One of them involves a transition state such as:

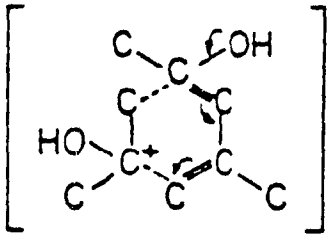

This process will be sterically hindered in the ZSM-5 channels, which would be an example of transition state shape selectivity. Therefore, over HZSM-5 catalyst, hydrocarbon selectivity to mesitylene was observed to be less than that for HY.

The other factor which may assist the formation of larger molecules over the HY zeolite is the high acid density present on such a catalyst surface.

The observations obtained with aqueous and pure acetone conversion over HZSM-5 and HY, and information based on research by C. D. Chang and F. C. Whitmore suggest that the formation of isobutylene is via cracking of diacetone alcohol and the formation of mesitylene is through the dehydration of diacetone and further transformation. More specifically designed tests for confirmation of such a mechanism for this reaction were performed and a detailed discussion of this will be presented in the next section.

3.3 Reaction Network

Various mechanisms for aldol condensation of acetone leading to isobutylene and other products are summarized in Figure 3.19.

Scheme I which was proposed by Chang[41] suggests that the adsorbed diacetone alcohol undergoes cracking to isobutylene and acetic acid (pathway [1]). This is basically the same reaction pathway as suggested by Le Van Mao et al[57] based on the results of Zaki and Sheppard[58] and shown in Figure 3.20.

Schemes II and III of Figure 3.19 hypothesize the dehydration of diacetone alcohol into mesityl oxide (pathway [2]). According to Kubelkova et al,[42] mesityl oxide may undergo cracking to isobutylene and acetic acid (pathway [4]) while the conventional pathway [3] as envisaged by Whitemore[39] leads to C_9 aromatics by a sequence of (further) condensation, ring formation and dehydration reactions.

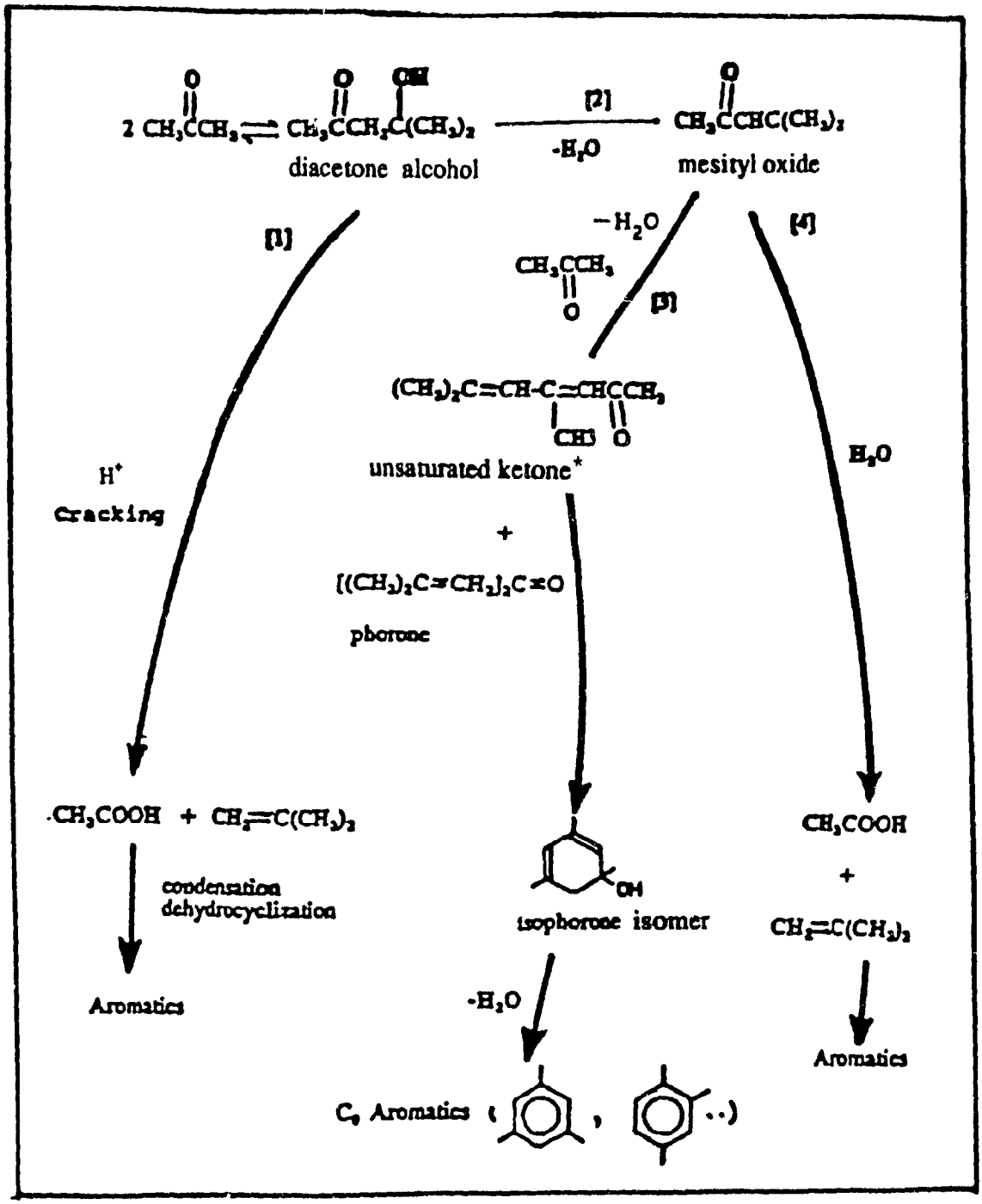

* 4,6 dimethyl hepta-3,5 diene-2 one.

Figure 3.19 Reaction scheme of aqueous acetone conversion over HZSM-5 catalyst

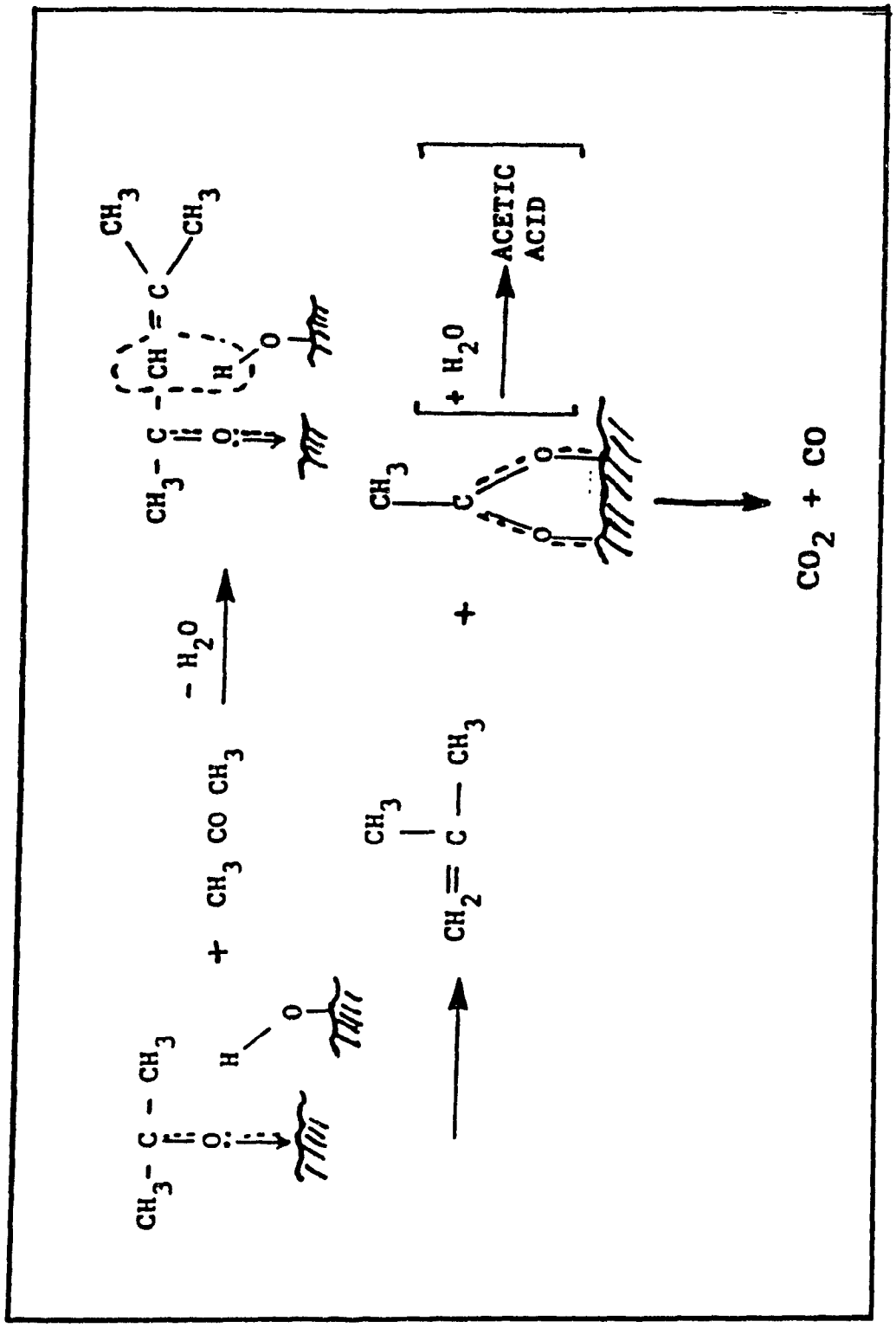

Figure 3.20 Hypothesis for the formation of hydrocarbons

Table 3.16 Effect of feed diacetone alcohol concentration on conversion over HZSM-5(22) catalyst at 210^0C

Reaction Conditions				
Concentration (wt%)	5.00[a]	6.18[a]	47.35[a]	100
WHSV (h^{-1})	0.10	0.10	0.09	0.09
Conversion (C-Atom%)	100	100	100	100
Carbon Selectivity (C-Atom%)				
Acetone[b]	0	0	12.9	36.6
Acetic Acid	11.8	17.3	22.9	32.0
Other O-compounds	0	0	0.7	2.2[c]
Hydrocarbons	39.9	41.6	29.2	20.3
CO_2+CO	48.3	41.1	34.3	8.9
Hydrocarbon Distribution (C-Atom%)				
Isobutylene	86.1	85.3	53.2	56.5
Other C_2-C_4 Olefins	6.6	6.0	13.6	12.8
C_1-C_4 Paraffins	0.5	0.6	3.5	5.3
C_5^+ Aliphatics	5.3	7.4	16.5	16.5
Mesitylene+Isomers	0	0	0	8.4
Other Aromatics	1.5	0.7	13.2	0.5

[a] Some acetone found through GC analysis.

[b] Produced through the reaction.

[c] Mainly mesityl oxide isomer $CH_3\overset{\overset{O}{|}}{C}CH_2C(CH_3)_2$. There are some C_4 alcohols.

Table 3.17 Effect of temperature on pure diacetone alcohol conversion over HZSM-5(22) catalyst

Reaction Conditions			
Temperature (^{0}C)	160	190	210
WHSV (h^{-1})	0.10	0.10	0.09
Conversion (C-Atom%)	99.3	100	100
Carbon Selectivity (C-Atom%)			
Acetone	65.2	50.3	36.6
Acetic Acid	3.1	16.2	32.0
Mesityl Oxide	10.9	0.4	trace
Other O-compounds[a]	2.0	0.9	2.2
Hydrocarbons	7.9	10.9	20.3
CO_2+CO	10.9	21.3	8.9
Hydrocarbon Distribution (C-Atom%)			
Isobutylene	67.1	72.4	56.5
Other C_2 -C_4 Olefins	0.5	9.9	12.8
C_1 -C_4 Paraffins	0	0.8	5.3
C_5^+ Aliphatics	0	5.9	16.5
Mesitylene+Isomers	11.5	3.3	8.4
Other Aromatics	20.9	7.7	0.5

[a] Mainly mesityl oxide isomer. There are some C_4 alcohols.

In order to elucidate the reaction mechanism, diacetone alcohol was used as feed over the ZSM-5 zeolite catalyst. Table 3.16 reports the results obtained with diacetone alcohol to which water was added to provide various concentrations of the diacetone alcohol aqueous solution.

It is seen that when water was present in the feed, acetic acid and isobutylene were produced in significant amounts. Aromatics were formed at the expense of isobutylene; however, no mesitylene and its isomers were produced. This means that pathway [1] (Figure 3.19) was the one followed by the reaction when aqueous diacetone alcohol (and aqueous acetone) was used. In these cases, pathway [2] was strongly inhibited by the massive presence of water. However, if the feed was pure diacetone alcohol (Table 3.16), a great amount of mesitylene (and isomers) were produced. This indicates that pathway [2] going through mesityl oxide was also effective for the reaction. The presence of acetic acid, isobutylene and aromatics other than mesitylene (and isomers) indicates that pathway [1] and [4] should co-exist with pathway [2] in a case of pure diacetone alcohol feed. This was also confirmed by the tests carried out with pure diacetone alcohol at different temperatures (Table 3.17, where large amounts of mesitylene and isomers were formed).

It is worth noting that, although only a trace amount of mesityl oxide was obtained with pure diacetone alcohol as feed at 210^0C, a significant amount of an isomer of mesityl oxide was formed (Table 3.16). Thus, such a result does not alter the hypothesis that the absence of water in the feed induces some diacetone alcohol in the feed to go through mesityl oxide ((or its isomer); and this results in the formation of mesitylene and its isomers. These results are also in agreement with those of Table 3.17 and Table 3.18. In fact, as shown in Table 3.18, CaO not only decomposed pure diacetone alcohol into acetone but also dehydrated diacetone alcohol into mesityl oxide and its isomer. This resulted in a high yield in mesitylene and its isomers. Moreover, since CaO does not have any acid sites (e.g. any cracking properties) the production of

Table 3.18 Conversion of diacetone alcohol over HZSM-5 and CaO catalysts at 210^0C

Reaction Conditions		
Catalyst	HZSM-5	CaO
WHSV (h^{-1})	0.09	0.10
Conversion (C-Atom%)	100	99.7
Carbon Selectivity (C-Atom%)		
Acetone	36.6	58.9
Acetic Acid	32.0	0
Mesityl Oxide	trace	9.4
Other O-compounds[a]	2.2	2.2
Hydrocarbons	20.3	3.7
CO_2+CO	8.9	25.8
Hydrocarbon Distribution (C-Atom%)		
Isobutylene	56.5	0.6
Other C_2 -C_4 Olefins	12.8	0
C_1 -C_4 Paraffins	5.3	2.7
C_5^+ Aliphatics	16.5	13.7
Mesitylene+Isomers	8.4	83.0
Other Aromatics	0.5	0

[a] Mainly mesityl oxide isomer.

Table 3.19 Comparative study of diacetone alcohol and mesityl oxide conversion over HZSM-5(22) catalyst at 210^0C

Reaction Conditions		
Reactant	diacetone alcohol	mesityl oxide
WHSV (h^{-1})	0.09	0.09
Conversion (C-Atom%)	100	48.4
Carbon Selectivity (C-Atom%)		
Acetone	36.6	2.7
Acetic Acid	32.0	11.1
Mesityl Oxide	0	--
Diacetone Alcohol	--	0
Other O-compounds[a]	2.2	24.2
Hydrocarbons	20.3	36.0
CO_2+CO	8.9	26.0
Hydrocarbon Distribution (C-Atom%)		
Isobutylene	56.5	57.9
Other C_2 -C_4 Olefins	12.8	3.1
C_1 -C_4 Paraffins	5.3	0.7
C_5^+ Aliphatics	16.5	11.0
Mesitylene+Isomers	8.4	7.9
Other Aromatics[b]	0.5	19.3

[a] Mainly mesityl oxide isomer.

[b] Mainly Probable presence of C_9 oxygenates, mostly with mesityl oxide as feed.

acetic acid, isobutylene and aromatics other than mesitylene (and its isomers) was practically nil (pathways [1] and [4] of Figure 3.19 prohibited).

Table 3.19 reports the results obtained with pure mesityl oxide as feed. It can be seen that:

i) mesityl oxide is not as reactive as diacetone alcohol; thus, mesityl oxide does not seem to be the main reaction intermediate;

ii) there was no diacetone alcohol formed; so there was no reverse reaction for pathway [2] as shown in Figure 3.19;

iii) acetic acid, isobutylene and aromatics other than mesitylene (and isomers) were produced in significant amounts., indicating that reaction through pathway [4] from Figure 3.19 was likely to have occurred;

iv) mesitylene and its isomers were indeed formed, along with some C_9 oxygenates, mostly in the case of mesityl oxide as feed.

In summary, we believe that the main reaction pathway for acetone conversion goes through diacetone alcohol and ends up with acetic acid (and carbon oxides) and isobutylene (and resulting aromatics) (Figure 3.19). This hypothesis is in perfect agreement with that of Chang [41]. With dilute aqueous solutions of acetone, only one such pathway [1] is used by the reaction. However, with pure acetone, a minor portion of reactant undergoes a dehydration which leads to mesityl oxide (or its isomer) as intermediate and finally to mesitylene and its isomers.

3.4 Apparent Activation Energy

The mechanism of surface catalysis is very complex. According to Hougen and Watson,[59] seven steps are involved when heterogeneous catalytic reactions occur on a molecular scale as in the following:

1. Mass transfer of reactants from the main body of the bulk phase to the gross exterior surface of the catalyst particle;
2a. Diffusion of the reactant molecules from the exterior surface of the catalyst particle into the interior pore structure;
3. Adsorption of the reactants on the surface;
4. Reaction on the surface-molecular rearrangements at active surface sites;
5. Desorption of chemically adsorbed species from the surface of the catalyst;
6b. Diffusion of the products into the fluid; and
7. Mass transfer of products from the exterior surface of the particle into the bulk phase.

In zeolite catalysis, two additional steps must be envisaged:

2b. Diffusion of the reactant molecules within the zeolite pore system;
6a. Diffusion of the products within the zeolite pore system;

Steps 1, 2, 6, and 7 are physical processes, whereas steps 3 and 5 are essentially of chemical character. Steps 1 and 7 are highly dependent on the fluid-flow characteristics of the system. The mass velocity of the fluid stream, the particle size, and the diffusional characteristics of the various molecular species are the pertinent parameters on which the rates of these steps depend.

In order to evaluate the apparent activation energy when zeolites are used as catalysts, E_{app}, the experimental conditions were chosen such that the reaction rate would not be influenced by external diffusion, the effects of which were verified by passing the gas at high velocity through the catalyst. Data of conversions obtained with aqueous (5 wt)% acetone while varying feed rate and maintaining WHSV are listed in Table 3.20. A reasonable constancy of the conversion was obtained, which suggests that the diffusion of the gases outside the zeolite particles was not a rate limiting step.

Table 3.20 Effects of external diffusion on aqueous acetone (5 wt%) conversion over HZSM-5 at 210^{0}C and 0.1 h^{-1}

Feed (g/h)	Weight of Catalyst (g)	Total Conversion (C-Atom%)
5.25	2.5	57.9
4.20	2.0	58.6
2.10	1.0	60.6

Table 3.21 Kinetic results of aqueous acetone (5 wt%) conversion over HZSM-5(22) catalyst

Temperature (K)	k* (h^{-1})	f(t) = a + bt + ct^2 +·· Correlation coefficient	E_{app} (kJ/mole)	A (h^{-1})
443	0.038	0.999		
463	0.071	0.996	61.1	5.7x10^5
483	0.15	0.992		

* $k = [df(t)/dt]_{t=0} = b$

One assumption can be made in order to simplify the kinetic analysis: the molecular diffusion of the reactants and the products is small and thus need not to be taken into account. In that case, the process depends on the adsorption, the reaction, and desorption steps, with apparent activation energy written as follows:

$$E_{app} = H_{ads} - E_{rxn} - H_{des} \qquad (4.1)$$

In any event, the activation energy of a reaction is obtained, in general, with the Arrhenius equation as expressed in:

$$k = A \exp(-E/RT) \qquad (4.2)$$

Where k is the rate constant.

A is the pre-exponential factor.

E is the apparent activation energy.

R is the gas constant

Under the experimental conditions, the reaction rate could be expressed as:

$$r = k P_A^n$$

$$r = kP_A = A \exp (- E/RT) P_A$$

for a first-order reaction, as shown in Appendix III. (4.3)

where r is the reaction rate.

k is the rate constant.

P_A is the partial pressure of the reactant.

n is the order of reaction

By combining (4.2) and (4.3) together, we obtain:

$$r = A \exp(-E/RT)\, P_A^{\,n} \qquad (4.4)$$

According to C. G. Hill,[60] the reaction rate per gram of catalyst is expressed as:

$$r = \frac{F \cdot x}{W} \qquad (4.5)$$

where x is the fraction of reactant converted into products (in mole or pressure units)

W is the weight of the catalyst in grams.

F is the molar feed in mole/h (or g/h)

x can be expressed as a function of partial pressure P_A and conversion C (in C-atom%),

$x = \Delta C \cdot P_A$

Rearrangement of above equation (4.5)

$$r = \frac{\Delta C \cdot P_A}{W/F} = \frac{\Delta C}{\Delta t} \cdot P_A \qquad (4.6)$$

where t is the contact time in g.h./mole or h.

At a zero value of contact time, the rate which is now called the initial rate, can be written as follows:

$$r_0 = (\text{Lim } r)_{t \to 0} = [dC/dt]_{t \to 0} \cdot P_A = kP_A \qquad (4.7)$$

Thus:

$$k = A \exp(-E/RT) = [dC/dt]_{t \to 0} \qquad (4.8)$$

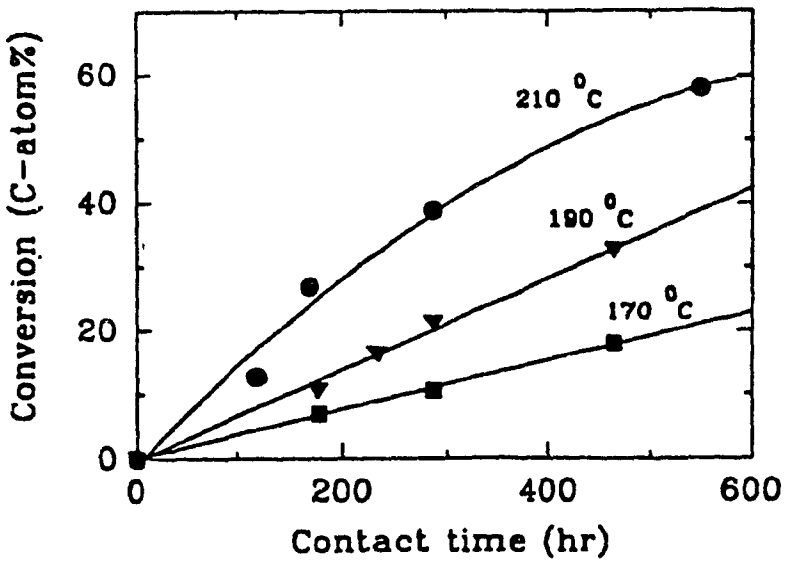

Figure 3.21 Conversion versus contact time for aqueous acetone (5 wt%) conversion over HZSM-5(22) catalyst at different temperatures

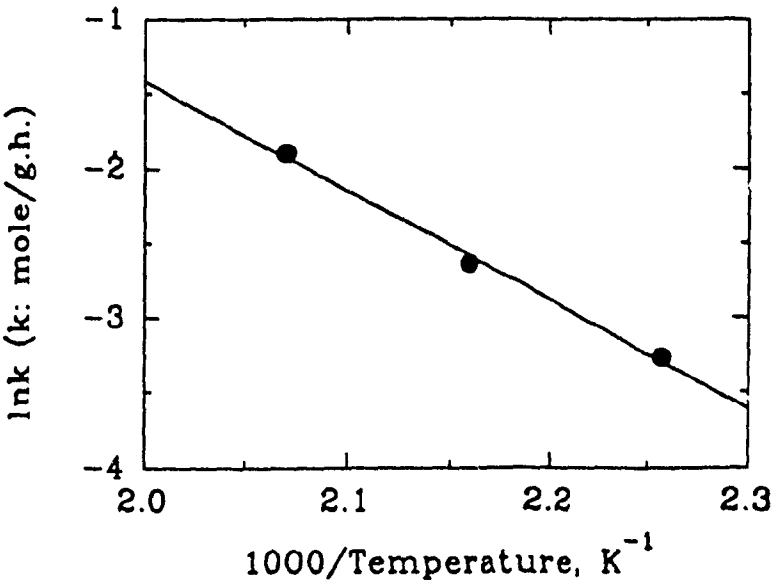

Figure 3.22 Arrhenius plot for aqueous acetone (5 wt%) conversion over HZSM-5(22) catalyst

If the conversion C can be expressed as a function f(t) of the contact time t, we will have

$$k = [df(t)/dt]_{t=0} = A \exp(- E/RT) \qquad (4.9)$$

We have used a non-linear regression analysis (polynomial function) to find out the function f(t) and its first derivation under initial reaction conditions. By plotting lnk versus 1/T, the apparent activation energy E and the pre-exponential factor A could be calculated.

Figure 3.21 shows the plots of aqueous acetone (5 wt%) conversion versus contact time over the HZSM-5(22) catalyst at three temperatures. At 170^0C and 190^0C, good results were obtained with first order plots while data at 210^0C best fit with a second order polynomial. Figure 3.22 is the Arrhenius plot with all related results listed in Table 3.21.

As seen in Table 3.21, the apparent activation energy of the aqueous acetone (5 wt%) conversion with HZSM-5(21) is 14.6 kcal/mole or 61.1 kJ/mole, and the pre-exponential factor is 5.7E+5 h^{-1}.

The conversion of aqueous acetone (5 wt%) with the ZSM-5 catalysts is the first-order and the data and graphs for the regression are given in Appendix III.

CHAPTER 4 - CONCLUSION

The one step conversion of very dilute acetic acid present in fermentation products to hydrocarbons, mainly isobutylene, has been proven to be a feasible reaction through the formation of acetone as the primary step. The reaction for the production of acetone from aqueous acetic acid can be carried out over strong base catalysts, such as CaO, and the reaction conditions include a space velocity of 0.2 h^{-1} (WHSV) and a reaction temperature of 425-450^{0}C.

The second step which involves the formation of isobutylene from aqueous acetone, makes use of molecular shape-selective zeolites as catalysts, such as triflic acid bearing HZSM-5 zeolite having a Si/Al ratio of 18. The best conditions are: a space velocity of 0.1 h^{-1} and a reaction temperature of 210^{0}C.

The activity and isobutylene selectivity can be improved by HZSM-5 loaded with TFA super acid and a TFA concentration of 2 wt% is found to be most effective. The catalyst is relatively stable at the temperatures below 220^{0}C. The high thermal stability of the acid species on the ZSM-5 surface is probably due to the strong chemical bonding (H bonds) of the adsorbed triflic acid molecules with the zeolite protonic acid sites.

HZSM-5 catalyst treated with strong base solution of KOH containing $Al_2(SO_4)_3$ shows the enhancement in the production of isobutylene from aqueous acetone solution, with respect to the parent HZSM-5 under the same reaction conditions. The effective concentration of KOH is 1.2-1.5N.

The reaction network for aqueous acetone conversion over HZSM-5 zeolite catalyst does not greatly depend on the water content in the feed. For dilute acetone solutions, the reaction follows the pathway in which diacetone alcohol acts as the intermediate followed by an acid-catalyzed cracking resulting in acetic acid and isobutylene as main products. The absence of water in the feed favors the formation of mesitylene and isomers. The presence of water in the feed has beneficial effects because

it not only prevents rapid deactivation but also provides a higher hydrocarbon selectivity toward isobutylene.

The apparent activation energy and pre-exponential factor are found to be 61.1 kJ/mole and 5.7E+5 h^{-1}.

In the future, such a process for isobutylene production may be very attractive for the chemical and petrochemical industries because the reactants can be obtained from natural, renewable resources, and isobutylene is a valuable precursor for MTBE and ETBE, two octane boosters for gasoline.

REFERENCES

1. A. Chauvel and G. Lefebvre, *Petrochemical Processes: Technical and Economic Characteristics, 2*, Technip, Paris, 1989.
2. I. S. Goldstein, *Organic Chemical from Biomass*, CRC Press, 1981.
3. G. L. Chauvel, and L. Castex, *Production of Petrochemicals and Characteritic Technique*, Imprimerie Nouvelle, 1989 p. 339.
4. J. Scherzer, *Octane-Enhancing Zeolitic FCC Catalysts*, Marcel Dekker, New York, 1990.
5. L. Pazner, and H. J. Cho, *Biomass*, 1985.
6. J. S. Robinson, *Fuels from Biomass*, Park Ridge, New Jersey, 1980.
7. O. P. Ward, *Fermentation Biotechnology*, Milton Keynes, England, 1989.
8. R. Le Van Mao, G. Mclaughlin and B. Sjiariel, Preceedings of the seventh Canadian Bioenergy R&D Seminar, Ottawa, Canada, April 24-26, 1989, p.623.
9. S. Bhatia, *Zeolite Catalysis: Principles and Applications*, CRC Press, Boca Raton, Florida, 1989.
10. D. W. Breck, *Zeolite Molecular Sieves: Structure, Chemistry, and Use*, Wiley, London, 1974, Chap. 1-2.
11. R. Szostak, *Molecular Sieves: Principles of Synthesis and Identification*, Van Nostrand Reinhold, New York, 1989.
12. G. T. Kokotailo and C. A. Fyfe, *J. Phys. Chem. Solids* Vol. 50, No. 5, 441-447 (1989).
13. N. Y. Chen, W. E. Garwood and F. G. Dwyer, *Shape Selective Catalysis in Industrial Applications*, Marcel Dekker, New York, 1989.
14. D. Decroocq, *Catalytic cracking of Heavy Petroleum Fractions*, Technip, Paris, 1984.
15. D. freude, M. Hunger and H. Pfeifer, *Zeitschrift Physikalische Chemie Neue*

Folge, **152,** 171 (1987).

16. E. Brunner, H. Rmst, D. Freude, T. Frohlich, M. Hunger and H. Pfeifer, *J. Catal.*, **127**, 34 (1991).
17. J. Klinowski, *Hydrothermal Alumination Zeolites*, 1990 p. 40.
18. E. Brunner, H. Ernst, D. Freude, M. Hunger, C. B. Krause and d. Prager, *Zeolites* vol. 9, July, 282 (1989).
19. Q. L. Wang, G. Giannetto and M. Guisnet, *Zeolites,* Vol. 10, April/May, 301 (1990).
20. M. W. Anderson, J. Klinowski and X. Liu, *J. Chem. Soc., Chem. Commum.*, 1596 (1984).
21. C. D. Chang, C. T. W. Chu, J. N. Miale, R. F. Bridger and R. B. Calvert, *J. Am. Chem. Soc.*, **106**, 8143 (1984).
22. R. M. Dessau and G. T. Kerr, *Zeolites*. Vol. 4, October, 315 (1984).
23. K. Yamagishi, S. Namba and T. Yashima, *J. Catal.*, **121,** 47 (1990).
24. W. F. Holderich, Proceedings of the International Symposium on Acid-Base Catalysis, Sapporo, VCH, 1989, p. 6.
25. G. T. Kokotailo, S. L. Lawton, D. H. Olson and W. M. Meier, *Nature*, **272,** 438 (1978).
26. S. L. Meisel, J. P. McCullough, C. H. Lechthaler, and P. B. Weisz, *Chemtech.*, **6**, 86 (1976).
27. C. D. Chang and A. J. Silvestri, *J. Catal.*, **47**, 249 (1977).
28. L. M. Parker, D. M. Bibby, and I. J. Miller, *J, Catal.*, **129**, 438-446 (1991).
29. S. Sugiyama, K. Sato, S. Yamasaki, K. Kawashiro and H. Hayashi, *Catalysis Letters*, **14**, 127 (1992).
30. Z. Dolejsek, J. Novakova, V. Bosacek, and L. Kubelkova, *Zeolites*, vol 11, March (1991).

31. J. Novakova, L. Kubelkova, V. Bosacek, and K. Mach, *Zeolites*, Vol 11, February (1991).

32. G. A. Olah and W. M. Ip, *New J. Chem.*, **12**, 299 (1988).

33. V. Bosacek and L. Kubelkova, *Zeolites*, Vol 10, January (1990).

34. L. Kubelkova and J. Novakova, *Zeolites*, vol 11, November/December (1991).

35. L. Kubelkova, J. Cejka and J. Novakova, *Zeolites*, Vol 11, January (1991).

36. G Zhang, H. Hattori and K. Tanabe, *Applied Catalysis*, **40**, 183-190 (1988).

37. M. I. Zaki and N. Sheppard, *J. Catal.*, **80**, 114 (1983).

38. R. Adams and R. W. Hufferd, *Org, Synth. Coll.*, Vol. I, Wiley, New York, 1961 p. 341.

39. F. C. Whitmore, *Organic Chemistry*, Van Nostrand, New York, 1937 p. 253.

40. G. M. Panchenkov, O. I. Kuznetsov, A. M. D. Guseinov and S. L. Mund, *Dokl. Akad*, Nauk SSSR, **204** (2), 390 (1972).

41. C. D. Chang, W. H. Lang and W. K. Bell , *Catalysis of Organic Reactions*, Marcel Dekker, New York, 1981, p. 73.

42. L. Kubelkova, J. Cejka, J. Novakova, V. Bosacek, I. Jirka, and P. Jiru, Proceedings 8th Intern. Zeolite Conf., Amsterdam, 1989, p. 1203.

43. S. H. McAllister, W. A. Bailey, Jr. and C. M. Bouton, *J. Amer. Chem. Soc.*, **62**, 3210 (1940).

44. O. A. Anunziata, O. A. Orio, E. R. Herrero, A. F. Lopez, C. F. Perez and A. R. Suarez, *Applied Catalysis*, **15**, 235 (1985).

45. J. P. Dejaifve, A. Auroux, P. C. Gravelle, J. C. Vedrine, Z. Gabelica and E. G. Derouane, *J. Catal.*, **70**, 123 (1981).

46. W. K. Hall, F. E. Lutinski and H. R. Geverick, *J. Catal.*, **3**, 512 (1964).

47. (a) R. J. Argauer and G.R. Landolt, U.S. Patent No. 3,702,886 (1972). (b) J. Yao, Ph.D. Thesis, Concordia University, August, 1992.

48. R. Le Van Mao, T. M. Nguyen and J. Yao, *Applied Catalysis*, **61**, 161 (1990).

49. G. C. Bond, *Heterogeneous Catalysis: Principles and Applications*, Clarendon Press, Oxford, 1987.

50. I. E. Sosnina,, and S. V. Lysenko, *Vestn. Mosk. Univ. Khim.*, **14**, 354 (1973).

51. R. Carvajal, P. Chy and J. H. Lunsford, *J. Catal.*, **125**, 123 (1990).

52. T. M. Nguyen, M.Sc. Thesis, Concordia University, July, 1988.

53. R. Le Van Mao and P. H. Bird, Can. Patent No. 1,195,311 (1985) and U.S. Patent No. 4,511,667 (1985).

54. P. Levesque, Ph.D. Thesis, Concordia University, June, 1987.

55. C. A. Fyfe, H. Grondey, Y. Feng and G. T. Kokotailo, *J. Am. Chem. Soc.*, **112**, 8812 (1988).

56. C. D. Chang, C.T-W. Chu, J. N. Miale and K. D. Schmitt, *J. Chem. Soc.*, Faraday Trans., 1, **81**, 2215 (1985).

57. R. Le Van Mao and L. Huang, "The Bioacids/Bioacetone to Hydrocarbons (BATH) Process" in *Novel Production Methods for Ethylene, Light Hydrocarbons, and Aromatics*, edited by L.F. Albright, B.L. Crynes and S. Nowak, p.425-442. Marcel Dekker, New York (1991).

58. M. I. Zaki and N. Sheppard, *J. Catal.*, **80**, 114 (1983).

59. R. D. Srivastava, *Heterogeneous Catalytic Science*, CRC Press, Boca Raton, Florida, 1988.

60. S. J. Thomson and G. Webb, *Heterogeneous Catalysis*, Oliver Boyd Ltd., 1968, p. 95.

APPENDIX I

Data for reproducibility tests:

Temperature (^{0}C)	210	210
WHSV (h^{-1})	0.10	0.10
Total Conversion (C-atom%)	57.1	59.9
Carbon Selectivity (C-atom%)		
Acetic Acid	7.2	6.2
Other O-compounds	0.5	0.4
Hydrocarbons	29.5	23.7
CO_2 + CO	62.8	69.7
Hydrocarbon Distribution (C-atom%)		
Isobutylene	47.0	50.2
Other C_2-C_4 Olefins	14.5	14.5
C_1-C_4 Paraffins	0.9	1.3
C_5^+ Aliphatics	27.8	26.7
Aromatics	9.8	7.3

The relative error both in terms of total conversion and selectivity to isobutylene, is quite acceptable (< 5%).

APPENDIX II

Data for Figure 3.8:

Temperature (^{0}C)	180	200	220
Total Conversion (C-atom%)	16.3	45.9	53.4
Carbon Selectivity (C-atom%)			
Hydrocarbons	45.5	54.0	60.5
O-compounds	9.8	14.3	13.4
CO_2 + CO	44.8	31.7	26.3
Hydrocarbon Distribution (C-atom%)			
Isobutylene	62.4	46.3	37.2
Other Hydrocarbons	37.6	53.7	62.8

Data for Figure 3.9:

Contact Time (h)	6	14	20	40	36	118
Total Conversion (C-atom%)	50.0	60.5	3.5	70.0	72.5	98.0
Conversion to						
Hydrocarbons	20.0	40.5	42.3	37.2	38.0	42.0
Acetic Acid	2.5	10.8	15.2	12.4	11.0	6.8
Isobutylene	12.0	15.6	19.5	14.5	12.5	3.4
Light Olefins	16.2	24.6	27.1	20.1	18.8	4.8

Data for Figure 3.17:

HY Content(wt%)	0	25	50	75	100
Total Conversion (C-atom%)	70.6	59.8	54.6	52.7	52.3
Carbon Selectivity (C-atom%)					
Hydrocarbons	32.0	32.5	28.8	27.7	26.1
O-compounds	18.2	17.0	12.6	11.9	9.8
$CO_2 + CO$	49.8	50.5	58.6	60.4	64.1
Hydrocarbon Distribution (C-atom%)					
C_2-C_4 Olefins	47.5	40.1	25.2	2.5	22.6
C_1-C_4 Paraffins	2.9	28.2	41.9	41.9	42.2
C_5^+ Aliphatics	36.6	21.7	20.5	18.9	18.5
Aromatics	13.0	7.0	12.4	16.7	16.7

APPENDIX III

Data and graphs of the regression for aqueous acetone conversion:

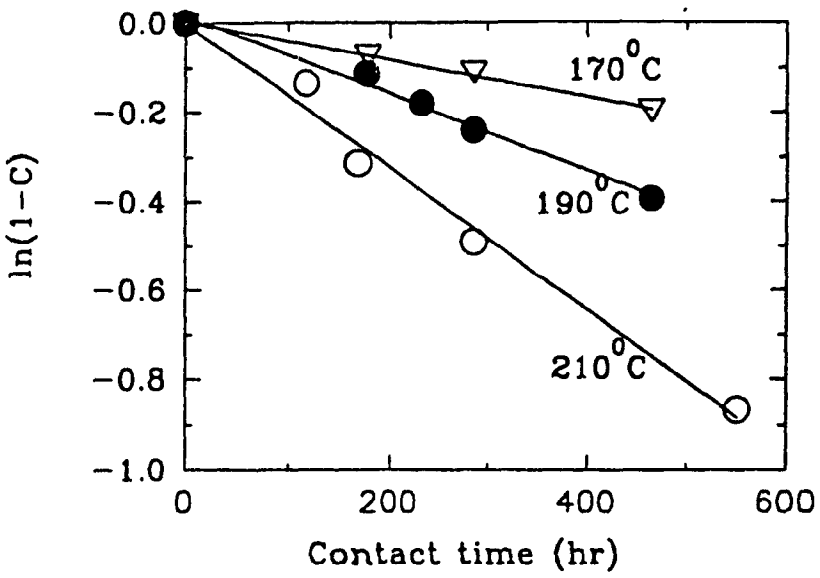

Temperature (°C)	170	190	210
Correlation coefficient	0.998	0.994	0.993

This reaction is of first-order because the total conversion C satisfies the following expression [P. Schulz and M. Baerns, Appl. Catal. 78, 15 (1991)]:

$$\ln (1-C) = kt \qquad (t = \text{contact time})$$